LULEÅ
UNIVERSITY
OF TECHNOLOGY

2003:19

DOCTORAL THESIS

MARTIN NILSSON – Restraint Factors and Partial Coefficients – DOCTORAL THESIS

Restraint Factors and Partial Coefficients for Crack Risk Analyses of Early Age Concrete Structures

Martin Nilsson

Department of Civil and Mining Engineering
Division of Structural Engineering

Restraint Factors and Partial Coefficients for Crack Risk Analyses of Early Age Concrete Structures

Martin Nilsson

Division of Structural Engineering
Department of Civil and Mining Engineering
Luleå University of Technology
SE – 971 87 Luleå
Sweden

Restraint Factors and Partial Coefficients for Crack Risk Analyses of
Early Age Concrete Structures
MARTIN NILSSON
Avdelningen för konstruktionsteknik
Institutionen för Väg- och vattenbyggnad
Luleå tekniska universitet

Akademisk avhandling

som med vederbörligt tillstånd av Tekniska fakultetsnämnden vid Luleå tekniska universitet för avläggande av teknologie doktorsexamen, kommer att offentligt försvaras i

universitetssal F1031, fredagen den 13 juni 2003, klockan 10.00.

Fakultetsopponent: *Professor emeritus Ferdinand S. Rostásy, Institut für Baustoffe, Massivbau und Brandschutz, Braunschweig, Tyskland.*

Betygsnämnd: *Professor Kent Gylltoft, Avdelningen för Betongbyggnad, Chalmers tekniska högskola.*
Professor emeritus Göran Fagerlund, Avdelningen för Byggnadsmaterial, Lunds tekniska högskola.
Professor Bernt Johansson, Avdelningen för Stålbyggnad, Luleå tekniska universitet.

Preface

In the beginning of August 1997, I started my second "journey" at Luleå University of Technology, a journey towards the doctor's degree. Now, in May 2003 I have reach my "destination" by presenting and defending this submitted dissertation. The journey has included both ascents and descent, sometimes even in high speed. The time flies by when you are enjoying yourself.

Finally, Ann, I do not have the words to thank you enough for the support you have given me during these years, but I promise you – I will never do this again! From now on, it is you, me and that little one you are carrying.

Luleå in May 2003, just when my journey ends. — Martin Nilsson

Abstract

Restraint factors and partial coefficients are essential in analyses of the risk of cracking of early age concrete structures. The degree of restraint in a structure or a structural element is almost proportional to the risk of cracking, and the partial coefficients are the statistic measures of the risk of thermal and moisture related cracking in early age concrete.

The accuracy in the determination of the degree of restraint is one of the most important issues that have to be considered in thermal stress analyses. The restraint is needed in order to enable reliable thermal crack risk estimation. Such a estimation will contribute to an improved service lifetime and function of a concrete structure. A semi-analytical method has been derived for the determination of the restraint variation in early age concrete elements cast on older and adjacent elements. The method is derived using the Compensation Plane method according to the linear elastic theory. The model depends on the geometry of the structure, the Young's modulus of the structural elements, the boundary restraint situation, and the location of the newly cast concrete element on the old element.

The model is further developed for the typical case wall-on-slab. Straightforward and simple expressions are derived for the restraint variation in the wall. In the model, effects of high walls are regarded in form of non-linear deformations for walls with completely restrained bases. The model is supplemented with effects concerning possible slip failure at the joint between the young and the old concrete. The decisive point for maximum tensile stresses and at where the restraint should be determined is briefly described and discussed.

Necessary adjustment tools are developed, determined and presented in order to achieve good correlation. Exactly 2920 3D elastic FEM calculations form the reference of the model. The adjustment tools consist of effective width of the slab, effects of relative location of walls on slabs, high wall effects, effects of possible slip failure in joints, and finally on the degree of boundary restraint. By use of the adjustment tools,

good agreement is achieved between the restraint variation determined by the semi-analytical method and by the reference values from the FEM calculations.

It has been shown that the structural restraint behaviour of structural elements can be described by means of restraint coefficients giving an agreeing thermal stress development compared to both more exact Finite Element (FE) calculations and measured stresses in a full-scale structure. The restraint coefficients are in a stress calculation applied as a direct reduction of the fixation stress during both the expansion and contraction phase of a hardening concrete in a structural element. The restraint coefficients established by the semi-analytical method give an acceptable accuracy compared to both more realistic viscoelastic approaches including models describing the hardening young concrete as well as the measured and observed restraint behaviour of a real full-scale structure.

Partial coefficients for thermal cracking problems have been determined by a probabilistic method. The calculated values of the partial coefficients have been compared to values stated in the Swedish building code for bridges. The values in the code are only based on experiences and logical reasoning, whereas the calculated coefficients are determined with various possible coefficients of variation of the used variables. Wide ranges of possible results depending on the input have been shown. However, with use of realistic material properties and reasonable assumptions related to thermal cracking problems, good agreement is achieved between the stated values in the code and the values obtained by the probabilistic method.

Sammanfattning

Tvångsfaktorer och partialkoefficienter är nödvändiga i sprickriskanalyser av unga betongkonstruktioner. Graden av tvång i en konstruktion eller ett konstruktionselement är så gott som proportionell mot risken för sprickbildning, och partialkoefficienter är det statistiska måttet på risken för termisk och fuktrelaterad sprickbildning i unga betongkonstruktioner.

Precisionen i bestämning av graden av tvång är en av de viktigaste frågeställningarna som måste beaktas för temperaturspänningsanalyser för att möjliggöra tillförlitliga termiska sprickriskuppskattningar. Detta i sin tur bidrar till förlängd livslängd och säkerställande av betongkonstruktioners funktion. En semi-analytisk metod har härletts för bestämning av tvångsvariationen i unga betongelement gjutna på äldre angränsande element. Metoden är härledd med grund i utjämnande planmetoden (Compensation Plane method) enligt linjär elasticitetsteori. Metoden beror på konstruktionens geometri, elasticitetsmodulen hos de ingående elementen, graden av randtvång och nyligen gjutna betongelements relativa läge på äldre och angränsande element.

Metoden är vidareutvecklad för typfallet vägg på platta. Ett enkelt och rättfram uttryck har härletts för tvångsvariationen i väggar. I modellen behandlas effekten av höga väggar genom ickelinjära deformationer för väggar med fullständigt fastlåsta bottenränder. Modellen är kompletterad med effekter rörande eventuella glidbrott i gjutfogen mellan den unga och den gamla betongen. Den bestämmande punkten för maximala dragspänningar och där tvånget bör bestämmas är övergripande beskrivet och genomgånget.

Nödvändiga justeringsverktyg för typfallet vägg på platta har utvecklats, bestämts och presenterat för att uppnå bra överensstämmelse med exakt 2920 3D elastiska FEM-beräkningar som utgör referensen för modellen. Justeringsverktygen består av effektiv plattbredd, effekter av väggars relativa läge på plattor, effekter av eventuella glidbrott i gjutfogar, och slutligen på graden av randtvång. Genom användandet av justeringsverk-

VII

tygen uppnås bra överensstämmelse mellan tvångsvariationer bestämda med den semi-analytiska metoden och referensvärdena från FEM-beräkningarna.

Tvångskoefficienterna enligt den semi-analytiska formuleringen har använts i en förenklad direkt beräkningsmetod för spänningar som har jämförts med mer exakta FEM-beräkningar och uppmätta spänningar i fullskalekonstruktioner. God överensstämmelse erhölls i båda fallen. Tvångskoefficienterna är i spänningsberäkningarna tillämpade som en direkt reduktion av fastlåsningsspänningen under både expansions- och kontraktionsfaserna hos en hårdnande betong i ett konstruktionselement. Tvångskoefficienterna i den direkta metoden är således helt jämförbara med både mer realistiska tvångsförhållandena erhållna enligt FEM-beräkningarna och observerade tvångsbeteenden i en riktig fullskalekonstruktion.

Partialkoefficienter för temperatursprickriskproblem har bestämts med en sannolikhetsteoretisk metod. De beräknade värdena på partialkoefficienterna har jämförts med värden givna i den svenska bronormen. Värden i normen är endast baserade på erfarenhet och logiska resonemang, medan de beräknade koefficienterna är bestämda med olika och möjliga variationskoefficienter för de ingående variablerna. En stor vidd av möjliga resultat beroende på indata har påvisats. Emellertid, med användande av realistiska materialegenskaper och förståndiga antaganden relaterande till den termiska sprickproblematiken har bra överensstämmelse erhållits mellan de givna värdena i normen och värden bestämda med den sannolikhetsteoretiska metoden.

Nyckelord: tvång, ung betong, sprickbildning, resiliens, gjutfogsglidning, vägg på platta, partialkoefficienter, sannolikhetsteoretisk metod

Table of Contents

1 Introduction

Restraint factors and partial coefficients are essential in analyses of the risk of cracking of early age concrete structures. The degree of restraint in a structure or a structural element is almost proportional to the risk of cracking, and the partial coefficients are the statistic measures of the risk of thermal and moisture related cracking in early age concrete.

Early age cracking of young concrete in civil engineering structures should be avoided, for instance in tunnels beneath the ground water level and in bridges exposed to chlorides and/or possible freezing and thawing cycles at high humidity situations. Through cracking in structures with water pressure on one side will lead to water flow through the structure for all visible cracks, i.e. for crack widths more than about 0.1 mm. The intrusion of chloride ions in cracks significantly may reduce the initiation period, i.e. the time before the reinforcement starts to corrode. If water entrains in arisen cracks, freezing and thawing may lead to increasing crack widths, with possible leakage and/or durability problems as consequence, see e.g. Fagerlund (1992 & 1994). Therefore, the understanding of the factors influencing the risks of thermal cracking is of great importance. Enhanced knowledge about the problem and the affecting parameters gain the building process and lower the final costs. The main factors affecting early age cracking in concrete are temperature and moisture conditions, degree of restraint, mechanical properties of the young concrete, and behaviour of adjoining structures, see Bernander (1998). In turn, these factors can be influenced already in the design phase for instance by choice of mix proportions, of pouring and curing conditions, and of the choice of structural system.

With beginning in the earlier part of the last century, see e.g. Carlson (1937), Reinius (1945) and Löfqvist (1946), estimation of the risk of cracking in newly cast concrete structures during the heating and cooling phases has been of great concern for engineers. However, it was not until the last decades, that, with the aid of modern computers and laboratory techniques, models for early age cracking risks based on stresses and/or strains were developed. Thus, extensive and thorough research and develop-

ment have been performed during the last years at many universities, organisations and companies within the field of early age thermal cracking, see e.g. Bernander (1973, 1982, 1998), ACI (1973, 1990 & 1995), Stoffers (1978), Harrison (1981), Fagerlund (1985), JCI (1992), RILEM (1998), Rostásy et al. (2001), CCEAC 2000 (2002).

At Luleå University of Technology, Division of Structural Engineering, thermal cracking of young concrete is one of the major research areas. This was started early in the 1980's, see Bernander (1982), influenced by work done by Cederwall et al. (1970). With Bernander, Cederwall and Elfgren as supervisors, the first academic theses were presented by Emborg (1985) and Emborg (1989). Thereafter, a number of licentiate and doctoral theses followed: Jonasson (1994), Westman (1995), Ekerfors (1995), Groth (1996), Hedlund (1996), Westman (1999), Larson (2000), Nilsson (2000), and Hedlund (2000).

Rules in different codes as well as a number of different recommendations and guidelines concerning cracking in early age concrete aim at: either minimizing widths of possible arisen cracks; or avoiding the origin of cracks. The predominant objective in the World is to minimize crack widths. In Sweden, the Building Codes for Bridges, BRO 2002 (2002) applicable to bridges and similar civil engineering structures, states that thermal induced cracking should be avoided. Therefore, the latter direction is the focus for the research presented in this thesis.

1.1   Early age cracking

During the hydration phase of a concrete structure, the chemical reaction between the cement and the water in the concrete generates heat. Due to this heat, young structural elements undergo temperature histories similar to what is shown in Figure 1a). During the heating phase, the structural elements expand, and later, when the chemical reaction subsides, the heat development decreases and the temperature starts to adjust to the surroundings implying in contraction of the young concrete. Meanwhile, the concrete matures and its strength increases, see Figure 1b).

The volume changes during the hydration phase can be hindered by adjoining structures, foundations or by internal parts not undergoing the same volume changes. This hindrance induces restraint stresses that may be so large that cracks possibly occur if the stresses are larger than the tensile strength of the concrete, see Figure 1b).

2

Introduction
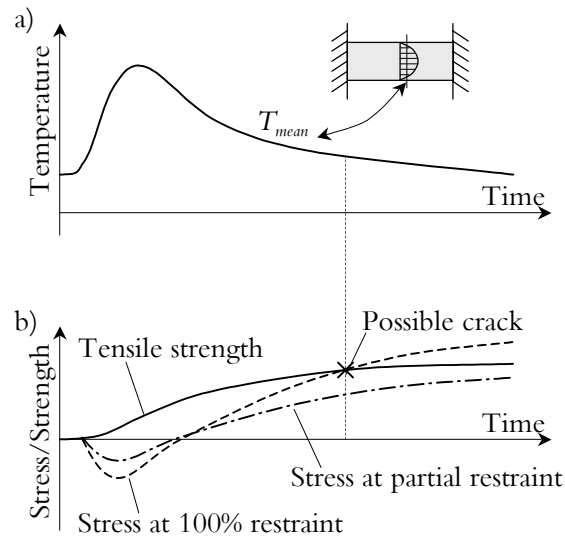
Figure 1 *Example of the a) mean temperature and b) stress and strength development in a hardening concrete element with partial restraint and total restraint (100%), respectively.*

The possible cracking of early age concrete structures can according to Bernander (1998) be divided into two groups, namely cracking during the expansion and during the contraction phases, respectively of which main features may be described as follows:

- Cracking during the expansion phase might occure both in the surfaces of elements and/or through the structural elements. Surface cracks in the expansion phase are induced in newly cast elements due to differences between internal movements within the elements. Through cracks in the expansion phase arise in older adjacent structural elements due to differences in movements between hydrating newly cast elements and the less or not at all hydrating older elements. Expansion phase cracks arise shortly after casting, within a few days, and tend to close by time. The influence by such cracks on the static capacity, the function and durability must be judged from case to case.
- Cracking during the contraction phase are usually in the shape of through cracks in newly cast elements. Depending on dimensions, environmental conditions etc. they might arise weeks, months and in extreme cases even years after casting. Cracks formed during the contraction phase are mostly through and lasting cracks, which are induced in the most recently cast elements due to the hindrance of the thermal movements from adjacent structural elements.

1.2   Crack risk estimations

The estimation of the risk of cracking of early age concrete structures can be based on five consecutive steps, see Figure 2. Firstly, the type of structure, the material proportions and possible measures to avoid cracks have to be chosen. Secondly, the temperature development has to be determined, either by calculations, diagrams/databases or by measurements. Thirdly, the restraint situation has to be determined, that is both the boundary and the structural restraint. Fourthly, structural calculation of the stress or strain ratios follows, i.e. the maximum tensile stress or strain is compared to the tensile strength or the ultimate strain capacity, respectively. Fifthly the crack risk design is based on partial coefficients, whose inverse the stress or strain ratios should not exceed. See e.g. Emborg & Bernander (1994), RILEM (1998), Rostásy et al. (2001) and Emborg et al. (2003) for a more thorough survey on the crack risk estimations.
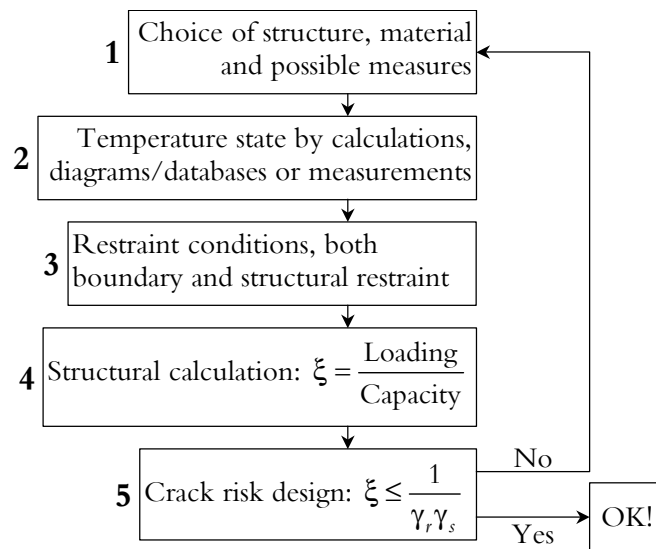
Figure 2 *Description of the principal steps in estimations of the risk of cracking in early age concrete structures. Nilsson (2000). ξ is the stress or strain ratio and $\gamma_r\gamma_s$ is the partial coefficient.*

The first step in Figure 2, *choice of structure, material and measures*, is the primary base of the outcome of estimations of risk of thermal cracking in early age concrete structures. Properly chosen type of structure and dimensions along with suitable mix design of the concrete are the foundation of the avoidance of cracking. In addition, possible measures such as cooling of hydrating parts, Bernander (1973 & 1998) and/or heating of adjacent older elements, see Wallin et al. (1997), might be required. In earlier days provision of movement joints, see e.g. Harrison (1981), and limitation of temperature differences within structures by use of low heat generating cement types, see Fagerlund (1985), composed commonly used measures. Combinations of several measures are in many situations necessary in order to avoid cracking.

4

The second step in Figure 2 comprises the *temperature development* during the hydration phase. It has to be determined either by finite element method calculations, see e.g. ConTeSt Pro (2003) and Kanstad et al. (2001), from diagrams/database, see Jonasson et al. (2001), from measurements in real structures, see Heimdal et al. (2001a & b), or by experiences from earlier cast similar structures.

As the third step, the *restraint condition* has to be determined, including the restraint within the studied structure elements, in the interface (joint) between parts of structures, from adjacent structural members and ground/rock. In Reinius (1945), ACI (1973, 1990 & 1995), Stoffers (1978) and Harrison (1981), the degree of restraint in base restrained walls is presented. In Emborg et al. (1997), several common cases of restraint conditions within structural elements are presented, and in e.g. Larson (1999 & 2000) the restraint from adjacent structures has been investigated. For determination of the degree of boundary restraint from adjacent ground material, several engineering models are reported in Rostásy et al. (1998) and (2001). Further, in e.g. Bernander (1993) and Nilsson (1998 & 2000) a method is presented for the determination of the degree of rotational boundary restraint, and Bernander (2001) also gives a method for the translational boundary restraint.

The determination of loading/capacity situation, step four in Figure 2, can be done by *structural calculations* e.g. by the finite element method according to ConTeSt Pro (2003) or JCI (1992). The loading/capacity situation can also be estimated by means of manual methods, see Reinius (1945), Löfquist (1946), Bernander (1982), Bernander & Emborg (1994), Emborg & Bernander (1994) and Larson (2000), or with help from diagrams/databases, e.g. through Emborg et al. (1997) and Jonasson et al. (2001).

Comparing the loading/capacity situation with stated partial coefficients for thermal cracking problems forms the final step in the *crack risk design*. The partial coefficients are given in design codes, e.g. BRO2002 (2002). The partial coefficients can be derived by probabilistic methods, see e.g. Cornell (1969), AK79/81 (1982), NKB87 (1987), Schneider (1997), and especially for thermal cracking problems, see Nilsson (2000) and Rostásy and Krauß (2002).

1.3   Identification of the problem

Improvement and development of new analyse tools in each of the steps in crack risk estimation according to Figure 2 are always important and necessary. The need of fast and reliable tools is of utmost importance.

One of the main issues is the estimation of the degree of restraint in a structure or a structural element, step 3 in Figure 2. Today, estimations are based either on time-consuming finite element method calculations or on more or less simplified engineering tools. Especially for the typical-case wall-on-slab, e.g. abutments and tunnel walls, the need is evident of faster and sufficiently accurate tools considering e.g. three-dimensional effects, effects of non-linearly varying strains and possible slip failure at the joints between walls and slabs.

The crack risk design of early age concrete structures, step 5 in Figure 2, should be based on partial coefficients, or their inverse safety-factors. The partial coefficients should be based on scientific basis. Since calculated stresses or strains are based on material data, geometric properties etc. that almost all are stochastic variables, the calculated stress or strain ratios must, by some probability, be lower than certain values. The crack safety values stated in the Swedish building code for bridges, BRO2002 (2002) are based on experiences and reasonable judgements. Therefore, the need for more scientifically determined partial coefficients is both important and necessary.

1.4 Aim and scope

The scope of this thesis focuses on the analysis steps 2 and 5 in Figure 2 above. The main objective is to simplify and improve crack risk estimations of early age concrete structures, by means of the determination of the degree of restraint and the determination of partial coefficients concerning analyses of cracking in early age concrete.

The aim of the work

- is to invent and derive a fast and reliable method for the determination of restraint factors affecting early age concrete structural elements, especially for the typical case wall-on-slab.

- is to calculate partial coefficients for thermal cracking of young concrete by use of a probabilistic method and to verify and form an opinion of the stated values in the Swedish building code for bridges, BRO94 (1999).

At the time when the work on partial coefficients was performed, the Swedish building code for bridges was given in BRO94 (1999), but at present, a newer version, BRO2002 (2002), is in use. However, the partial coefficients (named crack safety values) stated in both codes are the same.

2 Outline and Obtained Results

The thesis presented here is bases on four papers, Paper A, B, C and D. The first three papers deal with the determination and estimation of restraint factors used in crack risk analyses of early age concrete. The fourth and last paper deals with the determination of partial coefficients for crack risk estimations.

2.1 Determination of restraint factors (Paper A, B and C)

2.1.1 Derivation of a semi-analytical method – Paper A

The restraint in young concrete structures is one of the most crucial parameters in crack risk analyses. Without accurate tools for estimation of the restraint, crack risk analyses and design of possible crack-avoiding measures will not be reliable.

By the Compensation Plane theory, see e.g. JCI (1992) and Rostásy et al. (1998), a fairly simple and accurate semi-analytical model have been derived for the determination of restraint variations in early age concrete structures built by one young element cast on an older one. The model is derived under the assumption of uniformly distributed elastic thermal deformation and shrinkage in each section. The formulation depends on the geometric properties of the young and the old sections, the modulus of elasticity, the boundary restraint (both translational and rotational), a factor taking into account possible slip failure in joints and finally on a factor for high wall effects completed with correction factors dependent on the degree of boundary restraint.

Two simple and applicable expressions are further developed from the general formulation of the model for the restraint determination in typical-case wall-on-slab. The first equation applies to structures in which plane sections remain plane, in which no slip failure takes place in the joint between the wall and the slab, and in which the boundary restraint is zero. The second equation takes into account possible slip failure in the joint between the wall and the slab as well as high wall effects, that is, resilience. For cases subjected to some degree of boundary restraint, more sophisticated methods are necessary, see below regarding Paper B.

The derived and presented model is a further development of methods for restraint determination for totally base restrained walls, see e.g. ACI (1973, 1990 & 1995), Stoffers (1978) and Emborg (1989).

Paper A is written by Martin Nilsson, Jan-Erik Jonasson, Mats Emborg, Kjell Wallin and Lennart Elfgren. Martin Nilsson's contribution to the paper is the derivation and calibration of the model, determination and calculation of the new adjustment tools and finally writing the paper and drawing all the figures.

2.1.2 *Verification and calibration of the semi-analytical method – Paper B*

The special formulations of the semi-analytical model for wall-on-slab structures are not applicable without verification and calibration to some reference restraint variations. Therefore, the wall-on-slab formulation is calibrated and adjusted by use of 2920 elastic three-dimensional finite element method calculations. Necessary adjustment tools are determined and presented in order to achieve good correlation with the FEM calculations. The adjustment tools consist of the effective width of slab, effects of relative location of walls on slabs, high wall effects - resilience, effects of possible slip failure in joints, the degree of boundary restraint, and, finally, on basic resilience corrections factors for boundary restraint.

The calculation of restraint variations by the semi-analytical method is both simple and fast. By adjustments to the FEM calculations, the method gives reasonable accurate results for practically all cases that usually need analyses.

For the case of no boundary restraint, any wall-on-slab structure is fast and easily calculated by the semi-analytical method. This case covers the very most of the interesting ones in practical applications. For structures subjected to some degree of boundary restraint, the application of the concept of basic resilience correction factors works properly for length to height ratios larger than a certain, easy to calculate limit. For shorter structures subjected to some degree of boundary restraint the method does not work properly. However, such structures are rare, in the reality. Anyway, shorter structures might be regarded, on the safe side, as if the limit situation is fulfilled. This situation will be analysed more thoroughly in the future.

Paper B is written by Martin Nilsson, Jan-Erik Jonasson, Mats Emborg, Kjell Wallin and Lennart Elfgren. Martin Nilsson's contribution to the paper is the derivation and calibration of the model and determination and calculation of the new adjustment tools and finally writing the paper and drawing all the figures.

2.1.3 *Restraint coefficients in thermal stress analysis – Paper C*

For a full-scale field casting, see Heimdal et al. (2001a & b), the restraint and thermal stress development have been determined by means of evaluating measured strains and temperatures from a field-test. By use of simple elastic and more realistic viscoelastic material approaches in the thermal stress models used, respectively, the early age stresses of the structure is estimated theoretically and compared.

It is thus shown that the complex structural restraint behaviour can be described by means of restraint coefficients giving an agreeing thermal stress development compared to both more exact finite element method calculations and measured stresses in a full-scale structure. The restraint coefficients are in the stress calculation applied as a direct reduction of the fixation stress during both expansion and contraction phase of a hardening concrete structural element.

Paper C is written by Mårten Larson, Martin Nilsson and Jan-Erik Jonasson. Martin Nilsson's contribution to the paper is calculation of the restraint coefficients by the semi-analytical method and in that context writing the belonging text and drawing some of the figures.

2.2   Determination of partial coefficients

2.2.1   Determination of partial coefficients by a probabilistic method – Paper D

The risk of thermal cracking in young concrete structures is commonly estimated as the ratio between the calculated maximum tensile stress and the actual tensile strength. Alternatively, the ratio between the calculated maximum tensile strain and the actual tensile strain capacity is used. If a determined ratio is smaller than certain values, a structure is assumed to fulfil the requirements for avoiding thermal cracking.

Depending on the effects of cracking and the accuracy in determining material properties the Swedish building codes for bridges, BRO94 (1999), states different values of the risk of cracking.

Partial coefficients for cracking problems in early age concrete have been determined by a probabilistic method and compared to the values in BRO94 (1999). The values calculated by the probabilistic method coincide well with the values stated in the BRO94 (1999). However, the values obtained are based on many assumptions and simplifications and they shall not be seen as the final proposal. Additional judgements, research and calculations are needed.

Paper D is written by Martin Nilsson and Lennart Elfgren. Martin Nilsson's contribution to the paper is the modelling including finding necessary input and calculation of all partial coefficients and finally writing the paper and drawing all the figures.

3 Suggestions for Future Research

3.1 The semi-analytical method for restraint

The method presented is adjusted and calibrated to elastic 3D FEM calculations. However, the method should be compared to more real restraint variations determined from full-scale tests and/or reliable FEM calculations using the models for hydrating concrete, by means of viscoelastic behaviour, maturing etc.

The derived semi-analytical method has a limit in application not being able to be used for short structures for non-zero boundary restraint situations. Therefore, there is a need for future development of a method covering this area.

The models suggested for determination of the adjustment tools can always be improved by better models or by increasing the data behind the models.

An area that certainly needs theoretical and experimental research is foundation of concrete structures on rock. Important task is how the boundary restraint should be regarded and how interlocking and fracture zone in rock does influence the restraint in newly cast concrete elements.

3.2 Partial coefficients

The calculated partial coefficients for thermal cracking problems determined by the probabilistic method are based on many assumptions and simplifications. Data regarding the coefficient of variation for e.g. the concrete strength, the accuracy in the methods estimating the thermal stresses etc. should be more thoroughly investigated. Further, the determination does not include all possible parameters affecting the risk of cracking. However, the more parameters that are included in the model, the more complicated expressions will be the result.

References

ACI (1973). Effect of Restraint, Volume Change, and Reinforcement on Cracking of Massive Concrete. ACI Committee 207. ACI Journal / July 1973. Title No. 70-45. pp. 445-470.

ACI (1990). Effect of Restraint, Volume Change, and Reinforcement on Cracking of Massive Concrete. ACI Committee 207. ACI Materials Journal / May-June 1990. Title No. 87-M31. pp. 271-295.

ACI Committee 207 (1995). Effect of Restraint, Volume Change, and Reinforcement on Cracking of Massive Concrete. ACI Committee 207. ACI 207.2R-95.

AK79/81 (1982). *Allmänna regler för bärande konstruktioner. Principer, rekommendationer och kommentarer samt exempel på tillämpning.* (General Regulations for Structures. Principles, Recomendations, Comments and Examples of Application). Stockholm, Sweden: Statens Planverk, Rapport nr 50, Liber 1982, pp. 159. ISBN 91-38-07090-1. (In Swedish).

Bernander, S (1973). Cooling by Means of Embedded Cooling Pipes. Applications in Connection with the Construction of the Tingstad Tunnel, Göteborg. *Nordisk Betong, n:o 2-73.* pp. 21-31. (In Swedish).

Bernander, S (1982). Temperature Stresses in Early Age Concrete Due to Hydration. In: *Proceedings from International Conference on Concrete at Early Ages, RILEM, held in Paris, France on 6-8 April 1982.* Vol II. pp. 218-221.

Bernander, S (1993). *Balk på elastiskt underlag åverkad av ändmoment M_1* (Beam on Resilient Ground Loaded by Bending End Moments M_1). Göteborg, Sweden: ConGeo AB. Notes and calculations with diagrams. (In Swedish).

Bernander, S (1998). Practical Measures to Avoiding Early Age Thermal Cracking in Concrete Structures. In: *Prevention of Thermal Cracking in Concrete at Early Ages.* Ed. by

Springenschmidt, R. London, UK: E & FN Spon. RILEM Report 15. pp. 255-314. ISBN 0-419-22310-X.

Bernander, S (2001). *Analysis of Deformations in an Elastic Halfspace due to Horisontal Loading*. Göteborg, Sweden: Con-Geo AB. Notes and calculations with diagrams. pp. 47.

Bernander, S & Emborg, M (1994). Temperaturförhållanden och sprickbegränsning i grova betongkonstruktioner (Temperature conditions and crack limitation in mass concrete structures). In: *Betonghandbok − Arbetsutförande, projektering och byggande* (Concrete Handbook − Performance, projecting and building). Solna, Sweden: AB Svensk Byggtjänst. pp. 639-666. ISBN: 91-7332-586-4.

BRO94 (1994). *Bro 94. Allmän teknisk beskrivning för broar, 9. Förteckning.* (General Technical Description for Bridges, 9. Catalogue). Borlänge, Sweden: Swedish National Road Administration. Publ. 1999:20. pp. 139. ISSN: 1401-9612. (In Swedish).

BRO 2002 (2002). *Bro 2002. Allmän teknisk beskrivning för broar, 4 Betongkonstruktioner.* (General Technical Description for Bridges, 4. Concrete structures). Borlänge, Sweden: Swedish National Road Administration. (In Swedish).

Carlson, R W (1937). Drying Shrinkage of Large Concrete Members. In: *ACI Journal, Proceedings V. 33,* No. 3, Jan.-Feb. 1937, pp. 327–336.

Cederwall, K, Elfgre, L & Losberg, A (1970). Prestressed Concrete Columns under Long-Time Loading. In: *Symposium on the Design of Concrete Structures for Creep, Shrinkage and Temperature Changes, Madrid 1970.* IABSE Reports or Working Commissions, Volume 5, International Association for Bridge and Structural Engineering, Zürich 1970. pp. 181–189.

CCEAC 2000 (2002). *Proceedings of the International Workshop on Control of Cracking in Early Age Concrete, Sendai, Japan Aug. 23-24 2000.* Ed. by H. Mihashi & F. Wittmann. Lisse, the Netherlands: Swets & Zeitlinger. ISBN: 90 5809 506 1. pp. 399.

ConTeSt Pro (2003). *Users manual - Program for Temperature and Stress Calculations in Concrete*. Developed by JEJMS Concrete AB in co-operation with Luleå University of Technology, Cementa AB and Peab AB. Luleå, Sweden: Luleå University of Technology. (In progress May 2003).

Cornell, C A (1969). A probability-based structural code. In: *ACI Journal, Vol. 66*, pp. 974-985.

Ekerfors, K (1995). *Mognadsutveckling i ung betong. Temperaturkänslighet, hållfasthet och värmeutveckling.* (Maturity Development in Young Concrete. Temperature Sensitivity, Strength and Heat Development). Luleå, Sweden: Division of Structural Engineering, Luleå University of Technology. Licentiate Thesis 1995:34L. pp. 136.

References

Emborg, M (1985). *Thermal Stresses in Massive Concrete Structures. Viscoelastic Models and Laboratory Tests.* Luleå, Sweden: Luleå University of Technology, Division of Structural Engineering. Litentiate Thesis 1985:011 L. pp. 163. ISSN: 0280-8242.

Emborg, M (1989). *Thermal Stresses in Concrete Structures at Early Ages.* Luleå, Sweden: Luleå University of Technology, Division of Structural Engineering. Doctoral Thesis 1989:73D. pp. 285.

Emborg, M & Bernander, S (1994). Thermal stresses computed by a method for manual calculation. In: *Proceedings of the International RILEM Symposium on Thermal Cracking in Concrete at Early Ages.* Munich, Germany, Oct. 10-12 1994. London, England: E & FN Spon. RILEM Proceedings 25. pp. 321-328. ISBN: 0 419 18710 3.

Emborg, M, Bernander, S, Ekefors, K, Groth, P & Hedlund, H (1997). *Temperatursprickor i betongkonstruktioner - Beräkningsmetoder för hydratationsspänningar och diagram för några vanliga typfall* (Temperature Cracks in Concrete Structures – Calculation Methods for Hydration Stresses and Diagrams for some Common Typical Examples). Luleå, Sweden: Luleå University of Technology. Technical Report 1997:02. 100 pp. ISSN 1402-1536. (In Swedish).

Emborg, M, Bernander, S, Jonasson, J-E & Nilsson, M (2003). Avoidance of Early Age Cracking – Principles and Recommendations. Luleå, Sweden: Luleå University of Technology, Division of Structural Engineering. IPACS-report BE96-3843/2003:xx, ISBN-91-89580-80-X.

Fagerlund, G (1985). *Flytande kväve kyler betong.* (Liquid Nitrogen cools concrete). Danderyd, Sweden: Cementa AB. Cementa nr 2, 1985. pp 16-19.

Fagerlund, G (1992). *Betongkonstruktioners beständighet, en översikt.* (Durability of Concrete Structures, an outline). Danderyd, Sweden: Cementa AB. pp. 101. ISBN: 91-87334-00-3.

Fagerlund, G (1994). Betongkonstruktioners beständighet och livslängd. Kapitel 20 i Betonghandbok Material (Red.av Christer Ljungkrantz, Göran Möller och Nils Petersons), utgåva 2, svensk byggtjänst och Cementa, Stockholm 1994, sid 711-726.

Groth, P (1996). *Cracking in Concrete. Crack prevention with air-cooling and crack distribution with steel fibre reinforcement.* Luleå, Sweden: Luleå University of Technology, Division of Structural Engineering. Litentiate Thesis 1996:37 L. 126 pp. ISSN: 0280-8242.

Harrison, T. A. (1981). *Early-age thermal crack control in concrete.* London, England: CIRIA, Construction Industry Research and Information Association. Report 91. ISSN: 0305-408X. ISBN: 0 86017 166 3. pp. 48.

Hedlund, H (1996). *Stresses in High Performance Concrete due to Temperature and Moisture variations at Early Ages.* Luleå, Sweden: Luleå University of Technology, Division of Structural Engineering. Litentiate Thesis 1996:38 L. 240 pp. ISSN: 0280-8242.

Hedlund, H (2000). *Hardening Concrete. Measurements and evaluation of non-elastic deformation and associated restraint stresses.* Luleå, Sweden: Luleå University of Technology, Division of Structural Engineering. Doctoral Thesis 2000:25. 394 pp. ISBN: 91-89580-00-1.

Heimdal, E, Kanstad, T & Kompen, R (2001a). *Maridal Culvert, Norway - Field test I.* Luleå, Sweden: Luleå University of Technology, Department of Civil and Mining Engineering. IPACS–report BE96-3843/2001:73-7. pp. 69. ISBN 91-89580–73–7.

Heimdal, E, Kanstad, T & Kompen, R (2001b). *Maridal Culvert, Norway - Field test II.* Luleå, Sweden: Luleå University of Technology, Department of Civil and Mining Engineering. IPACS–report BE96-3843/2001:74-5. pp. 20. ISBN 91-89580–74–5.

JCI (1992). *A Proposal of a Method of Calculating Crack Width due to Thermal Stress* (1992). Tokyo, Japan: Japan Concrete Institute, Committee on Thermal Stress of Massive Concrete Structures. JCI Committee Report. pp. 106.

Jonasson, J-E (1994). *Modelling of Temperature, Moisture and Stresses in Young Concrete.* Luleå, Sweden: Luleå University of Technology, Division of Structural Engineering. Doctoral Thesis 1994:153 D. ISSN: 0348-8373. pp. 225.

Jonasson, J-E, Wallin, K, Emborg, M, Gram, A, Saleh, I, Nilsson, M, Larson, M & Hedlund, H (2001). *Temperatursprickor i betongkonstruktioner − Handbok med diagram för sprickriskbedömning inclusive åtgärder för några vanliga typfall. Del D och E.* (Temperature cracks in concrete structures − Handbook with diagrams for crack risk judgement including measures for som typical cases. Part D and E). Luleå, Sweden: Division of Structural Engineering, Luleå University of Technology, Technical Report 2001:14. ISSN: 1402-1536, ISRN: LTU − TR − 01/14 − SE.

Kanstad, T, Bosnjak, D & Øverli, J A (2001). *3D Restraint Analyses of Typical Structures with Early Age Cracking Problems.* Luleå, Sweden: Luleå University of Technology, Department of Civil and Mining Engineering. IPACS–report BE96-3843/2001:32-X. ISBN 91-89580-32-X. pp. 27.

Larson, M (1999). *Evaluation of Restraint from Adjoining Structures.* Luleå, Sweden: Luleå University of Technology, Department of Civil and Mining Engineering. IPACS–report BE96-3843/2001:57-5. ISBN 91-89580–57–5. pp. 23.

Larson, M (2000). *Estimation of Crack Risk in Early Age Concrete.* Luleå, Sweden: Luleå University of Technology, Division of Structural Engineering. Licentiate Thesis 2000:10. pp. 170.

Löfqvist, Bertil (1946). *Temperatureffekter i hårdnande betong* (Temperature Effects in Hardening Concrete). Stockholm, Sweden: Royal Hydro Power Administration. Technical Bulletins, Serie B, No 22. pp. 195. (In Swedish).

Nilsson, M (1998). *Inverkan av tvång i gjutfogar och i betongkonstruktioner på elastiskt underlag* (Influence of Restraint in Casting Joints and in Concrete Structures on Elastic

References

Foundation). Luleå, Sweden: Luleå University of Technology, Division of Structural Engineering. Master Thesis 1998:090 CIV. pp. 61. (In Swedish).

Nilsson, M (2000). Thermal Cracking of Young Concrete – Partial Coefficients, Restraint Effects and Influence of Casting Joints. Luleå, Sweden: Luleå University of Technology, Division of Structural Engineering. Licentiate Thesis 2000:27. pp. 267. http://epubl.luth.se/1402-1757/2000/27/LTU-LIC-0027-SE.pdf

NKB87 (1987). *Retningslinier for last- og sikkerhetsbestemmelser for baerende konstruktioner* (Guiding Rules for Loads and Safety Regulations for Structures). NKB-rapport nr. 55. 107+55 pp. ISBN 87-503-6991-1, ISSN 0359-9981. (In Swedish).

Reinius, Erling (1945). Temperatur- och krympspänningar i betongskivor, som stå på fast underlag. (Temperature and shrinkage stresses in concrete plates that stand on solid foundation). In: *Betong, Svenska betongföreningens tidsskrift. Årg. 30, H. 1*. pp. 20. (In Swedish).

RILEM (1998). *Prevention of Thermal Cracking in Concrete at Early Ages*. Ed. by R. Springenschmid. London, England: E & FN Spon. RILEM Report 15. State-of-the Art Report by RILEM Technical Committee 119, Avoidance of Thermal Cracking in Concrete at Early Ages. pp. 348. ISBN: 0 419 22310 X.

Rostásy, F S & Krauß, M (2002). Effects of stress–strain relationship and relaxation on restraint, stress and crack formation in young concrete members. In: *Proceedings of the International Workshop on Control of Cracking in Early Age Concrete, Sendai, Japan Aug. 23-24 2000*. Ed. by H. Mihashi & F. Wittmann. Lisse, the Netherlands: Swets & Zeitlinger. pp. 305-316. ISBN: 90 5809 506 1.

Rostásy, F S, Budelmann, H, Flender, E & Krauß, M (2001). *Proceeding of the seminar on Rissbeherrschung massiger Betonbauteile: Bauwerk, Werkstoff, Simulation, Braunschweig, Germany, Mar. 20 2001*. ISBN: 3-89288-132-4, ISSN 1439-3875. pp. 152.

Rostásy, F S, Tanabe, T & Laube, M (1998). Assessment of External Restraint. In: *Prevention of Thermal Cracking in Concrete at Early Ages*. Ed. by R. Springenschmid. London, England: E & FN Spon. RILEM Report 15. State-of-the Art Report by RILEM Technical Committee 119, Avoidance of Thermal Cracking in Concrete at Early Ages. pp. 149-177. ISBN: 0 419 22310 X.

Rostásy, F, S, Gutsch, A–W & Krauß, M (2001). *Engineering models for the assessment of restraint of slabs by soil and in piles in the early age of concrete*. Luleå, Sweden: Luleå University of Technology, Department of Civil and Mining Engineering. IPACS-report BE96-3843/2001:59-1. ISBN 91-89580-59-1. pp. 135.

Schneider, J (1997). Introduction to Safety and Reliability of Structures. In: *Structural Engineering Documents, 5*. Zürich: IABSE, International Association for Bridges and Structural Engineering. 138 pp.

Stoffers, H (1978). Cracking due to Shrinkage and Temperature Variations in Walls. *Heron, vol. 23, no. 23*. pp. 5-68.

Wallin, K, Emborg, M & Jonasson, J-E (1997). *Värme ett alternativ till kyla* (Heat an alternative to cold). Luleå, Sweden: Luleå University of Technology, Division of Structural Engineering. Technical Report 1997:15. pp. 168. (In Swedish).

Westman, G (1995). *Thermal Cracking in High Performance Concrete. Viscoelastic models and laboratory tests*. Luleå, Sweden: Luleå University of Technology, Division of Structural Engineering. Litentiate Thesis 1995:27 L. pp. 120. ISSN: 0280-8242.

Westman, G (1999). *Concrete Creep and Thermal Stresses – New Creep models and their Effects on Stress Development*. Luleå, Sweden: Luleå University of Technology, Division of Structural Engineering. Doctoral Thesis 1999:10. ISSN: 1402-1544. pp. 301.

Paper A

Determination of Restraint in Early Age Concrete Walls on Slabs by a Semi-Analytical Method
Paper 1 Theory and Derivation

By

Martin Nilsson

Jan-Erik Jonasson

Mats Emborg

Kjell Wallin

Lennart Elfgren

Paper A

Determination of Restraint in Early Age Concrete Walls on Slabs by a Semi-Analytical Method – Paper 1 Theory and Derivation

By Martin Nilsson, Jan–Erik Jonasson, Mats Emborg, Kjell Wallin and Lennart Elfgren

M.Sc. Eng. and Tech. Lic. Martin Nilsson is a PhD-student in Structural Engineering at Luleå University of Technology, Sweden. His field of research is structural behaviour of young concrete structures.

Tech. Dr. Jan-Erik Jonasson is a Senior Lecturer and Assistant Professor in Structural Engineering at Luleå University of Technology, Sweden. His research speciality is modelling of thermal and moisture conditions and associated structural behaviour of concrete structures.

Tech. Dr. Mats Emborg is partly a Senior Lecturer and Assistant Professor in Structural Engineering at Luleå University of Technology, Sweden, partly Research and Development Manager at Betongindustri AB, Sweden. His research speciality is behaviour of fresh and hardening concrete including self-compacting concrete with and without fibre reinforcement.

Mr. Kjell Wallin is technical adviser in concrete with many years of experience of practical work at the Swedish contractor Peab. He is also a Research Engineer in Structural Engineering at Luleå University of Technology, Sweden. His research speciality is thermal cracking and self compacting concrete.

Tech. Dr. Professor Lennart Elfgren is Head of Division of Structural Engineering at Luleå University of Technology, Sweden. His research specialities include fracture mechanics, fatigue, fasteners, and combined bending, shear and torsion.

ABSTRACT

The restraint situation in early age concrete structures is one of the crucial factors in thermal crack analyses at early ages. Therefore, the accuracy in the determination of the restraint is of utmost importance. A semi-analytical method has been derived for the determination of the restraint variation in early age concrete structures. The method is derived using the Compensation Plane method according to the linear elastic theory. The model depends on the geometry of the structure, the Young's modulus of the structural elements, the boundary restraint situation, and the location of the newly cast concrete element on the old element. The model is further developed for the typical case wall on slab. Straightforward and simple expressions are derived for the restraint variation in the wall. In the model, effects of high walls are regarded in form of deformations in the wall when its base is completely restrained. The model is further supplemented with effects of possible slip failure at the joint between the young and the old concrete. The concept of effective width of the slab is introduced in the method as the only model parameter for correlation with about 3000 3D elastic FEM calculations. The decisive point for maximum tensile stresses, and at where the restraint should be determined, is briefly described and discussed.

This paper forms the first part of two papers presenting and describing the semi-analytical method for restraint determination. This part, Paper 1, deals with the derivation and general descriptions of the method. In the second part, Paper 2 by Nilsson et al. (2003), the method is firstly verified and adjusted to the FEM calculations and secondly its application and necessary adjustment tools are determined and presented.

Keywords: restraint; early age concrete; mass concrete; cracking; resilience; joint slip; wall on slab.

1   INTRODUCTION

It is well known for contractors that due to volume changes in concrete structures large stresses can arise if the movements of the structures are restrained. These restraint stresses can be so large that they may cause extensive cracking, which give rise to expensive repair and reduce both the durability and the function of the structures. Therefore, today hardly any contractors overlook the effects of these early age stresses. Still, and too often, newly cast concrete structures crack at many building sites.

Large resources are put into modern building to predict the restraint stresses and the risk of cracking, and to design appropriate counter-measures to avoid possible cracking. The measures, including safety limits, should be designed in the early production-planning phase. However, if the conditions are changed for the actual casting, e.g. the air and/or the concrete temperatures change, a new crack risk analysis is needed. Nevertheless, there is a need of fast and reliable tools to realize the analyses, especially if the conditions are changed very late in the building process. Unfortunately, sometimes the

analysis tools and/or models are too simplified, which introduce uncertainties in the results, an on the opposite, the tools can also be too complicated and time consuming.

As been indicated, one important part of every tool is to predict the degree of restraint and, consequently, the restraint calculation should neither be too simplified nor too complicated. In this paper an elastic and fairly simple model is presented for the determination of the restraint in newly cast concrete structural elements on existing ones and especially for the typical case wall on slab.

1.1 Early age cracking

During the hydration phase of a concrete structure, the chemical reaction between the cement and the water in the concrete generates heat. Due to this heat, young structural elements undergo temperature histories similar to what is shown in Figure 1a). During the heating phase, the structural elements expand and later when the chemical reaction subsides, the concrete starts to contract when the heat development decreases and the temperature starts to adjust to the surroundings. Meanwhile the concrete matures and its strength increases, see Figure 1b). In addition, for high performance concretes (low water-to-cement ratios) significant autogenous shrinkage is present in the same time as the thermal movements take place.

The volume changes during the hydration phase can be hindered by adjoining structures, foundations or by internal parts not undergoing the same volume changes. This hindrance induces restraint stresses that may be so large that cracks possibly occur if the stresses are larger than the tensile strength of the concrete, see Figure 1b).
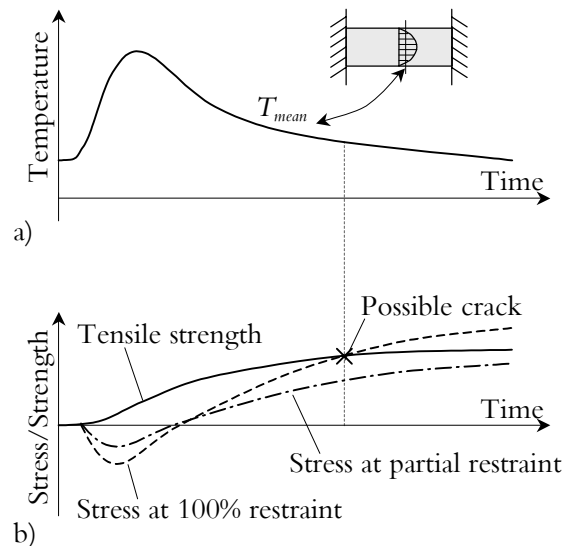

Figure 1 *Example of the a) mean temperature and b) stress and strength development in a hardening concrete element restrained at partial and totally (100 % degree).*

The possible cracking of early age concrete structures can be divided into two groups, namely cracking during the expansion and during the contraction phases, respectively.

- Cracking during the expansion phase might happen both in the surface and/or through the structural elements. Surface cracks in the expansion phase are induced in newly cast elements due to differences between the internal movements within the elements, and through cracks expansion phase can be found in adjacent structural elements due to the difference in movements between the different elements. Expansion phase cracks arise shortly after casting, within a few days, and tend to close by time. The influence by such cracks on the static capacity, the function and durability most be judged from case to case.

- Cracking during the contraction phase are usually in the shape of through cracks in newly cast elements. Depending on dimensions, environmental conditions etc. they might arise weeks, months and in extreme cases even years after casting. Cracks formed during the contraction phase are mostly through and lasting cracks, which are induced in the most recently cast elements due to the hindrance of the thermal movements from adjacent structural elements.

1.2   Crack risk estimations

The estimation of the risk of cracking of early age concrete structures can be based on five steps, see Figure 2. Firstly, the type of structure, the material proportions and possible measures to avoid cracks have to be chosen. Secondly, the temperature development has to be determined, either by calculations, diagrams/databases or by measurements. Thirdly, the restraint situation has to be determined, that is both the boundary and the structural restraint. Fourthly, structural calculation of the stress or strain ratios follows, i.e. the maximum tensile stress or strain is compared to the tensile strength or the ultimate strain capacity, respectively. Fifthly the crack risk design is based on so-called crack safety factors, the partial coefficients, which the stress or strain ratios should not exceed. Recommendations and guidelines regarding this whole process can be found in e.g. Emborg & Bernander (1994a) and Emborg et al. (2003).
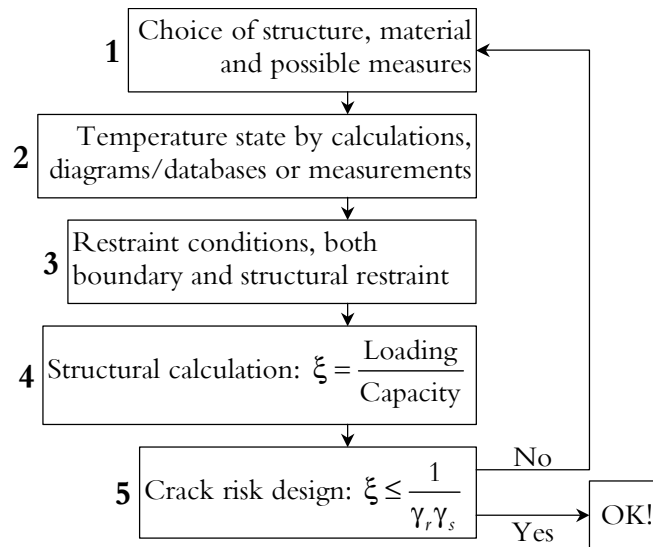
Figure 2 *Description of the principal steps in estimations of the risk of cracking in early age concrete structures. Nilsson (2000).*

The first step in Figure 2, *choice of structure, material and measures*, is the primary base of the estimation of risk of thermal cracking in early age concrete structures. Properly chosen type of structure and dimensions along with suitable mix design of the concrete is the foundation of the avoidance of cracking. In addition, possible measures such as cooling of hydrating parts, Bernander (1973 & 1998) and/or heating of adjacent older parts, e.g. see Wallin et al. (1997), might be required. The second step in Figure 2 comprises the *temperature development* during the hydration phase. It has to be determined either by calculations, see e.g. Jonasson et al. (1994) and ConTeSt Pro (2003), from diagrams/database, see Jonasson et al. (2001), or from measurements in real structures. From the temperature development, the stress and strength growth are obtained. As the third step, the *restraint condition* has to be determined, including the restraint within the studied structure, in the interface (joint) between parts of structures, from adjacent structural members and ground/rock. In Emborg et al. (1997), several common cases of internal restraint situations are presented, and in e.g. Larson (1999 & 2000) the restraint from adjacent structures has been investigated. In Rostásy et al. (2001) several engineering models are reported for the assessment of boundary restraint in the phases of pre-design and design and execution. For the rotational bending restraint from adjacent ground materials, e.g. in Bernander (1993) and Nilsson (1998 & 2000), methods for the determination of the boundary restraint coefficient are given. The determination of the stress/strength or strain/ultimate-strain situation, step four in Figure 2, can be done by *structural calculations*, e.g. with ConTeSt Pro (2003) or JCI (1992), by manual methods, see Löfquist (1946), Bernander (1982), Bernander & Emborg (1994), Emborg & Bernander (1994b) and Larson (2000), or with help from diagrams/databases, e.g. through Emborg et al. (1997). Comparing the stress/strength or

strain/ultimate-strain situations with stated partial coefficients for thermal cracking problems forms the final step in the *crack risk design*. The partial coefficients - or crack safety factors - are given in design codes, e.g. BRO 2002 (2002). The partial coefficients can be derived by probabilistic methods, see Nilsson (2000) and Nilsson & Elfgren (2003).

Below, a semi-analytical elastic model will be presented for the determination of the restraint in early age concrete walls cast on older slabs (step 3 in Figure 2). The model is derived using the Compensation Plane theory, see JCI (1992) and Rostásy et al. (1998), meaning plane sections remain plane after deformation in the structural analysis. The model is supplemented with the effects of high walls and the effects of possible slip failure in the joint between the young and the old concrete. In this paper only the derivation of the model will be presented as well as general descriptions of the parts included in the model. In the second paper, Paper 2 by Nilsson et al. (2003), the model is fitted to about 3000 three-dimensional elastic FEM calculations, deeper descriptions are given, and models and engineering tools for each part in the model are introduced and discussed. The approach presented in this paper is a modelling with respect to the effects of high walls as only the deformations in the wall are taken into consideration as in ACI (1973, 1990 & 1995), Stoffers (1978) and Emborg (1989).

2   THE SEMI-ANALYTICAL METHOD

As been described and visualised in Figure 2, one of the crucial factors in the estimation of the risk of early age cracking is the determination of the degree of restraint affecting a concrete structure. The restraint can be described as the hindrance of the free movements of young concrete structural elements or parts of elements during the hydration phase. If such elements or parts of elements are totally free to deform, when they are exposed to thermal induced movements and/or shrinkage, no restraint stresses will arise. On the opposite, if newly cast structural elements or parts of elements are hindered to move by adjacent sections or stiff foundation materials, different degrees of restraint stresses arise. E.g. in tunnel walls concreted on foundations and in walls on foundation slabs restraint stresses arise. The degree of restraint can be determined in different ways: e.g. by field measuring of actual strains in real structures and comparing them to the strain at total fixation, see Heimdal et al. (2001a & b) and Larson et al. (2003). It can also be determined by finite element method calculations, see e.g. JCI (1992) and Kanstad et al. (2001), or other more or less sophisticated theoretical models.

Below, a semi-analytical method will be presented that can be used as a fairly simple engineering tool adaptable in many situations. The model is presented both as a general formulation and as an applicable approach for the typical case wall on slab.

Generally, the restraint in a young concrete structural part, γ_R, can be defined as the quota between the principal stress at the studied time, σ_1, and the stress, σ^0, at total

26

fixation ($\varepsilon \equiv 0$) by volume changes in the young concrete (shrinkage and thermal strains):

$$\gamma_R = \frac{\sigma_1}{\sigma^0} \tag{1}$$

Based on Eq. (1) with the use of the Compensation Plane theory, see Appendix A, the degree of restraint in the length direction of a structure can be expressed as

$$\gamma_R = \delta_{res}\delta_{slip} - \gamma_R^t - \gamma_R^{r y} - \gamma_R^{y z} \tag{2}$$

where

δ_{res}	=	high wall effect, resilience, [–]
δ_{slip}	=	slip in joint effect, [–]
$\gamma_R{}^t$	=	translational restraint part, [–]
$\gamma_R{}^{r y}$	=	rotational restraint part for rotation around the y-axis (the vertical axis), [–]
$\gamma_R{}^{r z}$	=	rotational restraint part for rotation around the z-axis (the horizontal, transverse axis), [–]

Restraint determined by the semi–analytical model in Eq. (2) depends partly on effects of high walls in which the strains in the young parts do not vary linearly, partly on possible slip failure in the joint between the young and the old concrete, partly on three restraint parts, $\gamma_R{}^t$, $\gamma_R{}^{r y}$ and $\gamma_R{}^{r z}$, determined by the geometric properties of the structures as well as the boundary restraint situation from the adjacent foundation material. The first part of Eq. (2), $\delta_{res}\delta_{slip}$, forms the semi part of the method due to non-linear behaviour in high-wall structures, see below and Nilsson et al. (2003). The second part, $-\gamma_R{}^t-\gamma_R{}^{r y}-\gamma_R{}^{r z}$, forms the analytical part based on the Compensation Plane theory. The method includes adaptation to about 3000 3D elastic FEM calculations presented in Nilsson et al. (2003),

2.1 General formulation

A general expression is derived for the determination of the restraint variation in an early age concrete part cast on an older one, see also Appendix A. The derivation is based on the Compensation Plane theory (compare beam analysis) and uses an approach for pre-stressed concrete beams, see Collins & Mitchell (1991). Under assumption of uniform and elastic contraction in the whole young element and in the older element, respectively, the restraint variation can be described by

$$\gamma_R = \delta_{res}\delta_{slip} - (1 - \gamma_{RT})\frac{N_{RI}}{\Delta\varepsilon_c^0 \zeta E_{c28}A_{trans}}$$

$$-(1 - \gamma_{RR,y})\frac{M_{RI,y}(z_{cen} - z)}{\Delta\varepsilon_c^0 \zeta E_{c28}I_{trans,y}} - (1 - \gamma_{RR,z})\frac{M_{RI,z}(y_{cen} - y)}{\Delta\varepsilon_c^0 \zeta E_{c28}I_{trans,z}}$$

(3)

where

N_{RI}	=	compression force giving zero translational strain in the young concrete, [N]
$\Delta\varepsilon_c^0$	=	strain of applied volume changes in the young concrete (shrinkage and temperature induced strain), [-]
ζE_{c28}	=	modulus of elasticity of the young concrete at the studied time, [N/m^2]
A_{trans}	=	transformed area of the cross section, [m^2]
$M_{RI,y}$	=	internal bending moment around the y-axis for obtaining zero curvature in the xz-plane of the young concrete, [Nm]
$M_{RI,z}$	=	internal bending moment around the z-axis for obtaining zero curvature in the xy-plane of the young concrete, [Nm]
y_{cen}	=	vertical location of the centroid of the transformed section relatively the joint, [m]
y	=	vertical co-ordinate from the joint and up-wards, [m]
z_{cen}	=	horizontal location of the centroid of the transformed section relatively the centre of the slab, [m]
z	=	horizontal co-ordinate from the centre of the slab, [m]
$I_{trans,y}$	=	transformed second moment of inertia of the cross section for bending around the y-axis, [m^4]
$I_{trans,z}$	=	transformed second moment of inertia of the cross section for bending around the z-axis, [m^4]
γ_{RT}	=	translational boundary restraint, [-]
$\gamma_{RR,y}$	=	rotational boundary restraint for bending around the y-axis, [-]
$\gamma_{RR,z}$	=	rotational boundary restraint for bending around the z-axis, [-]

Note that this formulation is quite similar to the well-known Navier's formula for beam analyses.

The modulus of elasticity of the young concrete is expressed as a factor ζ times the 28-days value of the elasticity. This factor is introduced in order to take into account that most often cracking of young concrete (through cracks in the cooling phase) takes place fairly late in the hydration process but, for ordinary sized structures, not as late as at 28 days of maturity. In Larson (2000) a small study of the factor ζ was presented giving that $\zeta = 0.93$ is a good estimation of the somewhat lower stiffness of the young concrete during the contraction phase.

For simplicity at application, Eq. (3) is transformed to, see Appendix A,

$$\gamma_R = \delta_{res}\delta_{slip} - (1-\gamma_{RT})\frac{\delta_{slip}\int_{A_c}\delta_{res}dA_c + \frac{E_{a28}}{\zeta E_{c28}}\lambda\int_{A_{a,eff}}dA_{a,eff}}{\int_{A_c}dA_c + \frac{E_{a28}}{\zeta E_{c28}}\int_{A_{a,eff}}dA_{a,eff}}$$

$$-(1-\gamma_{RR,y})(z_{cen}-z)\frac{\delta_{slip}\int_{A_c}z'dA_c + \frac{E_{a28}}{\zeta E_{c28}}\lambda\int_{A_{a,eff}}z'dA_{a,eff}}{\int_{A_c}z'^2\,dA_c + \frac{E_{a28}}{\zeta E_{c28}}\int_{A_{a,eff}}z'^2\,dA_{a,eff}}$$

$$-(1-\gamma_{RR,z})(y_{cen}-y)\frac{\delta_{slip}\int_{A_c}\delta_{res}y'dA_c + \frac{E_{a28}}{\zeta E_{c28}}\lambda\int_{A_{a,eff}}y'dA_{a,eff}}{\int_{A_c}y'^2dA_c + \frac{E_{a28}}{\zeta E_{c28}}\int_{A_{a,eff}}y'^2dA_{a,eff}}$$

(4)

where

A_c = cross-section area of the young concrete, [m^2]

E_{a28} = 28 days modulus of elasticity of the adjacent older concrete, [N/m^2]

λ = factor describing the volume change in the old concrete relatively the volume change in the young concrete, $\lambda = \Delta\varepsilon_a^0/\Delta\varepsilon_c^0$, [–]

$A_{a,eff}$ = effective cross-section area of the adjacent older concrete, [m^2] (se subsection 2.6 and Paper 2 by Nilsson et al. (2003) for the meaning of the term effective)

y' = internal vertical lever arm to the total centroid for each part, [m]

As can be seen in Eqs. (3) and (4), the restraint variation depends on the cross-section areas of the structure, the geometric properties of the young part (high wall effects meaning non-linearly varying strain), possible slip failure in the joint between the young and the old parts, the modulus of elasticity of the young and the older concrete, and the translational and rotational boundary restraint situation from the foundation material, see Figure 3 for a brief description.
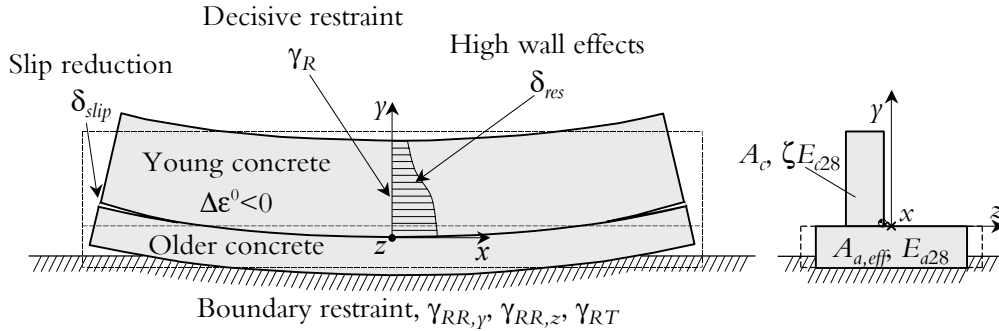
Figure 3 *Brief description of the including parts in the model for determination of the restraint variation.*

2.2   Effects of high walls

In not all early age concrete structures, the strains over the height of the young parts vary linearly during the deformation. In structures with low length to height ratios the strains vary non-linearly, which here is defined as effects of high walls. This means that plane sections do not remain plane under deformation and that a simple application of the Compensation Plane theory does not hold properly. In order to take into account the non-linearity so-called resilience functions can be used for the determination of the strain variations and thereby the restraint. The resilience is here based on a basic resilience factor that applies for fully base restrained walls, that is $\gamma_{RT} = \gamma_{RR,z} = 1$. The rotational boundary restraint for rotation around the vertical y-axis is without any further investigations in this model considered being zero, $\gamma_{RR,y} = 0$. For other base restraint situations than $\gamma_{RT} = \gamma_{RR,z} = 1$, resilience correction factors are used, see subsection 2.2.2. Basic resilience factors for fully base restrained walls have previously been presented in e.g. ACI (1973), Figure 4a), and Emborg (1989), Figure 4b).

The resilience factor is here determined as

$$\delta_{res} = \delta_{res}^0 \delta_{transl} \delta_{rot} \tag{5}$$

where

δ_{res}^0	=	basic resilience factor, [-]
δ_{transl}	=	resilience correction factor for translational boundary restraint, [-]
δ_{rot}	=	resilience correction factor for rotational boundary restraint, [-]

2.2.1 Basic resilience factors

High wall effects, basic resilience, referrer to structures with low length to height ratio and that are totally restrained at the base. In accordance with the presentation in Figure

4, the basic resilience is applicable for structures with length to height ratio smaller than e.g. about ten, $L/H_c < 10$, in Figure 4a), or about seven, $L/H_c < 7$, in Figure 4b).
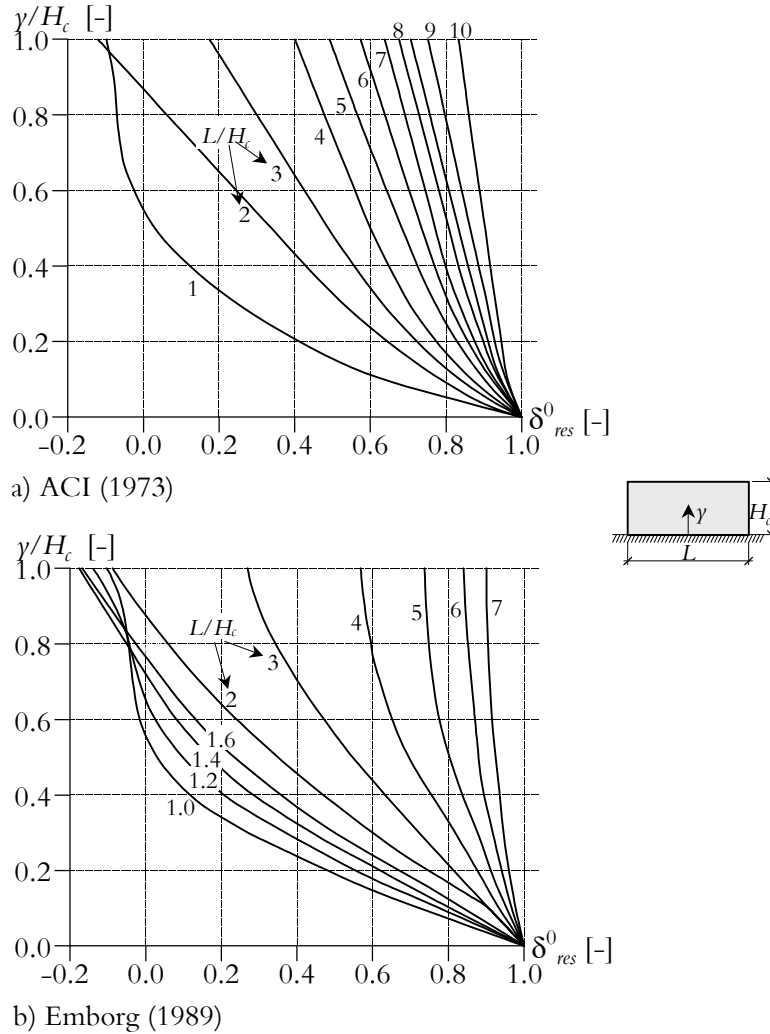
Figure 4 *Basic resilience factor δ^0_{res} at different distance from the base as function of the length to height ratio. Modified from a) ACI (1973) and b) Emborg (1989).*

The basic resilience curves in Figure 4a) originate from test data according to ACI (1973) whereas the curves in Figure 4b) where determined by elastic two-dimensional FEM calculations. The curves for $L/H_c > 2$ in Figure 4a) suggest "more" resilience than the curves in Figure 4b), which means that by using the basic resilience curves according to Figure 4b), higher restraint values will be obtained and thereby higher crack risks than by the curves in Figure 4a). Probably this is an effect of that the ACI-curves

are partly based on measurements, while the curves according to Emborg (1989) are calculated with a theoretically completely restrained wall base. For the moment the exact background for the ACI-curves has not been able to study thoroughly.

Since an analytical way of describing the resilience functions is needed here together with a more wide range of the length to height ratios L/H_c (<1 and >7, respectively), the curves from Emborg (1989) are here used as a base and are completed with more FEM calculations. Then all resulting curves are fitted to a polynomial function expressed as, see Paper 2 by Nilsson et al. (2003),

$$\delta_{res}^0 = \sum_{i=0}^{n} a_i \left(\frac{\gamma}{H_c} \right)^i \tag{6}$$

2.2.2 Resilience correction factors

The resilience correction factors are introduced, as been indicated above in Eq. (5), for cases in which the boundary restraint is not total. They are determined as

$$\delta_{transl} = \gamma_{RT} + \left(1 - \gamma_{RT}\right)\delta_{transl}^0$$
$$\delta_{rot} = \gamma_{RR,z} + \left(1 - \gamma_{RR,z}\right)\delta_{rot}^0 \tag{7}$$

where δ_{transl}^0 and δ_{rot}^0 are basic resilience correction factors for translation and rotation, respectively. See Paper 2 by Nilsson et al. (2003) for more details on the determination of the basic correction factors. Eq. (7) in Eq. (5) gives

$$\delta_{res} = \delta_{res}^0 \left(\gamma_{RT} + \left(1 - \gamma_{RT}\right)\delta_{transl}^0 \right)\left(\gamma_{RR,z} + \left(1 - \gamma_{RR,z}\right)\delta_{rot}^0 \right) \tag{8}$$

For case of free translation and free rotation, that is no boundary restraint $\gamma_{RT} = \gamma_{RR,z} = 0$, Eq. (8) becomes

$$\delta_{res} = \delta_{res}^0 \delta_{transl}^0 \delta_{rot}^0 \tag{9}$$

For no boundary restraint the 3D effect is considered only by introducing an effective width of the slab, $B_{a,eff}$, which means that formally $\delta_{transl}^0 \delta_{rot}^0 \equiv 1$ in this case. So, the basic resilience correction factor for rotation is determined as the inverse of the basic resilience correction factor for translation by

$$\delta_{rot}^0 = \frac{1}{\delta_{transl}^0} \tag{10}$$

This relation is used in the determination of the basic correction factor for bending, see Nilsson et al. (2003).

In Figure 5 the principles of the resilience correction factors are presented. The figure is drawn for a point above the joint in a structure where $\delta^0_{transl} < 1$ and consequently $\delta^0_{rot} > 1$, see Eq. (10). In another point of the structure the opposite situation might occur, i.e. $\delta^0_{transl} > 1$ and $\delta^0_{rot} < 1$. For $\gamma_{RT} = 0$ free translation prevails, and $\gamma_{RT} = 1$ means no translation, and for $\gamma_{RR,z} = 0$ a structure is free to rotate and for $\gamma_{RR,z} = 1$ no rotation prevails. When $\gamma_{RT} = 0$ and $\gamma_{RR,z} = 1$ structures are subjected to pure translation, and the opposite, for $\gamma_{RT} = 1$ and $\gamma_{RR,z} = 0$ only pure rotation is possible. For other values of γ_{RT} and $\gamma_{RR,z}$ the resilience correction factors are determined according to the lines between free and no translation and free and no rotation, respectively.

FEM calculations are used, see Paper 2 by Nilsson et al. (2003), for evaluation of the points at $\gamma_{RR,z} = 0$ and $\gamma_{RR,z} = 1$ at free translation ($\gamma_{RT} = 0$) yielding the resilience correction factor δ^0_{transl} (left part of Figure 5). With the prerequisite that $\delta^0_{transl}\delta^0_{rot} \equiv 1$ the corresponding value of δ^0_{rot} is obtained (the point where $\gamma_{RT} = \gamma_{RR,z} = 0$ in the right part of Figure 5). Interpolation along the lines is then possible which saves enormous amounts of calculations when establishing the model of resilience correction factors.
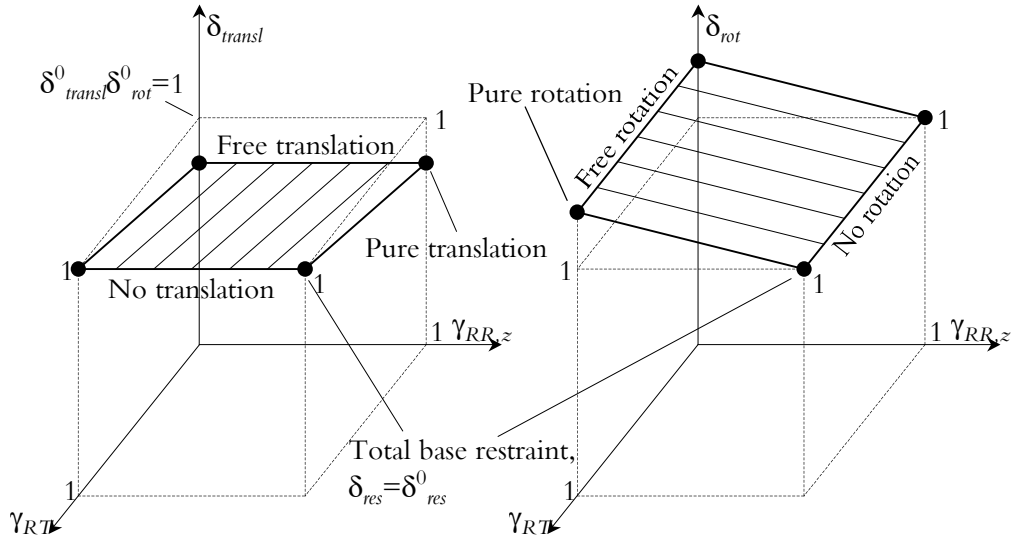

Figure 5 *Model description of resilience correction factors dependent on the boundary restraint situation.*

For symmetrical structures (no rotation around the γ-axis) subjected to total base restraint, $\gamma_{RT} = \gamma_{RR,z} = 1$, no correction is needed and the restraint is determined only by the basic resilience factor according to, Eqs. (4) and (8) with $\gamma_{RT} = \gamma_{RR,z} = 1$,

$$\gamma_R = \delta_{res}^0 \delta_{slip} \tag{11}$$

which also is shown in Figure 5 in the corners of the cubes where $\gamma_{RT} = \gamma_{RR,z} = \delta_{transl} = 1$ and $\gamma_{RT} = \gamma_{RR,z} = \delta_{rot} = 1$.

2.3 Effects of slip failure in joints

The restraint situation and thereby the cracking risk during the cooling phase of the young concrete depends to a large extent on the connecting joints between the young and the old parts. In Figure 6, the stress distribution before and after a possible slip failure in the joint is briefly described in a wall on a slab during the cooling phase. If a joint is very strong and contains a large amount of through reinforcement it is capable to transfer large restraining forces from the older part, Figure 6a), implying high horizontal stresses in the mid-section of the structure as well as high vertical and shear stresses at the ends of the joint. On the opposite, see Figure 6b), if the joint is weaker and does not contain much trough reinforcement, slip failure is possible and thereby the stresses in the mid-section and in the ends of the joint are reduced and consequently the risk of cracking. In longer structures, effects of possible slip failure in joints are not as obvious as in shorter structures since the middle parts of such structures do not respond to stress changes at the ends of the joints.

Due to the difficulty in knowing whether a joint will crack or not, decisions regarding possible measures as cooling of walls and heating of slabs will be quite uncertain. However, if a slip failure in a joint is predictable, a considerable amount of money can be saved. A predicted slip failure in a joint can be regarded as a controlled form of cracking and thereby a kind of measure, which is preferable compared to un-controlled cracking somewhere else in the young concrete. The usage of joint sealers and injection hoses in the joints are fairly simple measures to avoid leakage through any cracked joint.

Today the knowledge about the behaviour of the joints between young and older parts is limited. It is hard to determine how large forces that are transferred across a joint and to determine if any slip failure will occur. However, in Nilsson et al. (1999) and Nilsson (2000) three medium-scale tests of wall on slab cases are presented where slip failures where detected. It was found that failures start at the ends of the joints and progress in small steps towards the centre of the walls. The steps correspond to the distance between the reinforcement going through the joint from the slab to the wall. Further, in Bernander (2001) it is shown by basic classic theory of elasticity that for the typical case wall on slab for reasonable structure lengths the occurrence of slip failure in the joint is possible and probable.
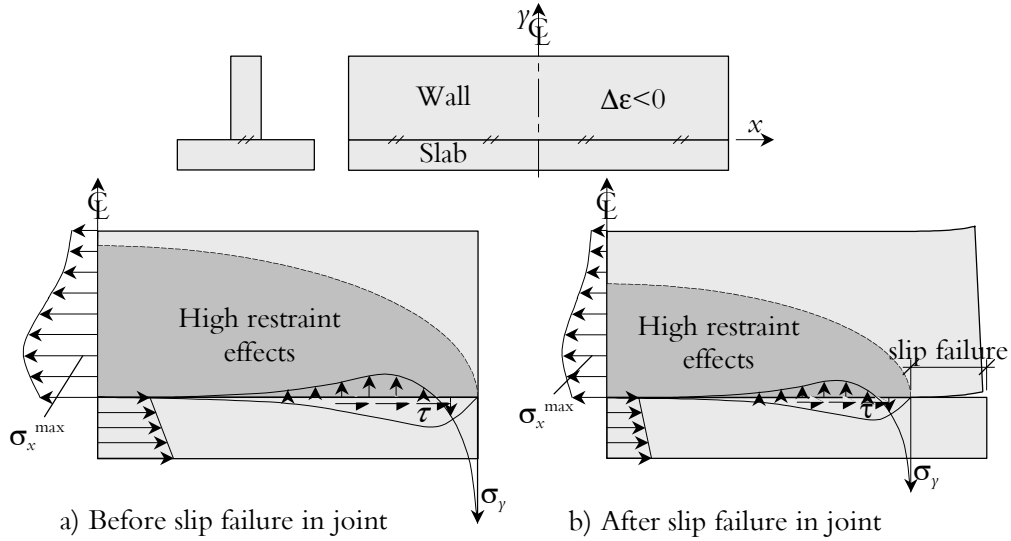
Figure 6 Principal description of the stresses in a structure a) before and b) after a possible slip failure in a joint. Nilsson (2000). By possible slip failure in the joint the horizontal stresses in the mid-section are reduced as well as the vertical and shear stresses in the end of the joint.

The effects of possible slip failure in joints are regarded by the slip failure factor δ_{slip}. This factor are smaller than 1 and therefore reduces the restraint values, see Eq. (4). For more details about values of the slip failure factor, see Nilsson et al. (2003) and Con-TeSt Pro (2003).

2.4 Applicable expressions

The model presented above in Eq. (4) is general and applies to any structure with a younger structural element cast on an older. For the case of a rectangular wall cast on a rectangular slab, simple, straightforward and sufficiently accurate semi-analytical expression can be derived, see Appendix A.

A simpler application of the semi-analytical model is derived if no volume change takes place in the slab, if slip failure in the joint is negligible, if plane sections remain plane (no effects of high walls), and if no translational nor rotational boundary restraint is present, $\gamma_{RT} = \gamma_{RR,x} = \gamma_{RR,y} = 0$. Then the expression for the determination of the restraint variation is changed from a semi-analytical expression to an analytical expression. That is, it is simplified to an expression exactly fulfilling the Compensation Plane method according to the linear elastic theory along the centre of the wall. The expression reads

$$\gamma_R = 1 - \cfrac{1}{1 + \cfrac{E_{a28}}{\zeta E_{c28}} \cfrac{A_{a,eff}}{A_c}}$$

$$- \cfrac{(\gamma_{cen} - \gamma)\left(\gamma_{cen} - \cfrac{H_c}{2}\right)}{\cfrac{H_c^2}{12} + \left(\gamma_{cen} - \cfrac{H_c}{2}\right)^2 + \cfrac{E_{a28}}{\zeta E_{c28}} \cfrac{A_{a,eff}}{A_c}\left(\cfrac{H_a^2}{12} + \left(\gamma_{cen} + \cfrac{H_a}{2}\right)^2\right)}$$

$$- \cfrac{\left(z_{cen} - \omega\cfrac{B_{a,eff} - B_c}{2}\right)^2}{\cfrac{B_c^2}{12} + \left(z_{cen} - \omega\cfrac{B_{a,eff} - B_c}{2}\right)^2 + \cfrac{E_{a28}}{\zeta E_{c28}} \cfrac{A_{a,eff}}{A_c}\left(\cfrac{B_{a,eff}^2}{12} + z_{cen}^2\right)}$$

$$\tag{12}$$

where

H_c	=	height of wall, [m]
H_a	=	height of slab, [m]
B_c	=	width of wall, [m]
$B_{a,eff}$	=	effective width of slab, [m]

ω is a coefficient describing the location of the wall on the slab in the z-direction. If $\omega = 0$, the wall is located in the middle of the slab, if $\omega = \pm1$, the wall is located at one of the sides of the slab, and for other values of ω the wall is located somewhere between the middle and the sides of the slab, see Figure A.9. ω is determined as

$$\omega = \frac{2u}{B_a - B_c} \tag{13}$$

where u is the real horizontal distance in the z-direction between the centre of the slab and the centre of the wall, [m].

Another situation, somewhat more complicated compared to above, is present when slip failure in the joint is possible and if sections do not remain plane under deformation (high wall effects), then the restraint in the wall is determined as, see Appendix A,

$$\gamma_R = \delta_{slip} \sum_{i=0}^{n} a_i \left(\frac{\gamma}{H_c}\right)^i - \delta_{slip} \frac{\displaystyle\sum_{i=0}^{n} \frac{a_i}{i+1}}{1 + \dfrac{E_{a28}}{\zeta E_{c28}} \dfrac{B_{a,eff} H_a}{B_c H_c}}$$

$$-\delta_{slip} \frac{(\gamma_{cen} - \gamma)\left(\gamma_{cen} \displaystyle\sum_{i=0}^{n} \frac{a_i}{i+1} - H_c \displaystyle\sum_{i=0}^{n} \frac{a_i}{i+2}\right)}{\dfrac{H_c^2}{12} + \left(\gamma_{cen} - \dfrac{H_c}{2}\right)^2 + \dfrac{E_{a28}}{\zeta E_{c28}} \dfrac{B_{a,eff} H_a}{B_c H_c} \left(\dfrac{H_a^2}{12} + \left(\gamma_{cen} + \dfrac{H_a}{2}\right)^2\right)} \qquad (14)$$

$$-\delta_{slip} \frac{\left(z_{cen} - \omega\dfrac{B_{a,eff} - B_c}{2}\right)^2}{\dfrac{B_c^2}{12} + \left(z_{cen} - \omega\dfrac{B_{a,eff} - B_c}{2}\right)^2 + \dfrac{E_{a28}}{\zeta E_{c28}} \dfrac{B_{a,eff} H_a}{B_c H_c} \left(\dfrac{B_{a,eff}^2}{12} + z_{cen}^2\right)}$$

A more comprehensive application formulation of the semi-analytical model is found if the boundary restraint may vary. In such cases, the resilience factor has to be determined according to Eq. (8) with the resilience correction factors. These factors can be determined from elastic FEM calculations with a method presented in Paper 2, see Nilsson et al. (2003). The determination of the resilience correction factors in its formulation is quite simple but due to mathematical/numerical reasons, limitations in the modelling arise.

2.5 Boundary restraint

As been introduced earlier, the boundary restraint is divided into one translational part and two rotational parts. The foundation material adjacent to deforming early age concrete structures restrains the free movements of the structures. Depending on the type of foundation material, the degree of compaction, different modulus of the subgrade and the geometry of the body resting on the ground etc., the boundary restraint varies.

The free translation of a structure is counteracted by the friction and/or cohesion properties of the foundation material. A low friction and/or low-cohesive foundation material gives almost no resistance to the free translation, which means that the translational boundary restraint is almost zero, $\gamma_{RT} \approx 0$.

The bending moment during the cooling phase tends to rotate the ends of structures upward and the centre parts downward. The stiffness of the foundation material prescribes how much a structure may bend down into the ground. A soft material offers almost no resistance to the free deformation of the structure, implying non or very little rotational bending restraint, $\gamma_{RR,z} \approx 0$. On the contrary, a structure that is founded on a stiff ground, for example rock or dense gravel, can hardly bend at all, that is, the rotational boundary restraint is about 100 percent, $\gamma_{RR,z} \approx 1$. If the stiffness of the founda-

tion material is high and/or the structure is relatively long, the structure rotates anyhow but lifts at its ends and rests on the ground only at intermediate parts of the structure. This lifting of the ends is hindered by the dead weight of the structure, see Nilsson (2000).

For structures founded on blasted rock, the restraint situation is much more complex. Interlocking between the concrete and the rock and influence from existing crack zones in the rock, determination of the degree of restraint is complicated. However, preliminary studies of the restraint from rock are given in Olofsson et al. (2001).

The axial force $\gamma_{RT}N_{RI}$ and the bending moments $\gamma_{RR,y}M_{RI,y}$ and $\gamma_{RR,z}M_{RI,z}$ in Eq. (3) are caused by the restraint/counteraction from adjacent older concrete members and/or more or less elastic foundations on the free movements of young concrete structures. The amount of translation and/or rotation depends partly on the length of the structures, partly on the friction and/or cohesion properties and stiffness of the foundation material. Methods for determination of the amount of boundary restraint can be found in Pettersson (1998), Rostásy et al. (2001) and Bernander (2001) and for the rotational boundary restraint an elastic approach can be found in Bernander (1993) and Nilsson (2000), see also Nilsson et al. (2003).

2.6   Effective width of slab

For a relatively thin and low wall cast on a very wide slab, it is obvious that not the whole width of the slab influences the movements of the wall. In such cases, only a certain part of the slab − here defined as the effective width − is active and should be used in the determination of the restraint in the assumed model. In Nilsson (2000), a small study on the effective width was presented. It was found in some examples analysed by FEM that in order to obtain the same curvature at the bottom of the wall, the width of the slab used in the semi-analytical model had to be different than the real widths.

In the recently finished Brite-Euram Project IPACS (Improved Production of Advanced Concrete Structures), about 3000 elastic FEM calculations of the restraint variation in rectangular walls on slabs were performed, see Nilsson (2003). Within the present work, the results from these calculations have been used to determine the effective width of the slabs that is needed in the semi-analytical model, Eq. (4), in order to obtain the same restraint variation as in the FEM calculations. Furthermore, from these results a method for the determination of the effective width is developed for geometric properties different from the ones used in the FEM calculations, see Paper 2 by Nilsson et al. (2003).

2.7   Decisive point

The cracking risk has of cause to be estimated at the point in a structure where the origin of a crack is most probable. In elastic analyses of wall on slab cases, the highest values of the restraint are located at the bottom of the wall. However, this is not the loca-

tion of the most critical point in real structures. In a wall on slab structure, the heat condition is non-uniformly distributed over the height the wall, that is, the heat is lower at the top and bottom of the wall than in the middle. Therefore, the decisive point is not located at the bottom of the wall where some cooling from the slab is present. Hence, the most critical point is located somewhere above the joint, but the location varies from case to case. In many cases one wall thickness above the joint is a good estimation of the location of the decisive point for a crack risk analysis, see Olofsson et al. (2001) and Figure 7.
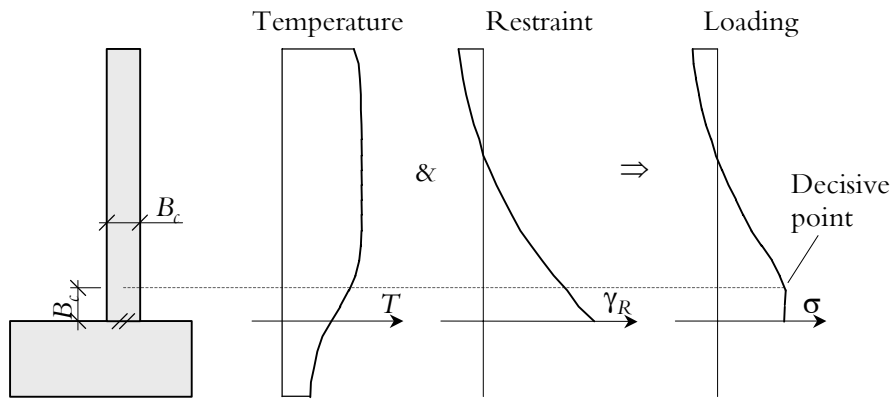
Figure 7 *Principle description of location of desicive point.*

3   EXAMPLE

By use of the two simple and applicable expressions presented above, Eqs. (12) and (14) , the restraint variation in the wall in Figure 8a) has been calculated and compared. Firstly, in the calculations the effective width of the slab is given the real value of the slab, Figure 8b). Secondly, the effective width in Eqs. (12) and (14) are given values according to the methodology presented in Nilsson et al. (2003), see Figure 8c) and d). The calculation with Eq. (12) does not depend on the length of the structure (Compensation Plane theory), which gives linearly varying restraint, Figure 8b) and d).

By Eq. (14) the length is an important parameter due to the high wall effects. The resilience factor depends on the length to height ratio, see Figure 4, in which it can be seen that with smaller length to height ratio the restraint varies more non-linearly. Further, the effective width of the slab also depends on the length of the structure, see Paper 2 by Nilsson et al. (2003).

In the diagrams of Figure 8 the final restraint variations determined by Eq. (14) for the different structural lengths are shown as well as the linear variation determined by Eq. (12). With increasing length, the restraint determined by Eq. (14) turns more and more into linear variation when the high wall effect subsides. Further, a comparison

between restraint determinations by the semi-analytical method presented in this paper and by evaluations of field measurements on a full-scale structure is presented in Larson et al. (2003).

L=10, 15, 25m

ω=0.655

B_c=0.65m

$$\frac{E_{a28}}{\zeta E_{c28}} = \frac{1}{0.93} = 1.075$$

0.65m

H_c=9m

H_a=1m

B_a=5m

a) Input

γ [m]

Linear variation

L=25m

L=15m

L=10m

γ_R

0

0.51 0.54   1

b) With and without high wall effects, $B_{a,eff} = B_a$

γ [m]

L=10m
$B_{a,eff}$=1.56m

L=25m
$B_{a,eff}$=3.50m

L=15m
$B_{a,eff}$=2.50m

0.65

γ_R

0   0.49 0.52   1
        0.51

c) High wall effects, $B_{a,eff} \neq B_a$

γ [m]

L=10m
$B_{a,eff}$=1.56m

L=15m
$B_{a,eff}$=2.50m

L=25m
$B_{a,eff}$=3.50m

0.65

γ_R

0   0.43 0.49   1
        0.47

d) No high wall effects, $B_{a,eff} \neq B_a$

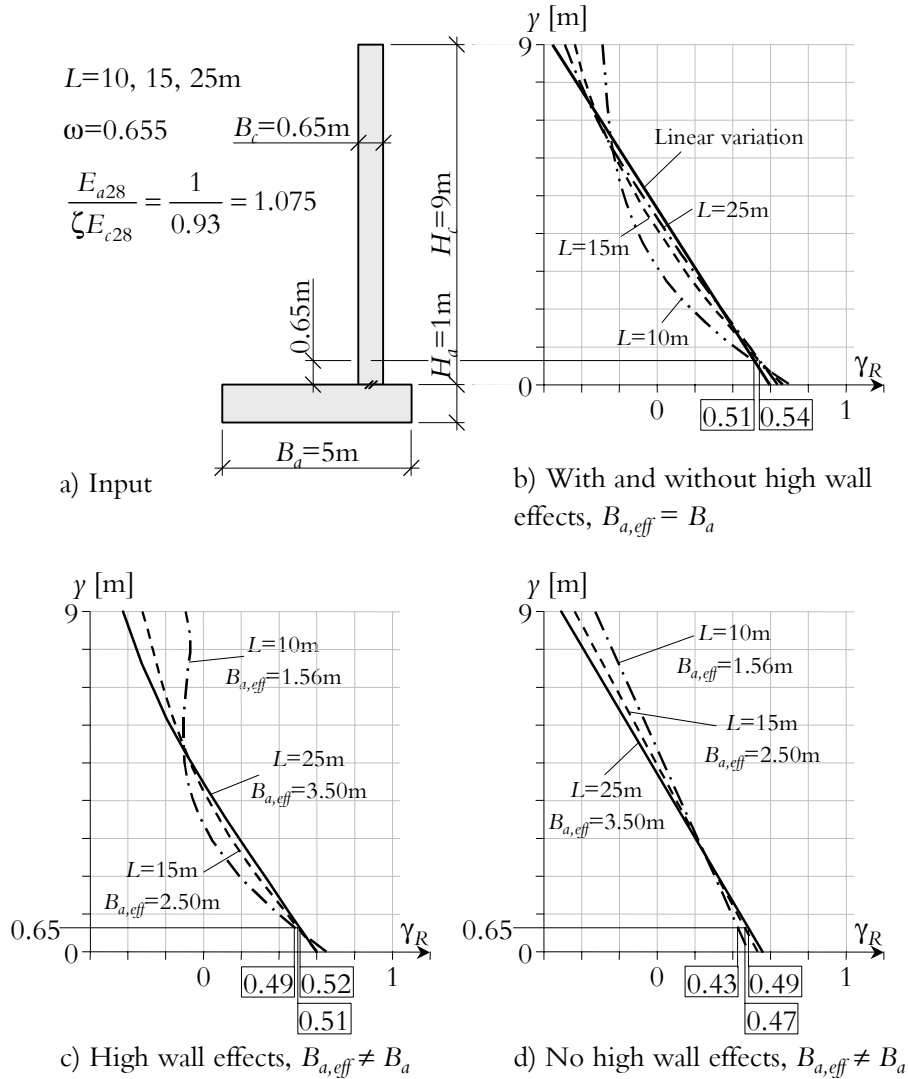**Figure 8** *Geometric properties and calculated restraint variations of wall on slab structure analysed in an example. Geometry from Kanstad et al. (2001).*

At one wall thickness above the joint, in this paper the default location of the decisive point, the restraint is found, Figure 8b), to be 0.51 for the linear variation by Eq. (12) and 0.51, 0.54 and 0.54 for L = 10, 15 and 25 m by Eq. (14) with $B_{a,eff} = B_a$, re-

spectively. By use of the effective width of slab, see paper 2 by Nilsson et al. (2003), the restraint values are found to be lower in this example. If high wall effects are included the differences by using the effective width are not so large, 4–6 %, but with no high wall effects the differences increase to 16, 8 and 4 % for $L = 10$, 15 and 25 m, respectively. Further, if the decisive point is located higher in the wall the difference will be larger, especially for shorter structures or for structures with higher walls.

4   SUMMARY AND CONCLUSIONS

The restraint in young concrete structures is one of the most crucial parameters in crack risk analyses. Without any accurate tools for estimation of the restraint, crack risk analyses and design of possible crack-avoiding measures will not be reliable.

By the Compensation Plane theory, a fairly simple and accurate semi-analytical model have been derived for the determination of the restraint variation in early age concrete structures built by one young section cast on an older one. The expression is derived under the assumption of uniformly distributed elastic thermal deformation and shrinkage in each part, respectively. The expression depends on the geometric properties of the young and the old sections, the modulus of elasticity, the boundary restraint (both translational and rotational), a factor taking into account effects of possible slip failure in joints and finally on a factor for high wall effects.

The model has been calibrated to about 3000 three-dimensional elastic finite element calculations with the introduction of the effective width of slab as the only model parameter, see Paper 2 by Nilsson et al. (2003).

Two simple and applicable expressions are developed from the general formulation of the model for the restraint determination in typical-case wall on slab. The first expression applies to structures in which plane sections remain plane, in which no slip failure takes place in the joint between the wall and the slab, and in which the boundary restraint is zero. The second expression takes into account possible slip failure in the joint between the wall and the slab as well as high wall effects, that is, resilience. For other boundary restraint situations more sophisticated methods are necessary, see Paper 2 by Nilsson et al. (2003).

5   ACKNOWLEDGEMENTS

6 REFERENCES

ACI (1973). Effect of Restraint, Volume Change, and Reinforcement on Cracking of Massive Concrete. ACI Committee 207. *ACI Journal / July 1973. Title No. 70-45.* pp. 445-470.

ACI (1990). Effect of Restraint, Volume Change, and Reinforcement on Cracking of Massive Concrete. ACI Committee 207. *ACI Materials Journal / May-June 1990. Title No. 87-M31.* pp. 271-295.

ACI Committee 207 (1995). Effect of Restraint, Volume Change, and Reinforcement on Cracking of Massive Concrete. ACI Committee 207. *ACI 207.2R-95.*

Bernander, S (1973). Cooling by Means of Embedded Cooling Pipes. Applications in Connection with the Construction of the Tingstad Tunnel, Göteborg. *Nordisk Betong, n:o 2-73.* pp. 21-31. (In Swedish).

Bernander, S (1982). Temperature Stresses in Early Age Concrete Due to Hydration. In: *Proceedings from International Conference on Concrete at Early Ages, RILEM, held in Paris, France on 6-8 April 1982.* Vol II. pp. 218-221.

Bernander, S (1993). *Balk på elastiskt underlag åverkad av ändmoment M_1* (Beam on Resilient Ground Loaded by Bending End Moments M_1). Göteborg, Sweden: ConGeo AB. Notes and calculations with diagrams. (In Swedish).

Bernander, S (1998). Practical Measures to Avoiding Early Age Thermal Cracking in Concrete Structures. In: *Prevention of Thermal Cracking in Concrete at Early Ages.* Ed. by Springenschmidt, R. London, UK: E & FN Spon. RILEM Report 15. pp. 255-314. ISBN 0-419-22310-X.

Bernander, S (2001). *Analysis of Deformations in an Elastic Halfspace due to Horisontal Loading.* Göteborg, Sweden: Con-Geo AB. Notes and calculations with diagrams. pp. 47.

Bernander, S & Emborg, M (1994). Temperaturförhållanden och sprickbegränsning i grova betongkonstruktioner (Temperature conditions and crack limitation in mass concrete structures). In: *Betonghandbok – Arbetsutförande, projektering och byggande* (Concrete Handbook – Performance, projecting and building). Solna, Sweden: AB Svensk Byggtjänst. pp. 639-666. ISBN: 91-7332-586-4.

BRO 2002 (2002). *Bro 2002. Allmän teknisk beskrivning för broar, 4 Betongkonstruktioner.* (General Technical Description for Bridges, 4. Concrete structures). Borlänge, Sweden: Swedish National Road Administration. (In Swedish).

Collins, M, P & Mitchell, D (1991). *Prestressed Concrete Structures.* Englewood Cliffs, New Jersey, U.S.A.: Prentice-Hall Inc. pp. 766. ISBN 0-13-691635-X.

ConTeSt Pro (2003). *Users manual - Program for Temperature and Stress Calculations in Concrete.* Developed by JEJMS Concrete AB in co-operation with Luleå University of

Paper A

Technology, Cementa AB and Peab AB. Luleå, Sweden: Luleå University of Technology. (In progress May 2003).

Emborg, M & Bernander, S (1994a). Assessment of the Risk of Thermal Cracking in Hardening Concrete. In: *Journal of Structural Engineering (ASCE), Vol 120, No 10, October 1994.* New York, U.S.A. pp. 2893-2912.

Emborg, M & Bernander, S (1994b). Thermal stresses computed by a method for manual calculation. In: *Proceedings of the International RILEM Symposium on Thermal Cracking in Concrete at Early Ages.* Munich, Germany, Oct. 10-12 1994. London, England: E & FN Spon. RILEM Proceedings 25. pp. 321-328. ISBN: 0 419 18710 3.

Emborg, M (1989). Thermal Stresses in Concrete Structures at Early Ages. Luleå, Sweden: Division of Structural Engineering, Luleå University of Technology. Doctoral Thesis 1989:73D. pp. 285.

Emborg, M, Bernander, S, Ekefors, K, Groth, P & Hedlund, H (1997). *Temperatursprickor i betongkonstruktioner - Beräkningsmetoder för hydratationsspänningar och diagram för några vanliga typfall* (Temperature Cracks in Concrete Structures – Calculation Methods for Hydration Stresses and Diagrams for some Common Typical Examples). Luleå, Sweden: Luleå University of Technology. Technical Report 1997:02. 100 pp. ISSN 1402-1536. (In Swedish).

Emborg, M, Bernander, S, Jonasson, J-E & Nilsson M (2003). *Avoidance of early age cracking - principles and recommendations.* Luleå, Sweden: Luleå University of Technology, Department of Civil and Mining Engineering. IPACS Report. pp. ISBN-91-89580-80-X. (In progress).

Heimdal, E, Kanstad, T & Kompen, R (2001a). *Maridal Culvert, Norway - Field test I.* Luleå, Sweden: Luleå University of Technology, Department of Civil and Mining Engineering. IPACS-report BE96-3843/2001:73-7. pp. 69. ISBN 91-89580–73–7.

Heimdal, E, Kanstad, T & Kompen, R (2001b). *Maridal Culvert, Norway - Field test II.* Luleå, Sweden: Luleå University of Technology, Department of Civil and Mining Engineering. IPACS-report BE96-3843/2001:74-5. pp. 20. ISBN 91-89580–74–5.

JCI (1992). *A Proposal of a Method of Calculating Crack Width due to Thermal Stress* (1992). Tokyo, Japan: Japan Concrete Institute, Committee on Thermal Stress of Massive Concrete Structures. JCI Committee Report. pp. 106.

Jonasson, J-E, Emborg, M & Bernander, S (1994). Temperatur, mognadsutveckling och egenspänningar i ung betong (Temperature, Maturity Growth and Eigenstresses in Young Concrete). In: *Betonghandbok - Material.* (Concrete Handbook - Material). Edition 2. Stockholm, Sweden: AB Svensk Byggtjänst and Cementa AB. pp. 547-607. ISBN 91-7332-709-3. (In Swedish).

Jonasson, J-E, Wallin, K, Emborg, M, Gram, A, Saleh, I, Nilsson, M, Larson, M & Hedlund, H (2001). *Temperatursprickor i betongkonstruktioner − Handbok med diagram för*

sprickriskbedömning inclusive åtgärder för några vanliga typfall. Del D och E. (Temperature cracks in concrete structures − Handbook with diagrams for crack risk judgement including measures for som typical cases. Part D and E). Luleå, Sweden: Division of Structural Engineering, Luleå University of Technology, Technical Report 2001:14. ISSN: 1402-1536, ISRN: LTU − TR − 01/14 − SE.

Kanstad, T, Bosnjak, D & Øverli, J A (2001). *3D Restraint Analyses of Typical Structures with Early Age Cracking Problems.* Luleå, Sweden: Luleå University of Technology, Department of Civil and Mining Engineering. IPACS-report BE96-3843/2001:32-X. ISBN 91-89580-32-X. pp. 27.

Larson, M (1999). *Evaluation of Restraint from Adjoining Structures.* Luleå, Sweden: Luleå University of Technology, Department of Civil and Mining Engineering. IPACS-report BE96-3843/2001:57-5. ISBN 91-89580−57−5. pp. 23.

Larson, M (2000). *Estimation of Crack Risk in Early Age Concrete.* Luleå, Sweden: Division of Structural Engineering, Luleå University of Technology. Licentiate Thesis 2000:10. pp. 170.

Larson, M, Nilsson, M & Jonasson, J-E (2003). *Restraint Coefficients in Thermal Stress Analysis − Application on a Full-Scale Field Test.* pp, 40. (Paper C in this thesis, aimed for external publication).

Löfquist, B (1946). *Temperatureffekter i hårdnande betong* (Temperature Effects in Hardening Concrete). Stockholm, Sweden: Royal Hydro Power Administration. Technical Bulletins, Serie B, No 22. pp. 195. (In Swedish).

Nilsson, M (1998). *Inverkan av tvång i gjutfogar och i betongkonstruktioner på elastiskt underlag* (Influence of Restraint in Casting Joints and in Concrete Structures on Elastic Foundation). Luleå, Sweden: Luleå University of Technology, Division of Structural Engineering. Master Thesis 1998:090 CIV. pp. 61. (In Swedish).

Nilsson, M (2000). Thermal Cracking of Young Concrete − Partial Coefficients, Restraint Effects and Influence of Casting Joints. Luleå, Sweden: Division of Structural Engineering, Luleå University of Technology. Licentiate Thesis 2000:27. pp. 267. http://epubl.luth.se/1402-1757/2000/27/LTU-LIC-0027-SE.pdf

Nilsson, M (2003). *Restraint Factors and Partial Coefficients for Crack Risk Analyses of Early Age Concrete Structures - Diagrams and Tables.* Luleå, Sweden: Division of Structural Engineering, Luleå University of Technology. Technical Report 2003:11. pp. 199.

Nilsson, M & Elfgren, L (2003). Partial Coefficients for Thermal Cracking Problems Determined by a Probabilistic Method. In: *Nordic Concrete Research, Publication 27-7.* pp. 16. (Paper D in this thesis).

Nilsson, M, Jonasson, J-E, Emborg, M, Wallin, K & Elfgren, L (2003). *Determination of Restraint in Early Age Concrete Walls on Slabs by a Semi-Analytical Method − Paper 2 Verification and Application.* pp. 33. (Paper B in this thesis, aimed for external publication).

Paper A

Nilsson, M, Jonasson, J-E, Wallin, K, Emborg, M, Bernander, S & Elfgren, L (1999). Crack Prevention in Walls and Slabs - The Influence of Restraint. In: *Innovation in Concrete Structures, Design and Construction. Proceedings of the International Conference held at the University of Dundee, Scotland, UK on 8-10 September 1999.* Ed. by R. K. Dhir & M. R. Jones. London, UK: Thomas Telford Publishing. pp. 461-471. ISBN: 0 7277 2824 5.

Olofsson, J, Uhlán, M & Hedlund, H (2001). *Slab cast on rock ground - Model for restraint estimation.* Luleå, Sweden: Luleå University of Technology, Department of Civil and Mining Engineering. IPACS-report BE96-3843/2001:66-4. ISBN 91-89580-66-4. pp. 34.

Olofsson, J, Uhlán, M & Hedlund, H (2001). *2D and 3D Restraint Analyses, Typical Structure − Wall on Slab.* Luleå, Sweden: Luleå University of Technology, Department of Civil and Mining Engineering. IPACS-report BE96-3843/2001:64-8. ISBN 91-89580-64-8. pp. 81.

Pettersson, D (1998). *Stresses in Concrete Structures from Ground Restraint.* Lund, Sweden: Department of Structural Engineering, Lund Institute of Technology. Report TVBK-1014. pp. 112.

Rostásy, F, S, Gutsch, A-W & Krauß, M (2001). *Engineering models for the assessment of restraint of slabs by soil and in piles in the early age of concrete.* Luleå, Sweden: Luleå University of Technology, Department of Civil and Mining Engineering. IPACS-report BE96-3843/2001:59-1. ISBN 91-89580-59-1. pp. 135.

Rostásy, F S, Tanabe, T & Laube, M (1998). Assessment of External Restraint. In: *Prevention of Thermal Cracking in Concrete at Early Ages.* Ed. by R. Springenschmid. London, England: E & FN Spon. RILEM Report 15. State-of-the Art Report by RILEM Technical Committee 119, Avoidance of Thermal Cracking in Concrete at Early Ages. pp. 149-177. ISBN: 0 419 22310 X.

Stoffers, H (1978). Cracking due to Shrinkage and Temperature Variations in Walls. *Heron, vol. 23, no. 23.* pp. 5-68.

Wallin, K, Emborg, M & Jonasson, J-E (1997). *Värme ett alternativ till kyla* (Heat an alternative to cold). Luleå, Sweden: Division of Structural Engineering, Luleå University of Technology. Technical Report 1997:15. pp. 168. (In Swedish).

7   LIST OF NOTATIONS, DEFINITIONS AND SYMBOLS

Roman upper-case letters

$A_{a,eff}$ = effective cross-section area of the adjacent older concrete, [m^2]

A_c = cross-section area of the young concrete, [m^2]

$B_{a,eff}$ = effective width of slab, [m]

45

B_c = width of wall, [m]

E_{a28} = 28 days modulus of elasticity of the old concrete, [MPa]

E_{c28} = 28 days modulus of elasticity of the young concrete, [MPa]

H_a = height of slab, [m]

H_c = height of wall, [m]

$I_{trans,y}$ = transformed second moment of inertia of the cross section for bending around the y-axis, [m^4]

$I_{trans,z}$ = transformed second moment of inertia of the cross section for bending around the z-axis, [m^4]

L = length of the structure, [m]

M = external flexural moment, [Nm]

$M_{RI,y}$ = internal bending moment around the y-axis for obtaining zero curvature in the xz-plane of the young concrete, [Nm]

$M_{RI,z}$ = internal bending moment around the z-axis for obtaining zero curvature in the xy-plane of the young concrete, [Nm]

N = external axial force, [N]

N_{RI} = compression force giving zero translational strain in the young concrete, [N]

Roman lower-case letters

x = horizontal co-ordinate in the length direction, [m]

y = vertical co-ordinate from the joint and up-wards, [m]

y' = internal vertical lever arm to the total centroid for each part, [m]

y_{cen} = vertical location of the centroid of the transformed section relatively the joint, [m]

z = horizontal co-ordinate from the centre of the slab, [m]

z' = internal horizontal lever arm to the total centroid for each part, [m]

z_{cen} = horizontal location of the centroid of the transformed section relatively the centre of the slab, [m]

Greek upper-case letters

$\Delta\varepsilon_a$ = strain of applied volume changes in the old concrete structure (shrinkage and temperature induced strain), [-]

$\Delta\varepsilon^0_c$ = strain of applied volume changes in the young concrete (shrinkage and temperature induced strain), [-]

Greek lower-case letters

δ_{res} = high wall effect, resilience, [-]

δ^0_{res} = basic resilience factor, [-]

δ^0_{transl} = basic resilience correction factor for translational boundary restraint, [-]

Paper A

δ^0_{rot} = basic resilience correction factor for rotational boundary restraint, [-]

δ_{slip} = slip in joint effect, [-]

ε = strain, [-]

ε_x^t = translational strain [-]

ε_x^{ry} = rotational strain around the y-axis [-]

ε_x^{rz} = rotational strain around the z-axis [-]

ϕ = curvature, $[m^{-1}]$

ϕ^0 = curvature at free rotation, $[m^{-1}]$

γ_R = restraint coefficient, [-]

γ_R^{ry} = rotational restraint part for rotation around the y-axis (the vertical axis), [-]

γ_R^{rz} = rotational restraint part for rotation around the z-axis (the horizontal, transverse axis), [-]

$\gamma_{RR,y}$ = rotational boundary restraint for bending around the y-axis, [-]

$\gamma_{RR,z}$ = rotational boundary restraint for bending around the z-axis, [-]

γ_R^t = translational restraint part, [-]

γ_{RT} = translational boundary restraint, [-]

λ = factor describing the volume change in the old concrete relatively the volume change in the young concrete, $\lambda = \Delta\varepsilon_a^0/\Delta\varepsilon_c^0$, [-]

σ^0 = stress at total fixation, [MPa]

σ_1 = principal stress at studied time, [MPa]

ζ = factor describing the modulus of elasticity of the young concrete in relation to the 28-days modulus of elasticity, [-]

ω = relative location of wall on slab, [-]

ζE_{c28} = modulus of elasticity of the young concrete at the studied time, $[N/m^2]$

APPENDIX A – DERIVATION OF RESTRAINT VARIATION IN WALL ON SLAB

Below a derivation of a semi-analytical expression for the determination of the restraint factor γ_R follows as function of the geometric properties of the cross-section, of the modulus of elasticity, and the boundary restraint condition. In addition, a high wall factor δ_{res} (resilience) is introduced for non-linear strain variations in high-wall structures. Also a so-called slip failure factor δ_{slip} is used.

A.1   Restraint

Let us assume that the wall in Figure A.1 is exposed to a non-elastic strain, $\Delta\varepsilon_c^0$. If every point of the cross section in Figure A.1 is totally restrained in the length direction (x-direction), and the deformations in the other directions (y- and z-directions) can take place without any restraint, the completely fixed stress in the x-direction is expressed by

$$\sigma_x^0 = \zeta E_{c28}(-\Delta\varepsilon_c^0) \tag{A.1}$$
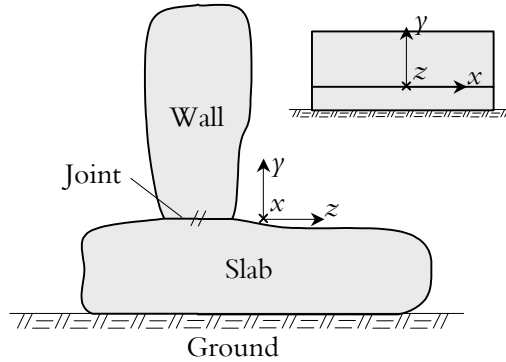
Figure A.1 *Cross section of the structure to be studied in the derivation of the restraint γ_R.*

For the actual situation, the stress in the x-direction, for instance determined by FEM calculations, is denoted σ_x. The restraint function for stresses in the x-direction is defined as the quota between the actual stress at the present time and the completely fixed stress according to Eq. (A.1), i.e.

$$\gamma_R = \frac{\sigma_x}{\sigma_x^0} \tag{A.2}$$

Alternatively, the analysis can be split into 1) a boundary restrained situation and 2) an additional deformation part. The first part is established when one of the boundaries

in the x-direction in the xy-plane of the structure is completely restrained. The boundary fixation stress function in the x-direction is then expressed as

$$\sigma_{xb}^0 = \zeta E_{c28}(-\delta_{res}\delta_{slip}\Delta\varepsilon_c^0) \tag{A.3}$$

where

ζE_{c28} =   modulus of elasticity of the young concrete at the studied time [MPa]
δ_{res} =   high wall effect, resilience [-]
δ_{slip} =   slip in joint effect [-]
$\Delta\varepsilon_c^0$ =   strain of applied volume changes in the young concrete structure (shrinkage and temperature induced strain) [-]

With the present boundary conditions in the xy-plane, the additional strain in the x-direction will be ε_x, and the total stress in the x-direction becomes

$$\sigma_x = \sigma_{xb}^0 + \zeta E_{c28}\varepsilon_x = -\zeta E_{c28}\delta_{res}\delta_{slip}\Delta\varepsilon_c^0 + \zeta E_{c28}\varepsilon_x \tag{A.4}$$

The restraint factor for stresses in the x-direction is now described by putting Eq. (A.3) in Eq. (A.4) which in turn together with Eq. (A.1) are put in to Eq. (A.2) giving

$$\gamma_R = \delta_{res}\delta_{slip} - \frac{\varepsilon_x}{\Delta\varepsilon_c^0} \tag{A.5}$$

A.2   General model

In accordance with the analysis method expressed by Eqs. (A.3) and (A.5), the additional strain in the length direction in any point of the cross section can be represented in the following way

$$\varepsilon_x = \varepsilon_x^t + \varepsilon_x^{ry} + \varepsilon_x^{rz} \tag{A.6}$$

where

ε_x^t =   translational strain [-]
ε_x^{ry} =   rotational strain around the y-axis [-]
ε_x^{rz} =   rotational strain around the z-axis [-]

Below, a semi-analytical model is being introduced by assumptions of non-linear functions with respect to deformations in the boundary fixation part (δ_{res} and δ_{slip}), and that plane section remains plane for the present boundary conditions with respect to

translation and rotations (ε_x^t, ε_x^{ry} and ε_x^{rz}, respectively). The model, see Figure A.2, is established on the following conditions

1. The boundary fixation part is defined for fixation of the lower part of the wall, i.e. for $y = 0$.
2. The effective area of the slab by adjustments of its width is introduced as the only free model parameter.

This basic modelling has the following consequences

- The first condition means that the boundary fixation functions (δ_{res} and δ_{slip}) depend only on the geometry of the wall.
- The second condition is chosen to be the only fitting parameter to be able to give acceptable agreement with three-dimensional finite element method calculations being performed.
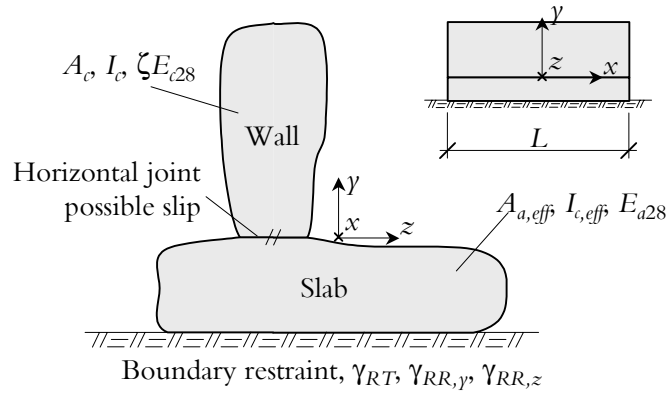
Figure A.2 *Basic properties used in the derivation of the restraint variation.*

With the introduction of Eq. (A.6) and the simplifications in the model, the restraint factor, see Eq. (A.5), becomes

$$\gamma_R = \delta_{res}\delta_{slip} - \gamma_R^t - \gamma_R^{ry} - \gamma_R^{rz} \tag{A.7}$$

where the restraint factor is divided into one boundary fixation part ($\delta_{res}\delta_{slip}$), one translational part ($\gamma_R^t = \varepsilon_x^t/\Delta\varepsilon_c^0$) and two rotational parts ($\gamma_R^{ry} = \varepsilon_x^{ry}/\Delta\varepsilon_c^0$ and $\gamma_R^{rz} = \varepsilon_x^{rz}/\Delta\varepsilon_c^0$).

Paper A

A.2.1 Translational restraint

The axial strain is determined from the horizontal equilibrium condition. The sum of all forces on the vertical cross-section of the young concrete and the effective cross-section of the older part is

$$\int_{A_c} \sigma_c dA_c + \int_{A_{a,eff}} \sigma_a dA_{a,eff} = N$$

which gives

$$\int_{A_c} \zeta E_{c28}(-\delta_{res}\delta_{slip}\Delta\varepsilon_c^0 + \varepsilon_x^t + \varepsilon_x^{ry} + \varepsilon_x^{rz})dA_c$$
$$+ \int_{A_{a,eff}} E_{a28}(-\Delta\varepsilon_a^0 + \varepsilon_x^t + \varepsilon_x^{ry} + \varepsilon_x^{rz})dA_{a,eff} = N \tag{A.8}$$

The effective cross-section for the adjacent structural element is used because the real width of the slab is not always giving the right movements in plane-section analyses compared with elastic 3-dimensional finite element calculations, see Nilsson (2000) and Nilsson (2003).

Further, the rotational strain is expressed as

$$\varepsilon_x^{ry} = -z'\phi_y$$
$$\varepsilon_x^{rz} = -y'\phi_z \tag{A.9}$$

Let the volume changes in the older concrete be expressed as a factor λ times the volume change in the young concrete, $\Delta\varepsilon_a^0 = \lambda\Delta\varepsilon_c^0$ which in Eq. (A.8) together with Eq. (A.9) gives

$$\zeta E_{c28}\varepsilon_x^t \left(\int_{A_c} dA_c + \frac{E_{a28}}{\zeta E_{c28}} \int_{A_{a,eff}} dA_{a,eff} \right)$$

$$-\zeta E_{c28}\phi_y \left(\int_{A_c} z'dA_c + \frac{E_{a28}}{\zeta E_{c28}} \int_{A_{a,eff}} z'dA_{a,eff} \right) -$$

$$\zeta E_{c28}\phi_z \left(\int_{A_c} y'dA_c + \frac{E_{a28}}{\zeta E_{c28}} \int_{A_{a,eff}} y'dA_{a,eff} \right)$$

$$-\zeta E_{c28}\Delta\varepsilon_c^0 \left(\delta_{slip} \int_{A_c} \delta_{res}dA_c + \frac{E_{a28}}{\zeta E_{c28}}\lambda \int_{A_{a,eff}} dA_{a,eff} \right) = N$$

51

The expression within the brackets in the first term defines the area of the transformed cross-section

$$A_{trans} = \int_{A_c} dA_c + \frac{E_{a28}}{\varsigma E_{c28}} \int_{A_{a,eff}} dA_{a,eff} \tag{A.10}$$

The second and third terms vanish, as the first moments of area about the centroidal axis are zero. The position of the centroid is calculated as

$$y_{cen} = \frac{\int_{A_c} y dA_c + \frac{E_{a28}}{\varsigma E_{c28}} \int_{A_{a,eff}} y dA_{a,eff}}{A_{trans}} \tag{A.11}$$

$$z_{cen} = \frac{\int_{A_c} z dA_c + \frac{E_{a28}}{\varsigma E_{c28}} \int_{A_{a,eff}} z dA_{a,eff}}{A_{trans}} \tag{A.12}$$

The fourth term defines the force for obtaining zero axial strain in the total structure expressed by

$$N_{RI} = -\Delta\varepsilon_c^0 \left(\varsigma E_{c28} \delta_{slip} \int_{A_c} \delta_{res} dA_c + E_{a28}\lambda \int_{A_{a,eff}} dA_{a,eff} \right) \tag{A.13}$$

Combining the expressions from equilibrium of axial forces gives the axial strain according to

$$\varepsilon_x^t = \frac{N - N_{RI}}{\varsigma E_{c28} A_{trans}} \tag{A.14}$$

The axial force N is defined by a translational boundary restraint factor expressed by

$$\gamma_{RT} = \frac{N}{N_{RI}} \tag{A.15}$$

which gives

$$\varepsilon_x^t = (1 - \gamma_{RT})\varepsilon_x^{t0} \tag{A.16}$$

where

$$\varepsilon_x^{t0} = -\frac{N_{RI}}{\zeta E_{c28} A_{trans}} \tag{A.17}$$

Now, the translational restraint can be determined as, the second term in Eq. (A.7),

$$\gamma_R^t = \frac{\varepsilon_x^t}{\Delta\varepsilon_c^0} = (1-\gamma_{RT})\frac{\varepsilon_x^{t0}}{\Delta\varepsilon_c^0} = -(1-\gamma_{RT})\frac{N_{RI}}{\Delta\varepsilon_c^0 \zeta E_{c28} A_{trans}} = \tag{A.18}$$

$$= (1-\gamma_{RT})\frac{\zeta E_{c28}\delta_{slip}\int\limits_{A_c}\delta_{res}dA_c + E_{a28}\lambda\int\limits_{A_{a,eff}}dA_{a,eff}}{\zeta E_{c28}\left(\int\limits_{A_c}dA_c + \dfrac{E_{a28}}{\zeta E_{c28}}\int\limits_{A_{a,eff}}dA_{a,eff}\right)} \Rightarrow$$

$$\gamma_R^t = (1-\gamma_{RT})\frac{\delta_{slip}\int\limits_{A_c}\delta_{res}dA_c + \dfrac{E_{a28}}{\zeta E_{c28}}\lambda\int\limits_{A_{a,eff}}dA_{a,eff}}{\int\limits_{A_c}dA_c + \dfrac{E_{a28}}{\zeta E_{c28}}\int\limits_{A_{a,eff}}dA_{a,eff}} \tag{A.19}$$

A.2.2 Rotational restraint

The strain from the rotation of the structure is determined from the condition of flexural moment equilibrium. The sums of all forces on the cross section of the young part and on the effective cross section of the old part times the lever arms to the total centroid, respectively, are

$$\int\limits_{A_c} z'\sigma_c dA_c + \int\limits_{A_{a,eff}} z'\sigma_a dA_{a,eff} = -M_y$$

and

$$\int\limits_{A_c} y'\sigma_c dA_c + \int\limits_{A_{a,eff}} y'\sigma_a dA_{a,eff} = -M_z$$

that with Eqs. (A.4), (A.6) and (A.9) are

$$\int\limits_{A_c} z'\zeta E_{c28}(-\phi_y z' - \delta_{slip}\delta_{res}\Delta\varepsilon_c^0)dA_c + \int\limits_{A_{a,eff}} z'E_{a28}(-\phi_y z' - \Delta\varepsilon_a^0)dA_{a,eff} = -M_y$$

and

$$\int\limits_{A_c} \gamma'\zeta E_{c28}(-\phi_z\gamma'-\delta_{slip}\delta_{res}\Delta\varepsilon_c^0)dA_c + \int\limits_{A_{a,eff}} \gamma' E_{a28}(-\phi_z\gamma'-\Delta\varepsilon_a^0)dA_{a,eff} = -M_z$$

Once again, the volume change in the old concrete is expressed as a factor λ times the volume change in the young concrete, $\Delta\varepsilon_a^0 = \lambda\Delta\varepsilon_c^0$, which gives

$$-\zeta E_{c28}\phi_y\left(\int\limits_{A_c} z'^2\,dA_c + \frac{E_{a28}}{\zeta E_{c28}}\int\limits_{A_{a,eff}} z'^2\,dA_{a,eff}\right)$$

$$-\zeta E_{c28}\Delta\varepsilon_c^0\left(\delta_{slip}\int\limits_{A_c} z'\delta_{res}dA_c + \frac{E_{a28a}}{\zeta E_{c28}}\lambda\int\limits_{A_{a,eff}} z'dA_{a,eff}\right) = -M_y$$

and

$$-\zeta E_{c28}\phi_z\left(\int\limits_{A_c} \gamma'^2\,dA_c + \frac{E_{a28}}{\zeta E_{c28}}\int\limits_{A_{a,eff}} \gamma'^2\,dA_{a,eff}\right)$$

$$-\zeta E_{c28}\Delta\varepsilon_c^0\left(\delta_{slip}\int\limits_{A_c} \gamma'\delta_{res}dA_c + \frac{E_{a28}}{\zeta E_{c28}}\lambda\int\limits_{A_{a,eff}} \gamma'dA_{a,eff}\right) = -M_z$$

The expressions within the brackets in the first terms in each expression define the transformed second moments of inertia

$$I_{trans,y} = \int\limits_{A_c} z'^2\,dA_c + \frac{E_{a28}}{\zeta E_{c28}}\int\limits_{A_{a,eff}} z'^2\,dA_{a,eff} \tag{A.20}$$

$$I_{trans,z} = \int\limits_{A_c} \gamma'^2\,dA_c + \frac{E_{a28}}{\zeta E_{c28}}\int\limits_{A_{a,eff}} \gamma'^2\,dA_{a,eff} \tag{A.21}$$

The second terms define the flexural moment for obtaining zero curvature in the total structure defined by

$$M_{RI,y} = \zeta E_{c28}\Delta\varepsilon_c^0\left(\delta_{slip}\int\limits_{A_c} z'\delta_{res}dA_c + \frac{E_{a28}}{\zeta E_{c28}}\lambda\int\limits_{A_{a,eff}} z'dA_{a,eff}\right) \tag{A.22}$$

$$M_{RI,z} = \zeta E_{c28}\Delta\varepsilon_c^0\left(\delta_{slip}\int\limits_{A_c} \gamma'\delta_{res}dA_c + \frac{E_{a28}}{\zeta E_{c28}}\lambda\int\limits_{A_{a,eff}} \gamma'dA_{a,eff}\right) \tag{A.23}$$

Combining the expressions from the equilibriums of flexural moment gives the curvatures

$$\phi_y = \frac{M_y - M_{RI,y}}{\zeta E_{c28} I_{trans,y}} \tag{A.24}$$

$$\phi_z = \frac{M_z - M_{RI,z}}{\zeta E_{c28} I_{trans,z}} \tag{A.25}$$

The external flexural moments M_y and M_z are defined by the rotational boundary restraint factors expressed as

$$\gamma_{RR,y} = \frac{M_y}{M_{RI,y}} \tag{A.26}$$

$$\gamma_{RR,z} = \frac{M_z}{M_{RI,z}} \tag{A.27}$$

which gives

$$\phi_y = (1 - \gamma_{RR,y})\phi_y^0$$

$$\phi_z = (1 - \gamma_{RR,z})\phi_z^0$$

where

$$\phi_y^0 = -\frac{M_{RI,y}}{\zeta E_{c28} I_{trans,y}} \tag{A.28}$$

$$\phi_z^0 = -\frac{M_{RI,z}}{\zeta E_{c28} I_{trans,z}} \tag{A.29}$$

Now, the rotational strain can be expressed as

$$\varepsilon_x^{ry} = -z'(1 - \gamma_{RR,y})\phi_y^0 \tag{A.30}$$

$$\varepsilon_x^{rz} = -y'(1 - \gamma_{RR,z})\phi_z^0 \tag{A.31}$$

With Eqs. (A.16) and (A.31) put into Eq. (A.6) the restraint factor is expressed by

$$\gamma_R = \delta_{slip}\delta_{res} - (1-\gamma_{RT})\frac{\varepsilon_x^{t0}}{\Delta\varepsilon_c^0} - (1-\gamma_{RR,\gamma})\frac{-z'\phi_{\gamma}^0}{\Delta\varepsilon_c^0} - (1-\gamma_{RR,z})\frac{-\gamma'\phi_z^0}{\Delta\varepsilon_c^0} \qquad (A.32)$$

The rotational parts of the restraint can now be determined as

$$\gamma_R^{r\gamma} = (1-\gamma_{RR,\gamma})\frac{-z'\phi_{\gamma}^0}{\Delta\varepsilon_c^0} = (1-\gamma_{RR,\gamma})\frac{z'M_{RI,\gamma}}{\Delta\varepsilon_c^0\zeta E_{c28}I_{trans,\gamma}} \Rightarrow$$

$$\gamma_R^{r\gamma} = (1-\gamma_{RR,\gamma})z'\frac{\delta_{slip}\displaystyle\int_{A_c} z'\delta_{res}dA_c + \frac{E_{a28}}{\zeta E_{c28}}\lambda\displaystyle\int_{A_{a,eff}} z'dA_{a,eff}}{\displaystyle\int_{A_c}\gamma'^2\,dA_c + \frac{E_{a28}}{\zeta E_{c28}}\displaystyle\int_{A_{a,eff}}\gamma'^2\,dA_{a,eff}} \qquad (A.33)$$

and

$$\gamma_R^{rz} = (1-\gamma_{RR,z})\frac{-\gamma'\phi_z^0}{\Delta\varepsilon_c^0} = (1-\gamma_{RR,z})\frac{\gamma'M_{RI,z}}{\Delta\varepsilon_c^0\zeta E_{c28}I_{trans,z}} \Rightarrow$$

$$\gamma_R^{rz} = (1-\gamma_{RR,z})\gamma'\frac{\delta_{slip}\displaystyle\int_{A_c} \gamma'\delta_{res}dA_c + \frac{E_{a28}}{\zeta E_{c28}}\lambda\displaystyle\int_{A_{a,eff}} \gamma'dA_{a,eff}}{\displaystyle\int_{A_c}\gamma'^2\,dA_c + \frac{E_{a28}}{\zeta E_{c28}}\displaystyle\int_{A_{a,eff}}\gamma'^2\,dA_{a,eff}} \qquad (A.34)$$

A.3 Effects of high walls

The high wall effects factor or the resilience factor is determined as

$$\delta_{res} = \delta_{res}^0\delta_{transl}\delta_{rot} \qquad (A.35)$$

where

δ_{res}^0 = basic resilience factor, [-]

δ_{transl} = resilience correction factor for translational boundary restraint, [-]

δ_{rot} = resilience correction factor for rotational boundary restraint, [-]

The basic resilience factor referrers to structures with low length to height ratio, which are totally restrained at the base, see Figure 4. The resilience correction factors are introduced for cases in which the boundary restraint is not total. They are determined as

$$
\delta_{transl} = \gamma_{RT} + \left(1 - \gamma_{RT}\right)\delta_{transl}^0
$$
$$
\delta_{rot} = \gamma_{RR,z} + \left(1 - \gamma_{RR,z}\right)\delta_{rot}^0
$$

(A.36)

where δ^0_{transl} and δ^0_{rot} are basic resilience correction factors for translation and rotation, respectively. See Nilsson et al. (2003) for more details on the determination of the basic resilience correction factors based on 3D elastic FEM calculations. Eq. (A.36) in Eq. (A.35) gives

$$
\delta_{res} = \delta_{res}^0 \left(\gamma_{RT} + \left(1 - \gamma_{RT}\right)\delta_{transl}^0\right)\left(\gamma_{RR,z} + \left(1 - \gamma_{RR,z}\right)\delta_{rot}^0\right)
$$

(A.37)

For the case free translation and free rotation, that is no boundary restraint $\gamma_{RT} = \gamma_{RR,z} = 0$, Eq. (A.37) becomes

$$
\delta_{res} = \delta_{res}^0 \delta_{transl}^0 \delta_{rot}^0
$$

(A.38)

For no boundary restraint the 3D effect is considered only by introducing an effective width of the slab $B_{a,eff}$, which means that formally $\delta^0_{transl}\delta^0_{rot} \equiv 1$ in this case. So, the basic resilience correction factor for rotation is determined as the inverse of the basic resilience correction for translation by

$$
\delta_{rot}^0 = \frac{1}{\delta_{transl}^0}
$$

(A.39)

which in Eq. (A.38) gives that for $\gamma_{RT} = \gamma_{RR,z} = 0$

$$
\delta_{res} = \delta_{res}^0
$$

(A.40)

A.4   Applicable formulations

Below a derivation of the restraint factor γ_R for un-symmetrically located rectangular walls cast on rectangular slabs follows as function of the height of the wall H_c, the width of the wall B_c, the height of the slab H_a, the effective width of the slab $B_{a,eff}$, and the relative location of the wall on the slab ω as well as the modulus of elasticity of the young and the old parts, see Figure A.9. For the case of no boundary restraint that is $\gamma_{RT} = \gamma_{RR,y} = \gamma_{RR,z} = 0$, the solution of Eq. (A.32) is performed analytically.

As been determined above, in Eq. (A.32), the restraint depends partly on the translational strain ε_x^{t0}, partly on the curvatures around the $y-$ and z-axes, ϕ_y^0 and ϕ_z^0. The translational strain is determined according to Eq. (A.17) by the force obtaining zero axial strain in the total structure, N_{RI}, by the modulus of elasticity of the young concrete, ζE_{c28}, and by the area of the transformed cross section, A_{trans}. The curvature, in turn, is determined according to Eqs. (A.28) and (A.29) by the flexural moments obtaining zero curvature in the total structure, $M_{RI,y}$ and $M_{RI,z}$, by the modulus of elasticity of the young concrete, ζE_{c28}, and by the second moments of inertia of the transformed cross section, $I_{trans,y}$ and $I_{trans,z}$.
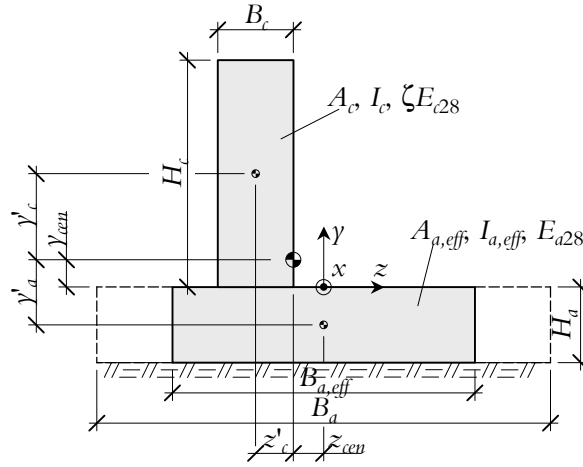
Figure A.9 *Cross sectional properties for a rectangular wall on a rectangular slab used in the derivation of the restraint* γ_R.

A.4.1 Translational restraint part

By assuming no volume change in the old concrete, $\lambda = 0$, the force obtaining zero strain in the total structure is

$$N_{RI} = -\Delta\varepsilon_c^0 \zeta E_{c28} \delta_{slip} B_c \int\limits_0^{H_c} \delta_{res}^0 dy$$

Now, let the high wall factor in Figure 4b), the basic resilience $\delta_{res}^0 = \delta_{res}^0(y/H_c)$, be described with a polynomial according to

$$\delta_{res}^0\left(\frac{y}{H_c}\right) = \sum_{i=0}^{n} a_i \left(\frac{y}{H_c}\right)^i \tag{A.41}$$

where a_i to a_n are coefficients that describe each curve in Figure 4b) above. Then

$$N_{RI} = -\Delta\varepsilon_c^0 \zeta E_{c28} \delta_{slip} B_c \int_0^{H_c} \sum_{i=0}^{n} a_i \left(\frac{\gamma}{H_c}\right)^i d\gamma \quad \Rightarrow$$

$$N_{RI} = -\Delta\varepsilon_c^0 \zeta E_{c28} \delta_{slip} B_c H_c \sum_{i=0}^{n} \frac{a_i}{i+1} \tag{A.42}$$

The area of the transformed cross section is

$$A_{trans} = \int_{A_c} dA_c + \frac{E_{a28}}{\zeta E_{c28}} \int_{A_{a,eff}} dA_{a,eff} =$$

$$= B_c \int_0^{H_c} d\gamma + \frac{E_{a28}}{\zeta E_{c28}} B_{a,eff} \int_{-H_a}^{0} d\gamma \Rightarrow$$

$$A_{trans} = B_c H_c + \frac{E_{a28}}{\zeta E_{c28}} B_{a,eff} H_a \tag{A.43}$$

The translational restraint part is now calculated as, Eqs. (A.42) and (A.43) in Eq. (A.18)

$$\gamma_R^t = -\frac{N_{RI}}{\Delta\varepsilon_c^0 \zeta E_{c28} A_{trans}} =$$

$$= \delta_{slip} \frac{B_c H_c \sum_{i=0}^{n} \frac{a_i}{i+1}}{B_c H_c + \frac{E_{a28}}{\zeta E_{c28}} B_{a,eff} H_a} \Rightarrow$$

$$\gamma_R^t = \delta_{slip} \frac{\sum_{i=0}^{n} \frac{a_i}{i+1}}{1 + \frac{E_{a28}}{\zeta E_{c28}} \frac{B_{a,eff} H_a}{B_c H_c}} \tag{A.44}$$

A.4.2 Rotational restraint for bending around the y-axis

By assuming no volume change in the old concrete, $\lambda = 0$, and no high wall effects (resilience), $\delta_{res} \equiv 1$, for bending around the y-axis, the flexural moment for obtaining zero curvature in the total structure is, Eq. (A.22)

$$M_{RI,y} = \Delta\varepsilon_c^0 \zeta E_{c28} \delta_{slip} H_c \int_{\omega\frac{B_{a,eff}-B_c}{2}-\frac{B_c}{2}}^{\omega\frac{B_{a,eff}-B_c}{2}+\frac{B_c}{2}} z' dz =$$

$$= \Delta\varepsilon_c^0 \zeta E_{c28} \delta_{slip} H_c \int_{\omega\frac{B_{a,eff}-B_c}{2}-\frac{B_c}{2}}^{\omega\frac{B_{a,eff}-B_c}{2}+\frac{B_c}{2}} \left(z_{cen} - z\right) dz =$$

$$= \Delta\varepsilon_c^0 \zeta E_{c28} \delta_{slip} H_c \left[z_{cen}z - \frac{z^2}{2} \right]_{\omega\frac{B_{a,eff}-B_c}{2}-\frac{B_c}{2}}^{\omega\frac{B_{a,eff}-B_c}{2}+\frac{B_c}{2}}$$

By introducing

$$C = \frac{B_{a,eff} - B_c}{2} \tag{A.45}$$

the expression is slightly simplified giving

$$= \Delta\varepsilon_c^0 \zeta E_{c28} \delta_{slip} H_c \left[z_{cen}z - \frac{z^2}{2} \right]_{\omega C - \frac{B_c}{2}}^{\omega C + \frac{B_c}{2}} =$$

$$= \Delta\varepsilon_c^0 \zeta E_{c28} \delta_{slip} H_c \left(z_{cen}\left(\omega C + \frac{B_c}{2}\right) - \frac{1}{2}\left(\omega C + \frac{B_c}{2}\right)^2 \right.$$

$$\left. -z_{cen}\left(\omega C - \frac{B_c}{2}\right) + \frac{1}{2}\left(\omega C - \frac{B_c}{2}\right)^2 \right) =$$

$$= \Delta\varepsilon_c^0 \zeta E_{c28} \delta_{slip} H_c \left(z_{cen}\omega C + z_{cen}\frac{B_c}{2} - \frac{(\omega C)^2}{2} - \frac{\omega C B_c}{2} - \frac{B_c^2}{8} - \right.$$

$$\left. z_{cen}\omega C + z_{cen}\frac{B_c}{2} + \frac{(\omega C)^2}{2} - \frac{\omega C B_c}{2} + \frac{B_c^2}{8} \right) =$$

$$= \Delta\varepsilon_c^0 \zeta E_{c28} \delta_{slip} H_c \left(z_{cen} B_c - \omega C B_c \right) \Rightarrow$$

$$M_{RI,y} = \Delta\varepsilon_c^0 \zeta E_{c28} \delta_{slip} H_c B_c \left(z_{cen} - \omega \frac{B_{a,eff} - B_c}{2} \right) \qquad \text{(A.46)}$$

z_{cen} is the distance to the centroid of the transformed cross-section relatively the centre of the slab (the chosen origin of the co-ordinate system, see Figure A.9), and it is calculated according to Eq. (A.12) as

$$z_{cen} = \frac{\displaystyle\int_{A_c} z dA_c + \frac{E_{a28}}{\zeta E_{c28}} \int_{A_{a,eff}} z dA_{a,eff}}{A_{trans}} =$$

$$= \frac{\displaystyle H_c \int_{\omega C - \frac{B_c}{2}}^{\omega C + \frac{B_c}{2}} z dz + \frac{E_{a28}}{\zeta E_{c28}} H_a \int_{-\frac{B_{a,eff}}{2}}^{\frac{B_{a,eff}}{2}} z dz}{A_{trans}} =$$

$$= \frac{\displaystyle H_c \left[\frac{z^2}{2}\right]_{\omega C - \frac{B_c}{2}}^{\omega C + \frac{B_c}{2}} + \frac{E_{a28}}{\zeta E_{c28}} H_a \left[\frac{z^2}{2}\right]_{-\frac{B_{a,eff}}{2}}^{\frac{B_{a,eff}}{2}}}{A_{trans}} =$$

$$= \frac{\displaystyle \frac{H_c}{2}\left(\left(\omega C + \frac{B_c}{2}\right)^2 - \left(\omega C - \frac{B_c}{2}\right)^2\right) + \frac{E_{a28}}{\zeta E_{c28}} \frac{H_a}{2}\left(\left(\frac{B_{a,eff}}{2}\right)^2 - \left(-\frac{B_{a,eff}}{2}\right)^2\right)}{A_{trans}} =$$

$$= \frac{\displaystyle \frac{H_c}{2}\left((\omega C)^2 + \omega C B_c + \frac{B_c^2}{4} - (\omega C)^2 + \omega C B_c - \frac{B_c^2}{4}\right)}{A_{trans}} =$$

$$= \frac{B_c H_c \omega C}{A_{trans}}$$

With A_{trans} according to Eq. (A.43), this becomes

$$\frac{B_c H_c \omega C}{B_c H_c + \dfrac{E_{a28}}{\zeta E_{c28}} B_{a,eff} H_a} =$$

$$= \frac{\omega C}{1 + \dfrac{E_{a28}}{\zeta E_{c28}} \dfrac{B_{a,eff} H_a}{B_c H_c}}$$

that in turn with Eq. (A.45) gives the final expression for the location of the centroid of the transformed cross-section

$$z_{cen} = \frac{\omega \dfrac{B_{a,eff} - B_c}{2}}{1 + \dfrac{E_{a28}}{\zeta E_{c28}} \dfrac{B_{a,eff} H_a}{B_c H_c}} \tag{A.47}$$

The transformed second moment of inertia $I_{trans,y}$ is calculated from Eq. (A.21), giving

$$I_{trans,y} = \int_{A_c} z'^2 \, dA_c + \frac{E_{a28}}{\zeta E_{c28}} \int_{A_{a,eff}} z'^2 \, dA_{a,eff} =$$

$$= H_c \int_{\omega C - \frac{B_c}{2}}^{\omega C + \frac{B_c}{2}} (z_{cen} - z)^2 \, dz + \frac{E_{a28}}{\zeta E_{c28}} H_a \int_{-\frac{B_{a,eff}}{2}}^{\frac{B_{a,eff}}{2}} (z_{cen} - z)^2 \, dz =$$

$$= H_c \left[z_{cen}^2 z - z_{cen} z^2 + \frac{z^3}{3} \right]_{\omega C + \frac{B_c}{2}}^{\omega C + \frac{B_c}{2}} + \frac{E_{a28}}{\zeta E_{c28}} H_a \left[z_{cen}^2 z - z_{cen} z^2 + \frac{z^3}{3} \right]_{-\frac{B_{a,eff}}{2}}^{\frac{B_{a,eff}}{2}} =$$

$$= H_c \left\{ z_{cen}^2 \left(\omega C + \frac{B_c}{2} \right) - z_{cen} \left(\omega C + \frac{B_c}{2} \right)^2 + \frac{1}{3} \left(\omega C + \frac{B_c}{2} \right)^3 - z_{cen}^2 \left(\omega C - \frac{B_c}{2} \right) \right.$$

$$\left. + z_{cen} \left(\omega C - \frac{B_c}{2} \right)^2 - \frac{1}{3} \left(\omega C - \frac{B_c}{2} \right)^3 \right\} + \frac{E_{a28}}{\zeta E_{c28}} H_a \left\{ z_{cen}^2 \frac{B_{a,eff}}{2} - z_{cen} \left(\frac{B_{a,eff}}{2} \right)^2 \right.$$

$$\left. + \frac{1}{3} \left(\frac{B_{a,eff}}{2} \right)^3 - z_{cen}^2 \left(-\frac{B_{a,eff}}{2} \right) + z_{cen} \left(-\frac{B_{a,eff}}{2} \right)^2 - \frac{1}{3} \left(-\frac{B_{a,eff}}{2} \right)^3 \right\} =$$

$$= H_c \left\{ z_{cen}^2 \omega C + z_{cen}^2 \frac{B_c}{2} - z_{cen} \left((\omega C)^2 + \omega C B_c + \frac{B_c^2}{4} \right) \right.$$

$$+ \frac{1}{3} \left((\omega C)^3 + 3(\omega C)^2 B_c + 3\omega C \frac{B_c^2}{4} + \frac{B_c^3}{8} \right)$$

$$- z_{cen}^2 \omega C + z_{cen}^2 \frac{B_c}{2} + z_{cen} \left((\omega C)^2 - \omega C B_c + \left(\frac{B_c}{2} \right)^2 \right)$$

$$\left. - \frac{1}{3} \left((\omega C)^3 - 3(\omega C)^2 B_c + 3\omega C \frac{B_c^2}{4} - \frac{B_c^3}{8} \right) \right\}$$

$$+ \frac{E_{a28}}{\zeta E_{c28}} H_a \left\{ z_{cen}^2 \frac{B_{a,eff}}{2} - z_{cen} \frac{B_{a,eff}^2}{4} + \frac{B_{a,eff}^3}{24} + z_{cen}^2 \frac{B_{a,eff}}{2} + z_{cen} \frac{B_{a,eff}^2}{4} + \frac{B_{a,eff}^3}{24} \right\} =$$

$$= H_c \left\{ z_{cen}^2 \omega C + z_{cen}^2 \frac{B_c}{2} - z_{cen} (\omega C)^2 - z_{cen} \omega C B_c - z_{cen} \frac{B_c^2}{4} + \frac{(\omega C)^3}{3} \right.$$

$$+ (\omega C)^2 \frac{B_c}{2} + \omega C \frac{B_c^2}{4} + \frac{B_c^3}{24} - z_{cen}^2 \omega C + z_{cen}^2 \frac{B_c}{2} + z_{cen} (\omega C)^2 - z_{cen} \omega C B_c + z_{cen} \frac{B_c^2}{4}$$

$$\left. - \frac{(\omega C)^3}{3} + (\omega C)^2 \frac{B_c}{2} - \omega C \frac{B_c^2}{4} + \frac{B_c^3}{24} \right\} + \frac{E_{a28}}{\zeta E_{c28}} H_a \left\{ z_{cen}^2 B_{a,eff} + \frac{B_{a,eff}^3}{12} \right\} =$$

$$= H_c \left(z_{cen}^2 \frac{B_c}{2} - z_{cen} \omega C B_c + (\omega C)^2 \frac{B_c}{2} + \frac{B_c^3}{24} + z_{cen}^2 \frac{B_c}{2} - z_{cen} \omega C B_c + (\omega C)^2 \frac{B_c}{2} + \frac{B_c^3}{24} \right)$$

$$+ \frac{E_{a28}}{\zeta E_{c28}} H_a \left(z_{cen}^2 B_{a,eff} + \frac{B_{a,eff}^3}{12} \right) =$$

$$= H_c \left(z_{cen}^2 B_c - 2 z_{cen} \omega C B_c + (\omega C)^2 B_c + \frac{B_c^3}{12} \right) + \frac{E_{a28}}{\zeta E_{c28}} H_a \left(z_{cen}^2 B_{a,eff} + \frac{B_{a,eff}^3}{12} \right) =$$

$$= \frac{H_c B_c^3}{12} + H_c B_c \left(z_{cen}^2 - 2 z_{cen} \omega C + (\omega C)^2 \right) + \frac{E_{a28}}{\zeta E_{c28}} \left(\frac{H_a B_{a,eff}^3}{12} + H_a B_{a,eff} z_{cen}^2 \right) =$$

$$= \frac{H_c B_c^3}{12} + H_c B_c \left(z_{cen} - \omega C \right)^2 + \frac{E_{a28}}{\zeta E_{c28}} \left(\frac{H_a B_{a,eff}^3}{12} + H_a B_{a,eff} z_{cen}^2 \right) =$$

$$= H_c B_c \left(\frac{B_c^2}{12} + \left(z_{cen} - \omega C \right)^2 + \frac{E_{a28}}{\zeta E_{c28}} \frac{H_a B_{a,eff}}{H_c B_c} \left(\frac{B_{a,eff}^2}{12} + z_{cen}^2 \right) \right)$$

that with Eq. (A.45) is

$$I_{trans,\gamma} = H_c B_c \left(\frac{B_c^2}{12} + \left(z_{cen} - \omega \frac{B_{a,eff} - B_c}{2} \right)^2 + \frac{E_{a28}}{\zeta E_{c28}} \frac{H_a B_{a,eff}}{H_c B_c} \left(\frac{B_{a,eff}^2}{12} + z_{cen}^2 \right) \right) \quad \text{(A.48)}$$

The rotational restraint part for bending around the γ-axis can now be determined accordingly to Eq. (A.34) with Eqs. (A.46) and (A.48) giving

$$\gamma_R^{r\gamma} = \frac{z' M_{RI,\gamma}}{\Delta \varepsilon_c^0 \zeta E_{c28} I_{trans,\gamma}} \Rightarrow$$

$$\gamma_R^{r\gamma} = \delta_{slip} \frac{\left(z_{cen} - z \right) \left(z_{cen} - \omega \frac{B_{a,eff} - B_c}{2} \right)}{\frac{B_c^2}{12} + \left(z_{cen} - \omega \frac{B_{a,eff} - B_c}{2} \right)^2 + \frac{E_{a28}}{\zeta E_{c28}} \frac{H_a B_{a,eff}}{H_c B_c} \left(\frac{B_{a,eff}^2}{12} + z_{cen}^2 \right)} \quad \text{(A.49)}$$

A.4.3 Rotational restraint for bending around the z-axis

By assuming no volume change in the old concrete, $\lambda = 0$, and letting the high wall effect factor, $\delta_{res}^0 = \delta_{res}^0(\gamma/H_c)$, be described with a polynomial, the flexural moment for obtaining zero curvature in the total structure is, Eq. (A.23)

$$M_{RI,z} = \Delta \varepsilon_c^0 \zeta E_{c28} \delta_{slip} B_c \int_0^{H_c} \gamma' \delta_{res}^0 \left(\frac{\gamma}{H_c} \right) d\gamma =$$

$$= \Delta \varepsilon_c^0 \zeta E_{c28} \delta_{slip} B_c \int_0^{H_c} \left(\gamma_{cen} - \gamma \right) \delta_{res}^0 \left(\frac{\gamma}{H_c} \right) d\gamma =$$

$$= \Delta \varepsilon_c^0 \zeta E_{28\gamma} \delta_{slip} B_c \int_0^{H_c} \left(\gamma_{cen} \sum_{i=0}^{n} a_i \left(\frac{\gamma}{H_c} \right)^i - \gamma \sum_{i=0}^{n} a_i \left(\frac{\gamma}{H_c} \right)^i \right) d\gamma \Rightarrow$$

$$M_{RI,z} = \Delta \varepsilon_c^0 \zeta E_{c28} \delta_{slip} B_c H_c \left(\gamma_{cen} \sum_{i=0}^{n} \frac{a_i}{i+1} - H_c \sum_{i=0}^{n} \frac{a_i}{i+2} \right) \quad \text{(A.50)}$$

γ_{cen} is the distance to the centroid relatively the joint and it is calculated according to Eq. (A.11) as

$$\gamma_{cen} = \frac{\int_{A_c} \gamma dA_c + \frac{E_{a28}}{\zeta E_{c28}} \int_{A_{a,eff}} \gamma dA_{a,eff}}{A_{trans}} =$$

$$= \frac{B_c \int_0^{H_c} \gamma d\gamma + \frac{E_{a28}}{\zeta E_{c28}} B_{a,eff} \int_{-H_a}^{0} \gamma d\gamma}{A_{trans}} =$$

$$= \frac{B_c \left[\frac{\gamma^2}{2} \right]_o^{H_c} + \frac{E_{a28}}{\zeta E_{c28}} B_{a,eff} \left[\frac{\gamma^2}{2} \right]_{-H_a}^{0}}{A_{trans}} =$$

$$= \frac{\frac{B_c H_c^2}{2} - \frac{E_{a28}}{\zeta E_{c28}} \frac{B_{a,eff} H_a^2}{2}}{A_{trans}}$$

that with Eq. (A.43) becomes

$$\frac{\frac{B_c H_c^2}{2} - \frac{E_{a28}}{\zeta E_{c28}} \frac{B_{a,eff} H_a^2}{2}}{B_c H_c + \frac{E_{a28}}{\zeta E_{c28}} B_{a,eff} H_a} \Rightarrow$$

$$\gamma_{cen} = \frac{\frac{H_c}{2} - \frac{H_a}{2} \frac{E_{a28}}{\zeta E_{c28}} \frac{B_{a,eff} H_a}{B_c H_c}}{1 + \frac{E_{28a}}{\zeta E_{c28}} \frac{B_{a,eff} H_a}{B_c H_c}} \tag{A.51}$$

The transformed second moment of inertia $I_{trans,z}$ is calculated from Eq. (A.21), giving

$$I_{trans,z} = \int_{A_c} \gamma'^2 dA_c + \frac{E_{a28}}{\zeta E_{c28}} \int_{A_{a,eff}} \gamma'^2 dA_{a,eff} =$$

$$= B_c \int_0^{H_c} (\gamma_{cen} - \gamma)^2 d\gamma + \frac{E_{a28}}{\zeta E_{c28}} B_{a,eff} \int_{-H_a}^{0} (\gamma_{cen} - \gamma)^2 d\gamma =$$

$$= B_c \left[\gamma_{cen}^2 \gamma - \gamma_{cen} \gamma^2 + \frac{\gamma^3}{3} \right]_0^{H_c} + \frac{E_{a28}}{\zeta E_{c28}} B_{a,eff} \left[\gamma_{cen}^2 \gamma - \gamma_{cen} \gamma^2 + \frac{\gamma^3}{3} \right]_{-H_a}^{0} =$$

$$= B_c \left(\gamma_{cen}^2 H_c - \gamma_{cen} H_c^2 + \frac{H_c^3}{3} \right) + \frac{E_{a28}}{\zeta E_{c28}} B_{a,eff} \left(\gamma_{cen}^2 H_a + \gamma_{cen} H_a^2 + \frac{H_a^3}{3} \right) =$$

$$= B_c H_c \left(\gamma_{cen}^2 - \gamma_{cen} H_c + \frac{H_c^2}{3} + \frac{H_c^2}{12} - \frac{H_c^2}{12} \right)$$

$$+ \frac{E_{a28}}{\zeta E_{c28}} B_{a,eff} H_a \left(\gamma_{cen}^2 + \gamma_{cen} H_a + \frac{H_a^2}{3} + \frac{H_a^2}{12} - \frac{H_a^2}{12} \right) =$$

$$= B_c H_c \left(\gamma_{cen}^2 - \gamma_{cen} H_c + \frac{H_c^2}{4} \right) + B_c H_c \frac{H_c^2}{12}$$

$$+ \frac{E_{a28}}{\zeta E_{c28}} \left(B_{a,eff} H_a \left(\gamma_{cen}^2 + \gamma_{cen} H_a + \frac{H_a^2}{4} \right) + B_{a,eff} H_a \frac{H_a^2}{12} \right) =$$

$$= \frac{B_c H_c^3}{12} + B_c H_c \left(\gamma_{cen} - \frac{H_c}{2} \right)^2 + \frac{E_{a28}}{\zeta E_{c28}} \left(\frac{B_{a,eff} H_a^3}{12} + B_{a,eff} H_a \left(\gamma_{cen} + \frac{H_a}{2} \right)^2 \right) \Rightarrow$$

$$I_{trans,z} = B_c H_c \left(\frac{H_c^2}{12} + \left(\gamma_{cen} - \frac{H_c}{2} \right)^2 + \frac{E_{a28}}{\zeta E_{c28}} \frac{B_{a,eff} H_a}{B_c H_c} \left(\frac{H_a^2}{12} + \left(\gamma_{cen} + \frac{H_a}{2} \right)^2 \right) \right) \quad (A.52)$$

The rotational restraint part can now be determined according to Eq. (A.34)

$$\gamma_R^{rz} = \frac{\gamma' M_{RI,z}}{\Delta \varepsilon_c^0 \zeta E_{c28} I_{trans,z}} \Rightarrow$$

$$\gamma_R^{rz} = \delta_{slip} \frac{(\gamma_{cen} - \gamma) \left(\gamma_{cen} \sum_{i=0}^n \frac{a_i}{i+1} - H_c \sum_{i=0}^n \frac{a_i}{i+2} \right)}{\frac{H_c^2}{12} + \left(\gamma_{cen} + \frac{H_c}{2} \right)^2 + \frac{E_{a28}}{\zeta E_{c28}} \frac{B_{a,eff} H_a}{B_c H_c} \left(\frac{H_a^2}{12} + \left(\gamma_{cen} + \frac{H_a}{2} \right)^2 \right)} \quad (A.53)$$

A.4.4 Final expressions

It is now possible to determine a final expression for the restraint in any point above the joint in a early ages concrete wall on a older slab subjected to no boundary restraint. Eqs. (A.41), (A.44), (A.48) and (A.53) in Eq. (A.7) give a final applicable expression for the restraint in the mid-section of a wall-on-slab structure according to

Paper A

$$\gamma_R = \delta_{slip} \sum_{i=0}^{n} a_i \left(\frac{\gamma}{H_c}\right)^i - \delta_{slip} \frac{\displaystyle\sum_{i=0}^{n} \frac{a_i}{i+1}}{1 + \frac{E_{a28}}{\zeta E_{c28}} \frac{B_{a,eff} H_a}{B_c H_c}}$$

$$-\delta_{slip} \frac{\left(z_{cen} - z\right)\left(z_{cen} - \omega \frac{B_{a,eff} - B_c}{2}\right)}{\frac{B_c^2}{12} + \left(z_{cen} - \omega \frac{B_{a,eff} - B_c}{2}\right)^2 + \frac{E_{a28}}{\zeta E_{c28}} \frac{H_a B_{a,eff}}{H_c B_c}\left(\frac{B_{a,eff}^2}{12} + z_{cen}^2\right)} \tag{A.54}$$

$$-\delta_{slip} \frac{\left(\gamma_{cen} - \gamma\right)\left(\gamma_{cen} \displaystyle\sum_{i=0}^{n} \frac{a_i}{i+1} - H_c \displaystyle\sum_{i=0}^{n} \frac{a_i}{i+2}\right)}{\frac{H_c^2}{12} + \left(\gamma_{cen}' - \frac{H_c}{2}\right)^2 + \frac{E_{a28}}{\zeta E_{c28}} \frac{B_{a,eff} H_a}{B_c H_c}\left(\frac{H_a^2}{12} + \left(\gamma_{cen}' + \frac{H_a}{2}\right)^2\right)}$$

An even simpler expression is found for structures with no high walls effects and with no possible slip failure in the joint. Eq. (A.54) is then simplified by excluding δ_{slip} and δ_{res}^0 from the derivations of Eqs. (A.44), (A.49) and (A.53) giving

$$\gamma_R = 1 - \frac{1}{1 + \frac{E_{a28}}{\zeta E_{c28}} \frac{B_{a,eff} H_a}{B_c H_c}}$$

$$- \frac{\left(z_{cen} - z\right)\left(z_{cen} - \omega \frac{B_{a,eff} - B_c}{2}\right)}{\frac{B_c^2}{12} + \left(z_{cen} - \omega \frac{B_{a,eff} - B_c}{2}\right)^2 + \frac{E_{a28}}{\zeta E_{c28}} \frac{H_a B_{a,eff}}{H_c B_c}\left(\frac{B_{a,eff}^2}{12} + z_{cen}^2\right)} \tag{A.55}$$

$$- \frac{\left(\gamma_{cen} - \gamma\right)\left(\gamma_{cen} - \frac{H_c}{2}\right)}{\frac{H_c^2}{12} + \left(\gamma_{cen}' - \frac{H_c}{2}\right)^2 + \frac{E_{a28}}{\zeta E_{c28}} \frac{B_{a,eff} H_a}{B_c H_c}\left(\frac{H_a^2}{12} + \left(\gamma_{cen}' + \frac{H_a}{2}\right)^2\right)}$$

which exactly correspond with the Compensation Plane method according to the linear elastic theory.

Paper B

**Determination of Restraint in Early Age Concrete Walls
on Slabs by a Semi–Analytical Method**
Paper 2 Verification and Application

By

Martin Nilsson

Jan-Erik Jonasson

Mats Emborg

Kjell Wallin

Lennart Elfgren

Paper B

Determination of Restraint in Early Age Concrete Walls on Slabs by a Semi-Analytical Method – Paper 2 Verification and Application

By Martin Nilsson, Jan–Erik Jonasson, Mats Emborg, Kjell Wallin and Lennart Elfgren

M.Sc. Eng. and Tech. Lic. Martin Nilsson is a PhD-student in Structural Engineering at Luleå University of Technology, Sweden. His field of research is structural behaviour of young concrete structures.

Tech. Dr. Jan-Erik Jonasson is a Senior Lecturer and Assistant Professor in Structural Engineering at Luleå University of Technology, Sweden. His research speciality is modelling of thermal and moisture conditions and associated structural behaviour of concrete structures.

Tech. Dr. Mats Emborg is partly a Senior Lecturer and Assistant Professor in Structural Engineering at Luleå University of Technology, Sweden, partly Research and Development Manager at Betongindustri AB, Sweden. His research speciality is behaviour of fresh and hardening concrete including self-compacting concrete with and without fibre reinforcement.

Mr. Kjell Wallin is technical adviser in concrete with many years of experience of practical work at the Swedish contractor Peab. He is also a Research Engineer in Structural Engineering at Luleå University of Technology, Sweden. His research specialities are thermal cracking and self compacting concrete.

Tech. Dr. Professor Lennart Elfgren is Head of Division of Structural Engineering at Luleå University of Technology, Sweden. His research specialities include fracture mechanics, fatigue, fasteners, and combined bending, shear and torsion.

ABSTRACT

A special formulation of the semi-analytical method derived and presented in Nilsson et al. (2003) is in this paper developed for the typical case wall on slab. This special formulation is calibrated and adjusted by use of 2920 elastic three-dimensional finite element method calculations. Necessary adjustment tools are determined and presented in order to achieve good correlation with the FEM calculations. The adjustment tools consist of the effective width of slab, effects of relative location of walls on slabs, high wall effects, effects of possible slip failure in joints, and finally on the degree of boundary restraint.

In a number of consecutive examples the need and use of the adjustment tools are presented. By use of the adjustment tools, good agreement is achieved between the restraint variation determined by the semi-analytical method and by the reference variation from the FEM calculations. By use of the adjustment tools the model is in its general form applicable to any degree of boundary restraint, both translational and rotational.

Keywords: restraint; early age concrete; mass concrete; cracking; resilience; joint slip; wall on slab.

1 INTRODUCTION

The determination of the degree of restraint that a hydrating concrete element is subjected to is of utmost importance for crack risk analyses of the young concrete. The degree of restraint can be determined in different ways, e.g. by calculations or evaluation of measurements.

This paper is the second paper out of two presenting a semi-analytical method for the determination of restraint variations in early age concrete structures. In the first paper, Paper 1 by Nilsson et al. (2003), the method was derived and all including parts and effects were described. The method is based on the Compensation Plane theory and should be seen as a fairly simple and straightforward engineering tool for restraint determination. A special formulation of the method is derived for the typical case wall on slab for which a number of adjustment tools are needed in order to achieve reliable restraint variations in walls for the typical case wall on slab structures. The necessary adjustment tools will be presented below, partly how they are derived and determined, partly how they are used. The presentation of the determination of the adjustment tools will be based on an example that will run through the whole paper in order to show the need and the result of each and every adjustment tool.

1.1 The semi-analytical method

The presentation in Nilsson et al. (2003) of the semi-analytical method contains only the derivation, the components and the basic principles of the method. No correlation or adjustments to any references of restraint variations are given. In order to assure the

72

method to correspond with the behaviour of real structures, a number of adjustments are necessary. The verification and adjustment of the method have been chosen to be done by elastic 3D FEM calculations of wall-on-slab structures. Exactly 2920 calculations have been performed, see Nilsson (2003), that hereby are chosen as references to the method.

The semi-analytical method in its general formulation is applicable to any early age concrete structure built by one young part cast on top of an older adjacent part, see Nilsson et al. (2003). For the typical case wall on slab with no volume change in the old part the general formulation reads

$$
\begin{aligned}
\gamma_R = \delta_{res}\delta_{slip} - (1 - \gamma_{RT})\frac{\delta_{slip}\int_{A_c}\delta_{res}dA_c}{A_{trans}} \\
-(1 - \gamma_{RR,z})(\gamma_{cen} - \gamma)\frac{\delta_{slip}\int_{A_c}\delta_{res}(\gamma_{cen} - \gamma)dA_c}{I_{trans,z}} \\
-(1 - \gamma_{RR,y})(z_{cen} - z)\frac{\delta_{slip}\int_{A_c}(z_{cen} - z)dA_c}{I_{trans,y}}
\end{aligned}
\tag{1}
$$

where

δ_{res}	=	high wall effect, resilience, [-]
δ_{slip}	=	slip in joint effect, [-]
A_c	=	cross-section area of the young concrete, [m^2]
A_{trans}	=	transformed cross-section area of the structure, [m^2]
$I_{trans,y}$	=	transformed second moment of inertia of the cross-section for bending around the y-axis, [m^4]
$I_{trans,z}$	=	transformed second moment of inertia of the cross-section for bending around the z-axis, [m^4]
γ_{RT}	=	translational boundary restraint, [-]
$\gamma_{RR,y}$	=	rotational boundary restraint for bending around the y-axis, [-]
$\gamma_{RR,z}$	=	rotational boundary restraint for bending around the z-axis, [-]
γ_{cen}	=	vertical location of the centroid of the transformed cross-section relatively the joint, [m]
γ	=	vertical co-ordinate from the joint and up-wards, [m]
z_{cen}	=	horizontal location of the centroid of the transformed cross-section relatively the centre of the slab, [m]
z	=	horizontal co-ordinate from the centre of the slab, [m]

The transformed cross-section properties as well as the location of the centroid are all calculated with the young concrete as the reference material, see Nilsson et al. (2003).

The high wall effect, resilience, is a correction factor for structures in which the strains do not vary linearly during the deformation, see Paper 1 by Nilsson et al. (2003) and below. For general cases subjected to some degree of boundary restraint, the resilience factor is determined as

$$\delta_{res} = \delta_{res}^0 \delta_{transl} \delta_{rot} \tag{2}$$

with

$$\delta_{transl} = \left(\gamma_{RT} + \left(1 - \gamma_{RT}\right)\delta_{transl}^0\right) \tag{3}$$

$$\delta_{rot} = \left(\gamma_{RR,z} + \left(1 - \gamma_{RR,z}\right)\delta_{rot}^0\right) \tag{4}$$

where

δ_{res}^0 = basic resilience factor, [-]
δ_{transl}^0 = basic resilience correction factor for translational boundary restraint, [-]
δ_{rot}^0 = basic resilience correction factor for rotational boundary restraint, [-]

which will be derived and more thoroughly described below.

In Nilsson et al. (2003) two simplified versions of the general semi-analytical method were presented for the typical case wall on slab, see Figure 1. The formulations assume rectangular cross-sections, horizontal joint between the wall and the slab, homogeneous and isotropic material in both parts and equal thermal contraction in the whole wall.

Paper B
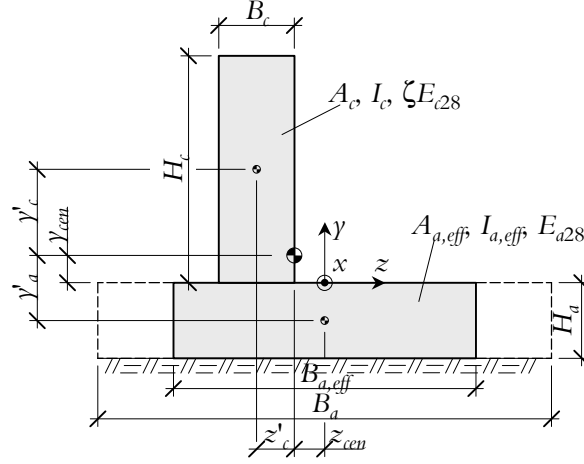
Figure 1 *Cross-section proerties used in the semi-analytical method for typical case wall on slab.*

The simplest expression does not use resilience and slip failure effects and is only applicable for structures not subjected to any boundary restraint. If the real width of slab is used and not the so-called effective width of slab that is introduced in Nilsson et al. (2003) and further explained and used below, the pure linear application of the semi-analytical method reads

$$
\gamma_R = 1 - \frac{1}{1 + \dfrac{E_{a28}}{\zeta E_{c28}} \dfrac{A_a}{A_c}}
$$
$$
- \frac{(\gamma_{cen} - \gamma)\left(\gamma_{cen} - \dfrac{H_c}{2}\right)}{\dfrac{H_c^2}{12} + \left(\gamma_{cen} - \dfrac{H_c}{2}\right)^2 + \dfrac{E_{a28}}{\zeta E_{c28}} \dfrac{A_a}{A_c}\left(\dfrac{H_a^2}{12} + \left(\gamma_{cen} + \dfrac{H_a}{2}\right)^2\right)}
$$
$$
- \frac{\left(z_{cen} - \omega\dfrac{B_a - B_c}{2}\right)^2}{\dfrac{B_c^2}{12} + \left(z_{cen} - \omega\dfrac{B_a - B_c}{2}\right)^2 + \dfrac{E_{a28}}{\zeta E_{c28}} \dfrac{A_a}{A_c}\left(\dfrac{B_a^2}{12} + z_{cen}^2\right)}
\qquad (5)
$$

where

E_{a28}	=	28 days modulus of elasticity of the adjacent older concrete, [N/m²]
ζE_{c28}	=	modulus of elasticity of the young concrete at the studied time, [N/m²]
A_a	=	real cross-section area of adjacent older concrete, [m²]
H_c	=	height of wall, [m]

75

H_a =   height of slab, [m]
B_c =   width of wall, [m]
B_a =   real width of slab, [m]
ω   =   relative location of wall on slab, see below, [-]

In Figure 2 an example of the restraint variation determined by Eq. (5) is shown for a 0.3m thick and 8m high wall located at the centre of a 1.4m high and 4m wide slab. The 28 days modulus of elasticity of the young and the old parts are set equal. Further, the maturity of the young concrete at the time of maximum crack risk is estimated by the factor ζ, which in this work has been given the value 0.93 according to Larson (2000). The figure 0.76 within the frame in Figure 2 marks a position one wall thick-ness above the upper surface of the slab − a position that in many practical applications has turned out to be an approximate critical design position in the wall.
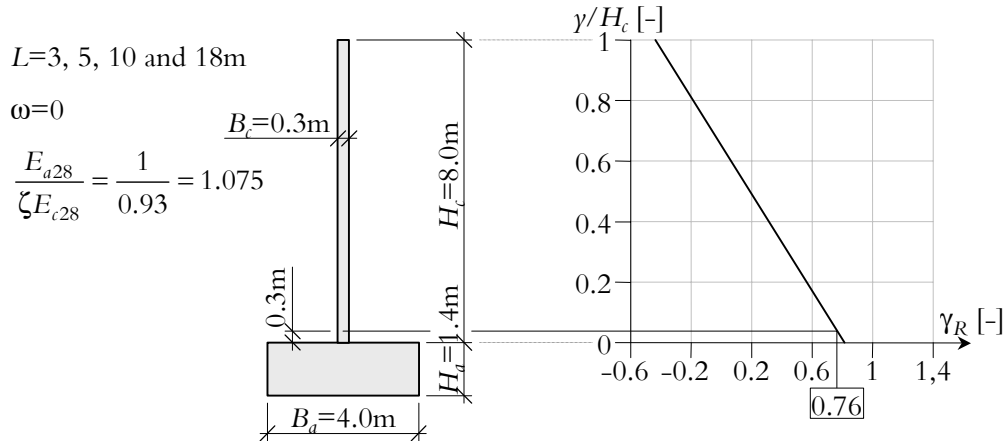
Figure 2 *Example of restraint distribution determined by Eq. (5) with the effective width of the slab set equal to the real width.*

Now one may ask oneself how well the restraint variation in Figure 2 corresponds with the real variations for the studied cross section and lengths. Calculations by Eq. (5) do not depend on the length of the structure. However, the length does influence. For short structures, or explicitly for structures with low length to height ratios, the strains over the height of the wall do not vary linearly, see Nilsson et al. (2003) and the subse-quent chapter. Further, if the slab is very wide compared to the wall, not the whole width of the slab influences the contraction of the wall. Instead, only an effective width of the slab affects the behaviour of the wall. In order to justify and improve the method it clearly has to be compared to some reference restraint variations, and adjustment tools of different kind are needed.

Paper B

2 REFERENCE RESTRAINT VARIATIONS

2.1 Restraint variations determined by Finite Element Method calculations

For the semi-analytical method presented in Nilsson et al. (2003) and further developed in this paper, finite element method (FEM) calculations have been chosen as a method of verifying and adjusting the method. Exactly 2920 elastic three-dimensional FEM calculations of the restraint variation in walls on slabs have been performed. The majority of the calculations were produced within the Brite-Euram Project IPACS (Improved Production of Advanced Concrete Structures), and the rest of the calculations were performed within the development of the semi-analytical method, see below for detailed description.
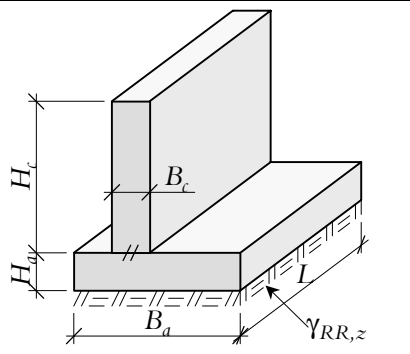
In all FEM calculations, the geometry of the structure has been varied as well as the rotational boundary restraint. The calculations were performed with the Dutch software DIANA. In the calculations, the temperature within the walls was lowered uniformly and linear elastic calculations were performed.

2.1.1 Input

The geometry of the wall on slab cases has been varied according to the following. Three different widths, B_a, and three different heights, H_a, of the slab have been used as well as three different widths, B_c, and five different heights of the wall, H_c. Four different lengths of the structure, L, and three different locations of the wall on the slab, ω, have been studied. Further, two different rotational boundary restraint situations have been regarded, $\gamma_{RR,z}$. All the parameters and their values are listed in Table 1. The coefficient ω describes the relative location of the wall on the slab. $\omega = 0$ means that the wall is centrically located on the slab and $\omega = \pm 1$ means the wall is located at one of the edges of the slab.

Table 1 List of parameters and their values used in the Finite Element Method calculations of the elastic restraint variations in the walls of wall-on-slab structures.

Parameter	Values	Num. of values
B_a [m]	2, 4, 8	3
H_a [m]	0.4, 1, 1.4	3
B_c [m]	0.3, 1, 1.8	3
H_c [m]	0.5, 1, 2, 4, 8	5
L [m]	3, 5, 10, 18	4
$\gamma_{RR,z}$ [–]	0, 1	2
ω [–]	0, 0.5, 1	3

77

In the calculations the modulus of elasticity of the slab was $E_{a28} = 30 \cdot 10^9$ N/m^2 and of the wall $\zeta E_{c28} = 27.9 \cdot 10^9$ N/m^2. The Poisson's ratio $\nu = 0.2$, the density $\rho = 2350$ kg/m^3 and the thermal dilation coefficient of the wall $\alpha = 1 \cdot 10^{-5} \, ^\circ$C^{-1}.

Due to symmetry, only half of the length of the structures was studied. For the cases with the walls located at the centre of the slabs, only one fourth of the structures was studied due to the double symmetry. For all calculations two different rotational boundary restraint cases have been studied, viz. free rotation $\gamma_{RR,z} = 0$ and totally hindered rotation $\gamma_{RR,z} = 1$, see Figure 3.
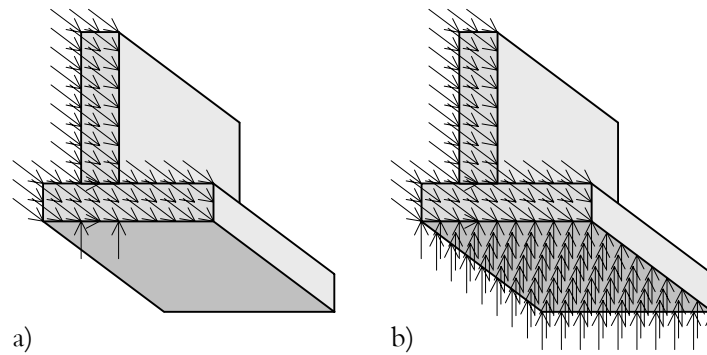
Figure 3 *Description of the constraints in the FEM calculations for the boundary conditions a) free rotation, $\gamma_{RR,z} = 0$, and b) totally hindered rotation, $\gamma_{RR,z} = 1$.*

The calculations were performed using eight-node isoparametric solid brick elements based on linear interpolation and Gauß integration. In all calculations the walls were subjected to a uniform temperature decrease of 10°C. The imposed temperature load was applied in each element as a momentary change of the temperature.

The total number of possible calculations is

$$n_{calc,possible} = 3 \cdot 3 \cdot 3 \cdot 5 \cdot 4 \cdot 2 \cdot 3 = 3240$$

but for $\omega = 0.5$ not all possible cases were calculated. Excluded were the cases with 1 and 1.8 m wide walls on 2 m wide slabs as well as 1 and 1.8 m wide walls on 8 m wide and 0.4 m thick slabs. The number of excluded calculations is

$$n_{excl} = (\underset{H_a}{3} \cdot \underset{B_c}{2} + \underset{H_a}{1} \cdot \underset{B_c}{2}) \cdot \underset{H_c}{5} \cdot \underset{L}{4} \cdot \underset{\gamma_{RR}}{2} = 320$$

which gives the total number of calculations

Paper B

$$n_{calc,performed} = n_{calc,possible} - n_{excl} = 3240 - 320 = 2920$$

2.1.2 Output

From the FEM calculations, the variations of the strain in the nodes along the line of symmetry (middle of the walls of the structures), ε_x, ε_y and ε_z, were stored. These strains have been used to determine the restraint variation by calculating the ratio between the stresses in the longitudinal direction and the one-dimensional stress at total fixation of the applied temperature decrease according to

$$\gamma_R = \frac{\sigma_{zz}}{\sigma^0} = \frac{\dfrac{\zeta E_{c28}}{1+\nu}\left(\varepsilon_z + \dfrac{\nu}{1-2\nu}\left(\varepsilon_x + \varepsilon_y + \varepsilon_z\right)\right) - \dfrac{\zeta E_{c28}\alpha\Delta T}{1-2\nu}}{\zeta E_{c28}\alpha\Delta T} \tag{6}$$

This formula implies that if no external strains are present ($\varepsilon_x = \varepsilon_y = \varepsilon_z = 0$) the restraint is exactly $1/(1-2\nu) = 1.67$. Normally the maximum amount of restraint is defined being exactly 1, but with three-dimensional FEM calculations as reference to a method applicable for one-dimensional crack risk analyses the restraint may be larger than 1 depending on the Poisson's ratio.

The values of the restraint determined by the FEM calculations have been plotted in diagrams as function of the relative distance above the joint between the walls and slabs, see Nilsson (2003). In each diagram, structures with the same cross-section but different lengths and rotational boundary restraint situations are presented.

In Figure 4 the restraint variation obtained by FEM calculations is shown for the wall on slab structure in Figure 2. In the figure only the restraint variations for the cases with no rotational boundary restraint $\gamma_{RR,z} = 0$ are shown. For $\gamma_{RR,z} = 1$, see Nilsson (2003). It is clearly seen that for the two shorter structures, $L = 3$ and 5 m, the high wall effects have great influence with non-linearly varying restraint due to the non-linearly varying strain. On the opposite, in the longest structure the strain varies linearly implying that the Compensation Plane theory is valid. This is also shown by the closeness to the straight dotted line showing the restraint variation in Figure 2 determined by Eq. (5).
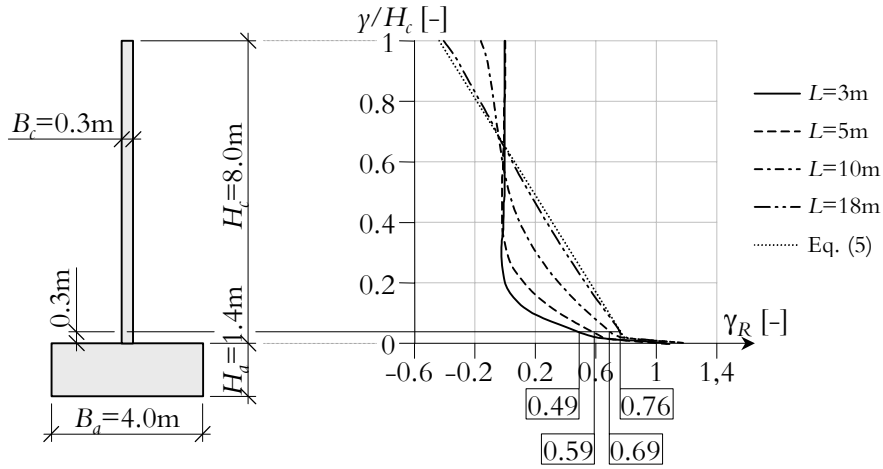
Figure 4 *The restraint distribution in the shown wall determined by 3D elastic FEM calculations for the lengths L = 3, 5, 10 and 18 m, see Nilsson (2003).*

From the results shown in Figure 4 it is clear that the need of some additional adjustment of the formulation in Eq. (5) is needed, especially for the structures exposed to high wall effects, the resilience.

3   ADJUSTMENT TOOLS

The application of the semi-analytical method needs, as been indicated above, a number of adjustment tools to obtain more correct restraint values for a wider range of structures. The determination of the adjustment tools will follow the same steps as they are used in restraint determination by the semi-analytical method.

The calculation of the restraint variation by the semi-analytical method is based on a number of consecutive steps, see Nilsson et al. (2003) for brief and general outline of the method. Firstly, the amount of boundary restraint has to be determined. Secondly, depending on the amount of boundary restraint, the resilience variation is determined by finding the basic resilience and basic resilience correction factors. Thirdly, the effective width of the slab has to be estimated. Finally, effects of possible slip failure at the joints between the walls and the slab are regarded.

3.1   Effects of high walls

As was shown in Figure 4 the restraint variation determined by Eq. (5) does not correspond to the variations determined by FEM calculations. Adapting the so-called high wall effects or resilience factor is the first and most important correction. In Nilsson et al. (2003) the concept of resilience were thoroughly described. In this paper additional basic resilience curves will be presented that are needed for adjustment of the semi-

analytical method to the reference restraint variations determined by the FEM calculations.

3.1.1 Basic resilience

In Nilsson et al. (2003) two different sets of basic resilience curves were presented, the first from ACI (1995) and the second from Emborg (1989). Below, the determination of four new resilience curves for base restrained walls for L/H_c = 0.25, 0.5 and L/H_c = 10 and 40 are presented. The determination of new resilience curves has been performed by elastic two-dimensional finite element method calculations by use of the Dutch software DIANA.

In the calculations a wall with the length L = 0.25, 0.5, 10 and 40m and the height H_c = 1m was used. The modulus of elasticity of the wall was ζE_{c28} = 22.5·10^9 Pa. The Poisson's ratio was ν = 0.2, the density ρ = 2350 kg/m^3 and the thermal dilation coefficient α = 1·10^{-5}°C^{-1}. The calculations were performed using eight-node quadrilateral isoparametric plane stress elements, which is based on quadratic interpolation and Gauß integration.

Due to symmetry, only half of the lengths of the walls were studied. The base of the wall was totally restrained both for bending and for translation, that is γ_{RT} = $\gamma_{RR,z}$ = 1, see Figure 5. In all calculations the walls were subjected to a temperature decrease of magnitude 10°C. The temperature load was applied in each element as a momentary change.
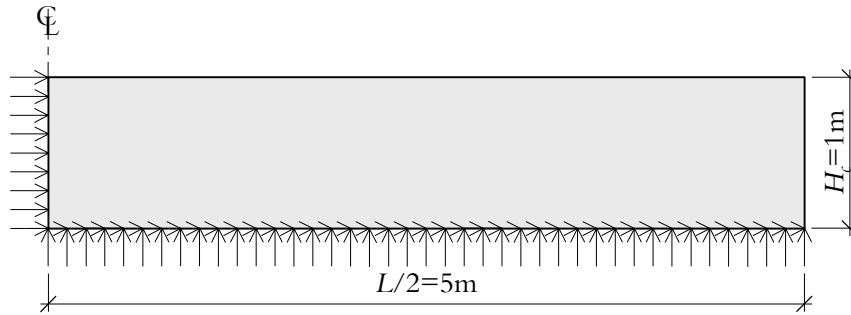
Figure 5 *Principle description of constraints in the FEM calculations for a wall with L/H_c = 10 and the boundary condition $\gamma_{RR,z}$ = 1.*

In the same way as for the FEM calculations of the restraint variation, the variations of the strain in the nodes along the line of symmetry (middle of the walls of the structures), ε_x, ε_y and ε_z, were stored. The strains in each node in the mid-section of the wall were then used to determine the restraint distribution. The determination is done

according to Eq. (6) giving the basic resilience curves shown in Figure 6 for L/H_c = 0.25, 0.5, 10 and 40, which are marked with bolder lines.
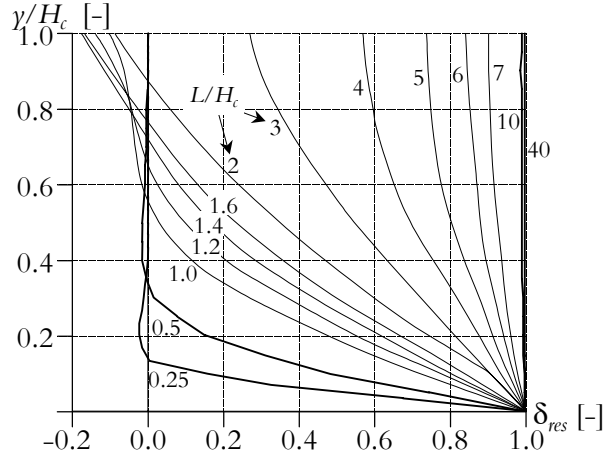
Figure 6 *Completed basic resilience factor δ^0_{res}, marked with bold lines, for L/H_c = 0.25, 0.5, 10 and 40 as function of the relative distance above the joint. Existing curves, marked with thin lines, according to Emborg (1989).*

For application purposes in the semi-analytical method the curves in Figure 6 can be described by polynomials of seventh order according to

$$\delta^0_{res}\left(\frac{\gamma}{H_c}\right) = a_0 + a_1\left(\frac{\gamma}{H_c}\right) + a_2\left(\frac{\gamma}{H_c}\right)^2 + a_3\left(\frac{\gamma}{H_c}\right)^3 + a_4\left(\frac{\gamma}{H_c}\right)^4$$
$$+ a_5\left(\frac{\gamma}{H_c}\right)^5 + a_6\left(\frac{\gamma}{H_c}\right)^6 + a_7\left(\frac{\gamma}{H_c}\right)^7 = \sum_{i=0}^{7} a_i\left(\frac{\gamma}{H_c}\right)^i$$

(7)

with coefficients according to Table 2.

Table 2 *Coefficients for polynomials describing the basic resilience curves in Figure 6.*

L/H_c		Coefficients						
	a_0	a_1	a_2	a_3	a_4	a_5	a_6	a_7
0.25	1	–14.43	73.76	–167.6	152.5	19.93	–117.5	52.36
0.5	1	–5.961	7.786	12.14	–30.91	5.168	24.24	–13.46
1	1	–3.112	1.913	1.863	–1.746	0	0	0
1.2	1	–2.392	0.227	3.072	–2.038	0	0	0
1.4	1	–1.907	–0.362	2.700	–1.588	0	0	0
1.6	1	–1.690	–0.304	1.907	–1.062	0	0	0
2	1	–1.238	–0.541	1.158	–0.441	0	0	0
3	1	–0.912	–0.041	0.189	0.054	0	0	0
4	1	–0.641	0.131	0.026	0.063	0	0	0
5	1	–0.387	0.036	0.132	–0.031	0	0	0
6	1	–0.206	–0.197	0.455	–0.202	0	0	0
7	1	–0.185	0.222	–0.253	0.127	0	0	0
10	1	–0.019	0.007	0	0	0	0	0
40	1	0	0	0	0	0	0	0

With use of the resilience curves in Figure 6 expressed by polynomials according to Eq. (7) and solving Eq. (1) the following expression is given for determination of restraint distributions in structures with high wall effects and subjected to no boundary restraint $\gamma_{RT} = \gamma_{RR,y} = \gamma_{RR,z} = 0$, see Nilsson et al. (2003),

$$
\gamma_R = \sum_{i=0}^{n} a_i \left(\frac{\gamma}{H_c} \right)^i - \frac{\displaystyle\sum_{i=0}^{n} \frac{a_i}{i+1}}{1 + \dfrac{E_{a28}}{\zeta E_{c28}} \dfrac{A_a}{A_c}}
$$

$$
- \frac{(\gamma_{cen} - \gamma)\left(\gamma_{cen} \displaystyle\sum_{i=0}^{n} \frac{a_i}{i+1} - H_c \sum_{i=0}^{n} \frac{a_i}{i+2} \right)}{\dfrac{H_c^2}{12} + \left(\gamma_{cen} - \dfrac{H_c}{2} \right)^2 + \dfrac{E_{a28}}{\zeta E_{c28}} \dfrac{A_a}{A_c} \left(\dfrac{H_a^2}{12} + \left(\gamma_{cen} + \dfrac{H_a}{2} \right)^2 \right)}
$$

$$
- \frac{\left(z_{cen} - \omega \dfrac{B_a - B_c}{2} \right)^2}{\dfrac{B_c^2}{12} + \left(z_{cen} - \omega \dfrac{B_a - B_c}{2} \right)^2 + \dfrac{E_{a28}}{\zeta E_{c28}} \dfrac{A_a}{A_c} \left(\dfrac{B_a^2}{12} + z_{cen}^2 \right)}
$$

(8)

where $i = 0, 1, \ldots n$ = degree of the polynomial with coefficients $a_i - a_n$. In this paper $n = 7$, see Table 2.

With the coefficients in Table 2 the restraint distributions for the structures in Figure 2 are calculated giving the results shown in Figure 7. Compared to the linear variation in Figure 2 the curves determined with Eq. (8) show a considerable improvement, i.e. a better agreement with expected real behaviour, achieved only by use of the resilience curves. However, there are still some differences between the curves obtained by Eq. (8) and by the FEM calculations, which are shown with thinner lines in the diagram in Figure 7. Further improvements are needed.
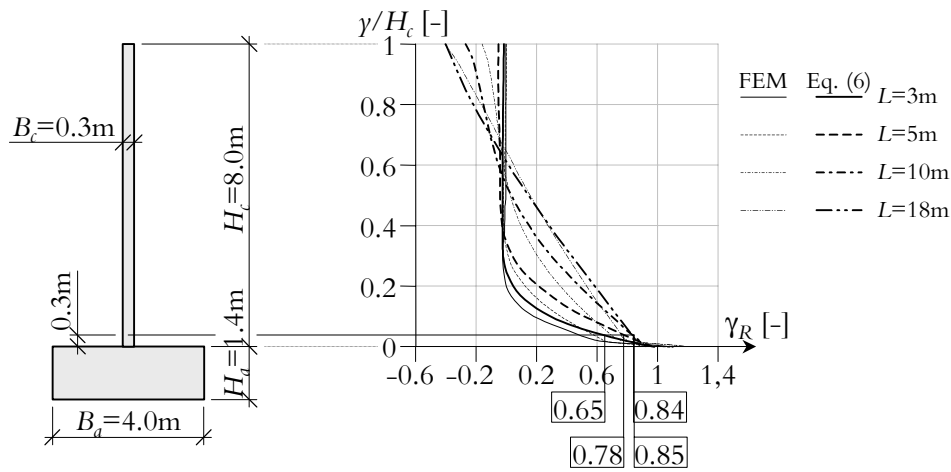

Figure 7 *Restraint distribution by use of resilience determined according to Eq. (8) with coefficients from Table 2.*

3.2   Effective width of slab

The restraint curves obtained with Eq. (8) and shown in Figure 7 give higher restraint values in the lower part of the wall than the curves from the FEM calculations. The lower part of the wall is of course the most interesting part regarding crack risk analyses. In this particular, case this difference is on the safe side, but that may not always be the case. As been described in Nilsson et al. (2003) and mentioned above, the so-called effective width of the slab is introduced as a model parameter to adjust the semi-analytical method to the reference restraint distributions from the FEM calculations.

Below, a description is presented of the determination of the effective width for the FEM-calculations with centrically located walls on slabs subjected to no boundary restraint. For other cases of boundary restraint, the so-called resilience correction factors δ_{transl} and δ_{rot} are used, see Nilsson et al. (2003) and below. The values of the effective width are stored in a database, see Nilsson (2003), that is used to give values for the semi-analytical method for structures different from the ones in the FEM calculations.

Paper B

3.2.1 Determination of effective width of slab

The determination of the effective width of slab $B_{a,eff}$ has been performed by varying the width of the slab in the semi-analytical method and comparing the restraint distribution with the results from the FEM calculations. Using the least square method for the difference in the restraint values over the height of the wall is expressed by

$$\min\left(\sum_{i=1}^{n}(\Delta\gamma_R)^2\right) = \min\left(\sum_{i=1}^{n}\left(\gamma_{R,FEM,i} - \gamma_{R,semi,i}\right)^2\right) \tag{9}$$

where $i = 1, 2, \dots n$ = number of nodes in the FEM calculations. The values of the effective width of slab for all the different geometries in the FEM calculations, see above, have been gathered in groups of nine structures with the same real width of the slab, B_a, the same height of the wall, H_c, and the same length of the structure, L. The values in each group were then sorted by a parameter X calculated as

$$X = \frac{\zeta E_{c28}A_c}{E_{a28}A_a}\frac{L}{H_c} = \frac{0.93 E_{c28}B_c H_c}{E_{a28}B_a H_a}\frac{L}{H_c} = 0.93\frac{B_c L}{B_a H_a} \tag{10}$$

where 0.93 is the value of the 28-days value of the modulus of elasticity of the concrete in the wall, see above. The 28-days values of the modulus of elasticity in the walls and the slabs are set to be equal.

3.2.2 Modelling of effective width of slab

By plotting the obtained values of the effective width as a function of the parameter X, fairly clear relations for each group of nine values of the effective width have been found. In order to get applicable relations for the determination of the effective width when using the semi-analytical method, functions based on polynomials of fourth order according to

$$B_{a,eff} = b_0 + b_1 X + b_2 X^2 + b_3 X^3 \tag{11}$$

have been established for the groups of nine values of the effective width. The establishment of the polynomials was done by use of regression analysis, where $b_0 - b_3$ are the coefficients for the polynomials, see below.

3.2.3 Results

In Nilsson (2003), the effective width as function of the parameter X is presented graphically. In the graphs, both the evaluated values of the effective width, and the corresponding values obtained by the polynomials for the same values of X, are plotted, see the example in Figure 8. In addition, the coefficients $b_0 - b_3$ of the polynomials for

each set of data are given together with the numerical values of the effective width be-hind each graph.

The most values of the effective width have been possible to use in the determination of the polynomials, however, not all. Some of the values have been too far away from the rest of the values in the groups of nine. Therefore, these values have been excluded in the establishing of the polynomials. The reason for this might originate from the iteration procedure when determining the values of the effective width of slab. In some cases several values of the effective width of slab gave almost the same restraint variations and which of the values to choose have not been studied in detail within this work.

In Figure 8 an example is shown of the effective width as function of the parameter X for structures with 4 m wide slab, 8 m high wall and that are 5 m long. In the figure both the values from the evaluation of the FEM data are shown as well as the values from the established polynomial, Eq. (11). It is seen that there is a clear relation between the effective width of slab and the parameter X for this group of nine values. Similar relations are found for each and every set of values, see Nilsson (2003).

$$B_{a,eff} = 0.405 + 0.722X + 0.081X^2 - 0.003X^3$$
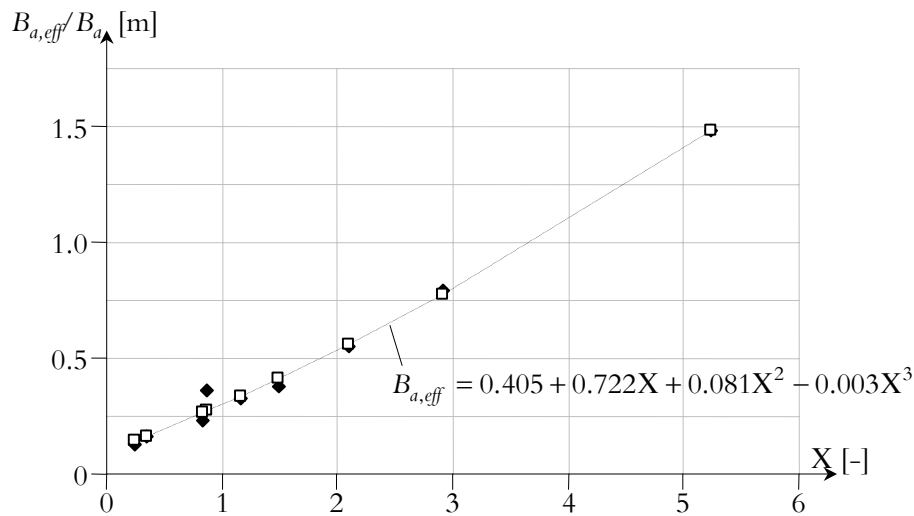
Figure 8 *Example of the effective width to real width as function of the paprmeter X for B_a = 4m, H_c = 8m and L = 5m.*

As an example of results, the calculations of the effective widths from the FEM calculations showed that for the actual structure, $B_{a,eff}$ = 0.531, 0.532, 0.682 and 1.655 m for L = 3, 5, 10 and 18 m, respectively. With coefficients from Nilsson (2003) for the polynomial in Eq. (11) the effective width of slab is calculated giving $B_{a,eff}$ = 0.523, 0.590, 0.829 and 1.956 m for L = 3, 5, 10 and 18 m respectively. The differences be-

tween these values are 1.6, 10.9, 21.6 and 18.2 %, which might seem large, but compared to the real width of the slab this corresponds to 0.2, 1.5, 3.7 and 7.5 %, respectively. With the introduction of the effective width of slab, $B_{a,eff}$, and corresponding effective area of slab, $A_{a,eff}$, Eq. (8) reads

$$
\gamma_R = \sum_{i=0}^{n} a_i \left(\frac{\gamma}{H_c} \right)^i - \frac{\displaystyle\sum_{i=0}^{n} \frac{a_i}{i+1}}{1 + \dfrac{E_{a28}}{\zeta E_{c28}} \dfrac{A_{a,eff}}{A_c}}
$$

$$
- \frac{(\gamma_{cen} - \gamma)\left(\gamma_{cen} \displaystyle\sum_{i=0}^{n} \frac{a_i}{i+1} - H_c \displaystyle\sum_{i=0}^{n} \frac{a_i}{i+2} \right)}{\dfrac{H_c^2}{12} + \left(\gamma_{cen} - \dfrac{H_c}{2} \right)^2 + \dfrac{E_{a28}}{\zeta E_{c28}} \dfrac{A_{a,eff}}{A_c} \left(\dfrac{H_a^2}{12} + \left(\gamma_{cen} + \dfrac{H_a}{2} \right)^2 \right)}
$$

$$
- \frac{\left(z_{cen} - \omega \dfrac{B_{a,eff} - B_c}{2} \right)^2}{\dfrac{B_c^2}{12} + \left(z_{cen} - \omega \dfrac{B_{a,eff} - B_c}{2} \right)^2 + \dfrac{E_{a28}}{\zeta E_{c28}} \dfrac{A_{a,eff}}{A_c} \left(\dfrac{B_{a,eff}^2}{12} + z_{cen}^2 \right)}
$$

(12)

that for the earlier studied example yields the restraint distributions depicted in the diagram in Figure 9. Now the agreement with the reference curves from the FEM calculations is quite acceptable, especially for $\gamma_R > 0$ (= tensile stresses).
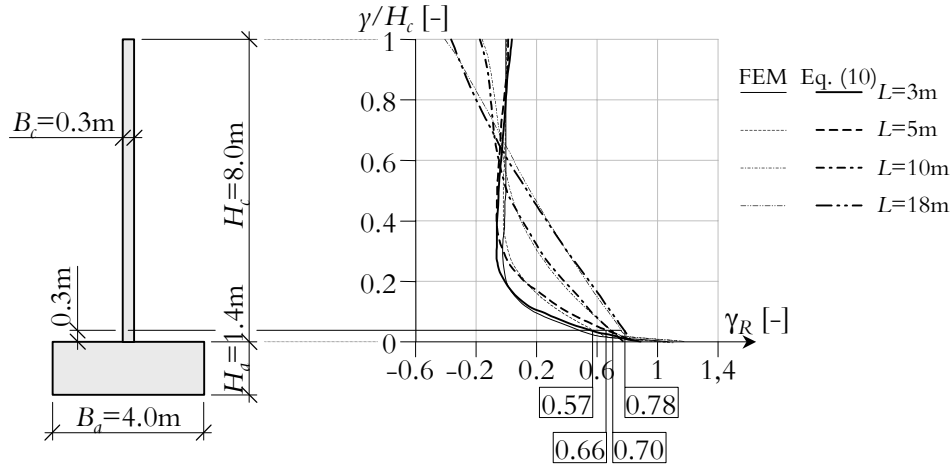

Figure 9 *Restraint distributions determined with resilience curves and effective width of slab according to Eq. (12).*

3.2.4 Walls not located at the centre of slabs

For structures with walls not located at the centre of the slab, the same type of calcula-tions as above have been carried trough with one additional adjustment of the effective width of the slab. In the determination of the effective width of slab, it was found that the values vary depending on the location of the walls on the slabs. In Nilsson (2003) the ratio between the effective width of slab for the un-symmetrically located walls, ω = 0.5 and 1, and the symmetrically located walls, ω = 0, of the same cross-section pa-rameters have been determined as

$$\omega_{corr} = \frac{B_{a,eff}(\omega \neq 0)}{B_{a,eff}(\omega = 0)} \tag{13}$$

Then for un-symmetrically located walls on slabs the effective width of slab is de-termined by these values of ω_{corr} that can be found in Nilsson (2003). Unfortunately, at present no simplifying relations for the determination of ω_{corr} have been found similar to what was established for the determination of the effective width of slab.

An example of the restraint variations from the FEM calculations and from the semi-analytical method determined with Eqs. (10) – (13) is shown in Figure 10. In this case ω_{corr} = 0.66, 0.67, 0.59 and 0.29 and consequently $B_{a,eff}$ = 0.345, 0.394, 0.487 and 0.563 m for L = 3, 5, 10 and 18 m, respectively. From comparison between Figure 9 and Figure 10 it is evident that the rather small differences from the FEM calculations are quite similar in both cases.
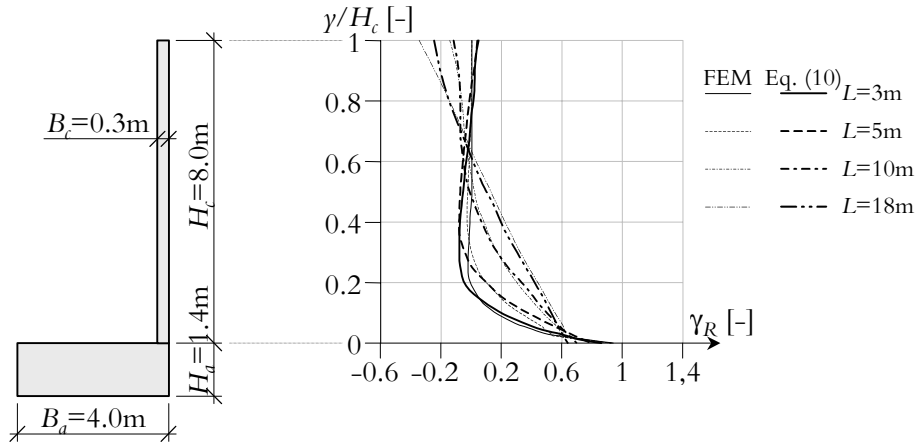

Figure 10 *Example of restraint distributions determined by Eq. (12) and ω_{corr} for a un-symmetrically located wall on slab structure.*

Paper B

3.3 Boundary restraint

The boundary restraint within this work is divided into a translational part γ_{RT} and two rotational parts $\gamma_{RR,y}$ and $\gamma_{RR,z}$. The rotational boundary restraint against rotation around the y-axis is set to be zero, $\gamma_{RR,y} = 0$, as it is assumed that the torsion of the structure on the ground is not hindered at all. This is assumed to be an acceptable simplification in cases where the subgrade consists of frictional/cohesive material like gravel, sand, clay, etc. The two other boundary restraint parts are coefficients that vary between 0 and 1 and can be determined according to different existing methods.

The rotational boundary restraint can be described by a modulus of subgrade reaction, see below, and the translational boundary restraint by friction analysis.

3.3.1 Rotational boundary restraint

The rotational boundary restraint against bending around the z-axis, see Figure 1, can be determined by different methods, e.g. from expressions for beams on elastic foundations valid for structures founded on elastic materials described by a modulus of compaction, see Bernander (1993) and Nilsson (1998 & 2000). In this case the rotational boundary restraint coefficient, $\gamma_{RR,z}(x)$, at any point along a structure is expressed by

$$
\begin{aligned}
\gamma_{RR,z}(x) = 1 - \frac{2}{\left(\sin \dfrac{L}{L_e} + \sinh \dfrac{L}{L_e} \right)} \\
\left\{ \left(\cos \frac{L}{2L_e} \sinh \frac{L}{2L_e} + \sin \frac{L}{2L_e} \cosh \frac{L}{2L_e} \right) \cos \frac{x}{L_e} \cosh \frac{x}{L_e} \right. \\
\left. - \left(\cos \frac{L}{2L_e} \sinh \frac{L}{2L_e} - \sin \frac{L}{2L_e} \cosh \frac{L}{2L_e} \right) \sin \frac{x}{L_e} \sinh \frac{x}{L_e} \right\}
\end{aligned}
\tag{14}
$$

where L_e is the so-called elastic length that is calculated as

$$
L_e = \sqrt[4]{\frac{2\zeta E_{c28} I_{trans,z} \kappa}{K_j}}
\tag{15}
$$

where

κ =   a shape factor for the surface resting on the ground, see below, [-]
K_j =   modulus of compression, [N/m^2]

The expression for the rotational boundary restraint generally originates from analysis of deformations for beams on elastic foundation loaded by equal and opposite bending moments at the ends, see Timoshenko (1958) and Nilsson (2000). From Eq. (14) it

can be seen that the rotational boundary restraint only depends on the length to elastic length ratio, which makes the expression very applicable. In the mid-section of a structure, $x = 0$, which in almost all cases is the decisive section, Eq. (14) is simplified to

$$\gamma_{RR,z} = 1 - \frac{2}{\sin\dfrac{L}{L_e} + \sinh\dfrac{L}{L_e}}\left(\cos\frac{L}{2L_e}\sinh\frac{L}{2L_e} + \sin\frac{L}{2L_e}\cosh\frac{L}{2L_e}\right) \qquad (16)$$

Different types of soils give different resistance on compressive loading depending on the degree of compaction. Examples of the modulus of compression for different types of foundation materials at different degrees of compaction, like soft, semi-solid, dense, are given in Table 3. Higher degree of compaction leads to higher modulus of compression.

Table 3 *Modulus of compression, K_j, for different types of foundation materials, from Bernander (1993) and Nilsson (2000).*

Type of soil and compaction	K_j [MN/m^2]
Clay, soft	0.5 – 2
Clay, semi-solid	1 – 3
Clay, sandy and silty	2 – 5
Sand, soft	3 – 10
Sand, medium dense to dense	10 – 60
Gravel, medium dense to dense	10 – 60

The shape factor κ in Eq. (15) can be determined according to for instance Löfling (1993) where it depends on the ratio between the width of the slab and the length of the slab, B_a/L, see Table 4.

Table 4 *The shape factor κ as function of the width to length ratio of the structure member resting on the ground, see Löfling (1993).*

B_a/L	0.2	0.4	0.6	0.8	1.0
κ	0.94	0.83	0.75	0.69	0.65

From Eq. (14) the length to elastic length ratio of structures that correspond to values of rotational boundary restraint between 0 and 100% have been calculated. The results depicted in Figure 11 for $x = 0$, $\pm0.1L$, $\pm0.2L$, $\pm0.3L$ and $\pm0.4L$ can be used to determine the rotational boundary restraint for a structure with given geometry that is founded on an elastic material with given modulus of compression.

Figure 11 *The rotational boundary restraint coefficient* $\gamma_{RR,z}(x)$ *as function of the length to elastic length ratio of the structure* L/L_e. *Nilsson (2000).*

For structures founded on rock or very stiff materials, it is also possible to estimate the rotational boundary restraint assuming no cohesion and/or friction between the concrete and sub-ground, Nilsson (2000). For such structures the ends tend to lift after the temperature maximum is reached and the cooling phase has started. Only the bending moment from the dead weight and the length of a structure counteracts the lifting. Further, by combining Eq. (14) for structures on elastic foundations with a formulation for structures on very stiff materials, cases of possible lifting ends of structures can also

be solved. In Nilsson (2000) this case is thoroughly studied and an explicit expression and a corresponding diagram are presented for determination of the rotational boundary restraint.

The determination of the rotational boundary restraint coefficient as stated above is a quite straightforward method and rather simple by use of Eq. (14) and/or Figure 11. A general three-dimensional presentation of the rotational boundary restraint coefficient can be drawn from Figure 11 for structures with no lifting ends, see Nilsson (2000) and Figure 12. In the figure it can be seen that with higher length to elastic length ratio in combination with the proximity to the midsection of the structure, the higher the rotational restraint coefficient will be.

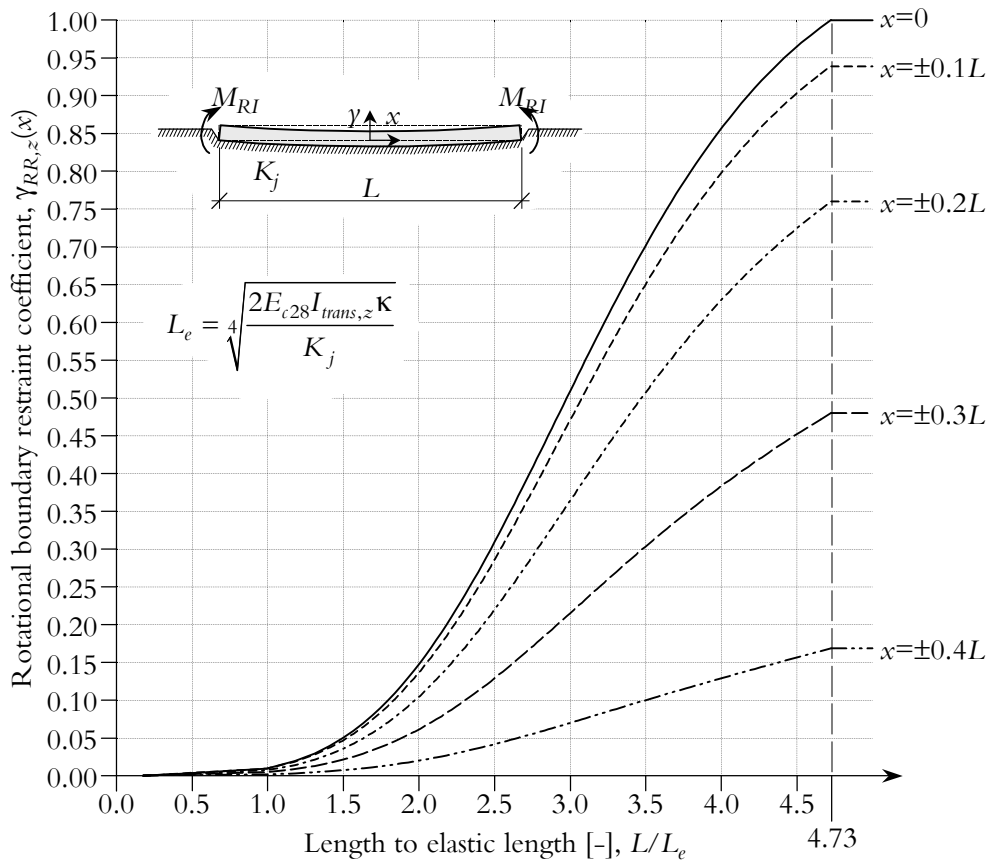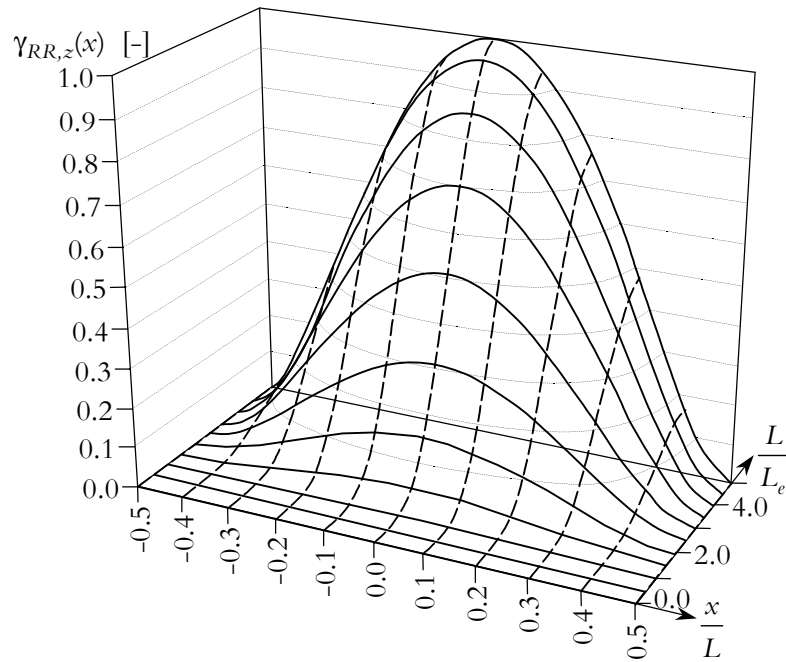**Figure 12** *Three-dimensional presentation of the rotational boundary restraint coefficient, $\gamma_{RR,z}(x)$, as function of the length to elastic length ratio, L/L_e, and the distance from the midsection of the structure, x. Nilsson (2000).*

The rotational boundary restraint can now be calculated for the example studied earlier. Assume that the slab is founded on dense gravel with modulus of compression $K_j = 60$ MN/m^2 and that the modulus of elasticity of the wall $\zeta E_{c28} = 27900$ MN/m^2. Further, the second moment of inertia of the cross-section $I_{trans,z} = 51.7$ m^4, $\kappa = 0.61$, 0.69, 0.83 and 0.93, respectively (by interpolation in Table 4). All these data used in Eq. (15) give the elastic lengths $L_e = 13.32$, 13.75, 14.39 and 14.79 m for $L = 3$, 5, 10

and 18 m, respectively. The rotational boundary restraint coefficient is then calculated by Eq. (16) giving $\gamma_{RR,z}$ = 2.7·10^{-5}, 1.8·10^{-4}, 2.4·10^{-3} and 2.2·10^{-2} for L = 3, 5, 10 and 18 m, respectively. These values are very small and in this particular case the rotational boundary restraint coefficient can be neglected, i.e. $\gamma_{RR,z}$ = 0 is a good approximation for the studied structure.

3.3.2 Translational boundary restraint

The translational boundary restraint coefficients can be determined by different methods, see e.g. Pettersson (1996 & 1998), Rostásy et al. (2001) and Bernander (2001).

In Rostásy et al. (2001) the three-layer method that assumes full interaction between a slab, a possible blinding and the ground is introduced. The model is derived under the assumption that plane sections remain plane, which involves very high degrees of boundary restraint. On the contrary, Bernander (2001) shows by basic and classic theory of elasticity that for the typical case wall on slab, the translational boundary restraint in the mid-section can be neglected for reasonable long structures. Based on the findings according to Bernander (2001) γ_{RT} = 0 is chosen as a good approximation.

3.4 Resilience correction

In cases where the boundary restraint is not negligible, the high wall effects, the resilience, depend, see Nilsson et al. (2003), on the degree of boundary restraint and is calculated as

$$\delta_{res} = \delta_{res}^0 \delta_{transl} \delta_{rot} \tag{17}$$

with

$$\delta_{transl} = \gamma_{RT} + \left(1 - \gamma_{RT}\right)\delta_{transl}^0 \tag{18}$$

$$\delta_{rot} = \gamma_{RR,z} + \left(1 - \gamma_{RR,z}\right)\delta_{rot}^0 \tag{19}$$

where

δ_{res}^0 $\quad$ = basic resilience factor, see Figure 6[–]

δ_{transl}^0 $\quad$ = basic resilience correction factor for translational boundary restraint, [–]

δ_{rot}^0 $\quad$ = basic resilience correction factor for rotational boundary restraint, [–]

In cases with free translation and free rotation, i.e. γ_{RT} = $\gamma_{RR,z}$ = 0, Eq. (17) becomes

$$\delta_{res} = \delta_{res}^0 \delta_{transl}^0 \delta_{rot}^0 \tag{20}$$

For no boundary restraint the 3D effect is considered only by introducing an effective width of the slab $B_{a,eff}$, which means that formally $\delta^0_{transl}\delta^0_{rot} \equiv 1$ in this case. So, the basic resilience correction factor for rotation is determined as the inverse of the basic resilience correction factor for translation by

$$\delta_{rot}^0 = \frac{1}{\delta_{transl}^0} \tag{21}$$

This relation is used in the determination of the basic correction factor for bending for structures subjected to rotational boundary restraint, see below.

The last case rises at total boundary restraint, $\gamma_{RT} = \gamma_{RR,y} = \gamma_{RR,z} = 1$, that with Eq. (17) in Eq. (1) gives

$$\gamma_R = \delta_{res}^0 \tag{22}$$

which exactly corresponds to the methodology in i.e. ACI (1995) for base restraint walls, see Figure 6.

3.4.1 Determination of basic resilience correction for translational boundary restraint

The determination of the basic resilience correction factors for translational boundary restraint has been done by evaluating the restraint distributions from the results of the FEM calculations with $\gamma_{RT} = 0$, $\gamma_{RR,z} = 1$ and $\delta_{slip} = 1$, see Nilsson (2003). The high wall effects are calculated from Eq. (17) giving

$$\delta_{res} = \delta_{res}^0\left(\frac{\gamma}{H_c}\right)\delta_{transl}^0\left(\frac{\gamma}{H_c}\right) \tag{23}$$

where $\delta_{res}^0\left(\dfrac{\gamma}{H_c}\right)$ is calculated by Eq. (7) with coefficients from Table 2. $\delta_{transl}^0\left(\dfrac{\gamma}{H_c}\right)$ is then determined by application of Eq. (1) with $\gamma_{RT} = 0$, $\gamma_{RR,z} = 1$, $\delta_{slip} = 1$ and Eq. (23) is transformed to

$$\gamma_R = \delta_{res}^0\left(\frac{\gamma}{H_c}\right)\delta_{transl}^0\left(\frac{\gamma}{H_c}\right) - \frac{\int_{A_c} \delta_{res}^0\left(\frac{\gamma}{H_c}\right)\delta_{transl}^0\left(\frac{\gamma}{H_c}\right)dA_c}{A_{trans}} \tag{24}$$

94

Thereafter, as the distribution of the restraint factor, $\gamma_{R,j}$, is known from the FEM calculations, the values of $\delta^0_{transl}\left(\dfrac{\gamma_j}{H_c}\right)$ can be established point-by-point ($j = 1, \ldots,$ n) using Eq. (24) expressed as

$$\delta^0_{transl}\left(\frac{\gamma_j}{H_c}\right) = \frac{\gamma_{R,j}}{\delta^0_{res}\left(\dfrac{\gamma_j}{H_c}\right) - \dfrac{1}{A_{trans}}\displaystyle\int_{A_c}\delta^0_{res}\left(\dfrac{\gamma}{H_c}\right)dA_c} \tag{25}$$

which by introducing Eq. (7) finally gives

$$\delta^0_{transl}\left(\frac{\gamma_j}{H_c}\right) = \frac{\gamma_{R,j}}{\displaystyle\sum_{i=0}^{7}a_i\left(\frac{\gamma_j}{H_c}\right)^i - \frac{A_c}{A_{trans}}\sum_{i=0}^{7}\frac{a_i}{i+1}} \tag{26}$$

For each set of restraint variations obtained in the FEM calculations with the rotational boundary restraint $\gamma_{RR,z} = 1$, see chapter 2, the variations of δ^0_{transl} are determined by use of Eq. (26). However, there is one limitation due to arisen mathematical/numerical problems when the denominator in Eq. (26) reaches zero and then change sign, which is the case for length to height ratios smaller than a certain value, usually between 2 and 3, see Figure 13 and Nilsson (2003) for the denominator below zero. This problem is also vaguely indicated in JCI (1992).

In Figure 13 the variation of the denominator of Eq. (26) is shown for six different values of the area ratio A_c/A_{trans} for structures with length to height ratio $L/H_c = 3$. It can be seen that with larger area ratios the denominator changes sign and consequently also δ^0_{transl} changes sign, which makes Eq. (26) impossible to use, as δ^0_{transl} reaches infinity.
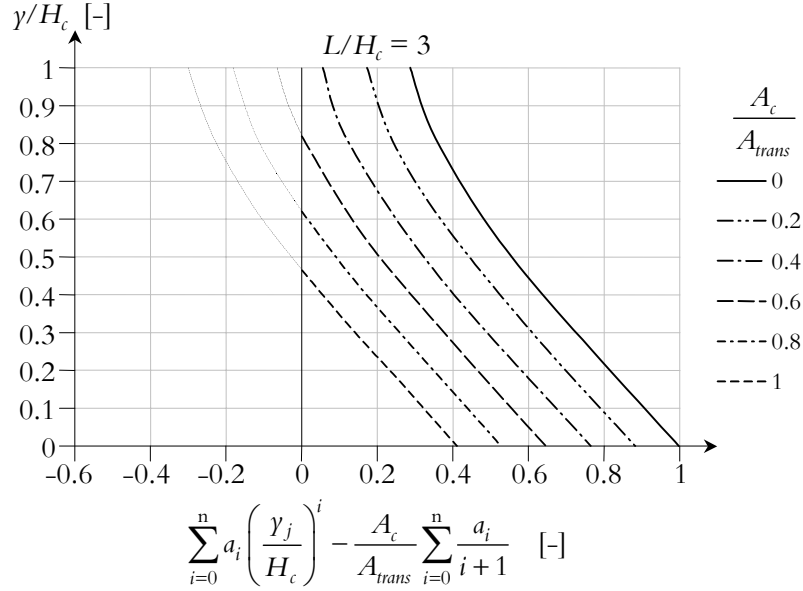
Figure 13 *The variation of the denominator of Eq. (26) for different values of the ratio A_c/A_{trans} for structures with $L/H_c = 3$.*

In Figure 14 the variations of the basic resilience correction factor for translational boundary restraint are shown for the example in Figure 9 (wall at the centre of the slab). Due to the denominator in Eq. (26) passing zero, it can be seen that δ^0_{transl} varies much between large negative and positive values for the length to height ratios $L/H_c = 0.375$, 0.625 and 1.25, respectively.

Thus, in the shown example, $L/H_c \geq 2.25$ is valid for the chosen basic technique "safely" using δ^0_{transl} and δ^0_{rot} according to Eq. (17). For the other structures, i.e. $L/H_c < 2.25$ in this example, the presented technique for determination of δ^0_{transl} is not possible. This means that at present, very short structures cannot be analysed for $\gamma_{RT} > 0$. Note that as long as the restraint values obtained from the FEM calculations $\gamma_{R,j} > 0$ the inverse of Eq. (26), $\delta^0_{rot} = 1/\delta^0_{transl}$, is still valid. Hereby, for somewhat shorter structures analyses for the case $\gamma_{RT} = 0$ and $\gamma_{RR,z} \neq 0$ can be performed.

It is however here noted that, in practice, the need of analyses of very short structures for $\gamma_{RT} > 0$ and for $\gamma_{RR,z} > 0$ when $\gamma_{RT} = 0$, respectively, is not so large. Still, but from theoretical point of view it is interesting to establish some useful method for these short structures in the future.
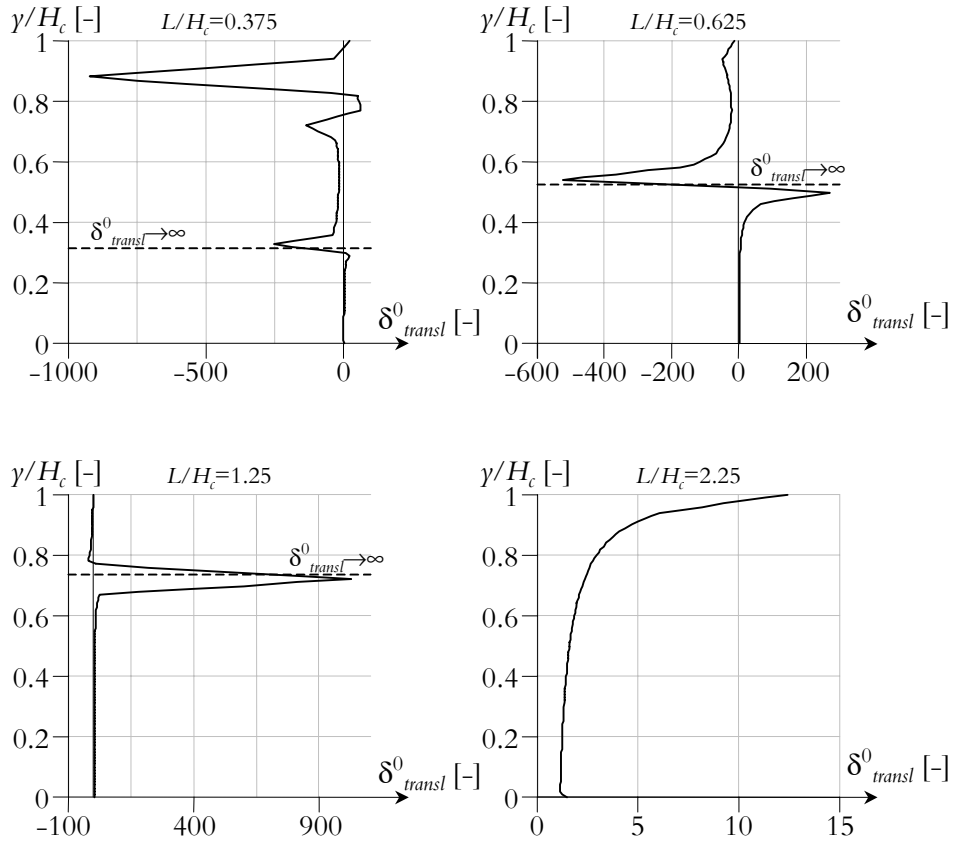
Figure 14 *Basic resilience correction factor* δ^0_{transl} *for the structure in the example in Figure 9. The position where* δ^0_{transl} *reaches infinity is marked, when it is valid.*

3.4.2 Resilience correction for rotational boundary restraint

Once the resilience correction for translational boundary restraint is determined, the resilience correction for rotation can be obtained according to Eq. (21). Therefore, no data of the resilience correction for rotational boundary restraint have been established.

3.5   Effects and slip failure in joints

The effects of possible slip failure in joints are regarded by the factor δ_{slip}. In Nilsson (2000) the slip effects factor is presented as it is used in ConTeSt Pro (2003), see Figure 15. The factor varies between the lower limits 0.5 and 1. Firstly, it depends on the free length of the casting section, and secondly on the height and width of the wall. The free length of the casting section is seen in the figure.

In Bernander (2001) a study by basic and classic theory of elasticity of the behaviour of joints between walls and slabs were performed. It was found that for fairly reasonable

data regarding material and geometry, the risk of slip failure in the ends of the joint between the walls and the slabs were most likely to occur.

Figure 15 *Factor for possible slip in joint effects* δ_{slip} *as function of the free length of casting, the height of the wall and the width of the wall. ConTeSt Pro (2003) and Nilsson (2000).*

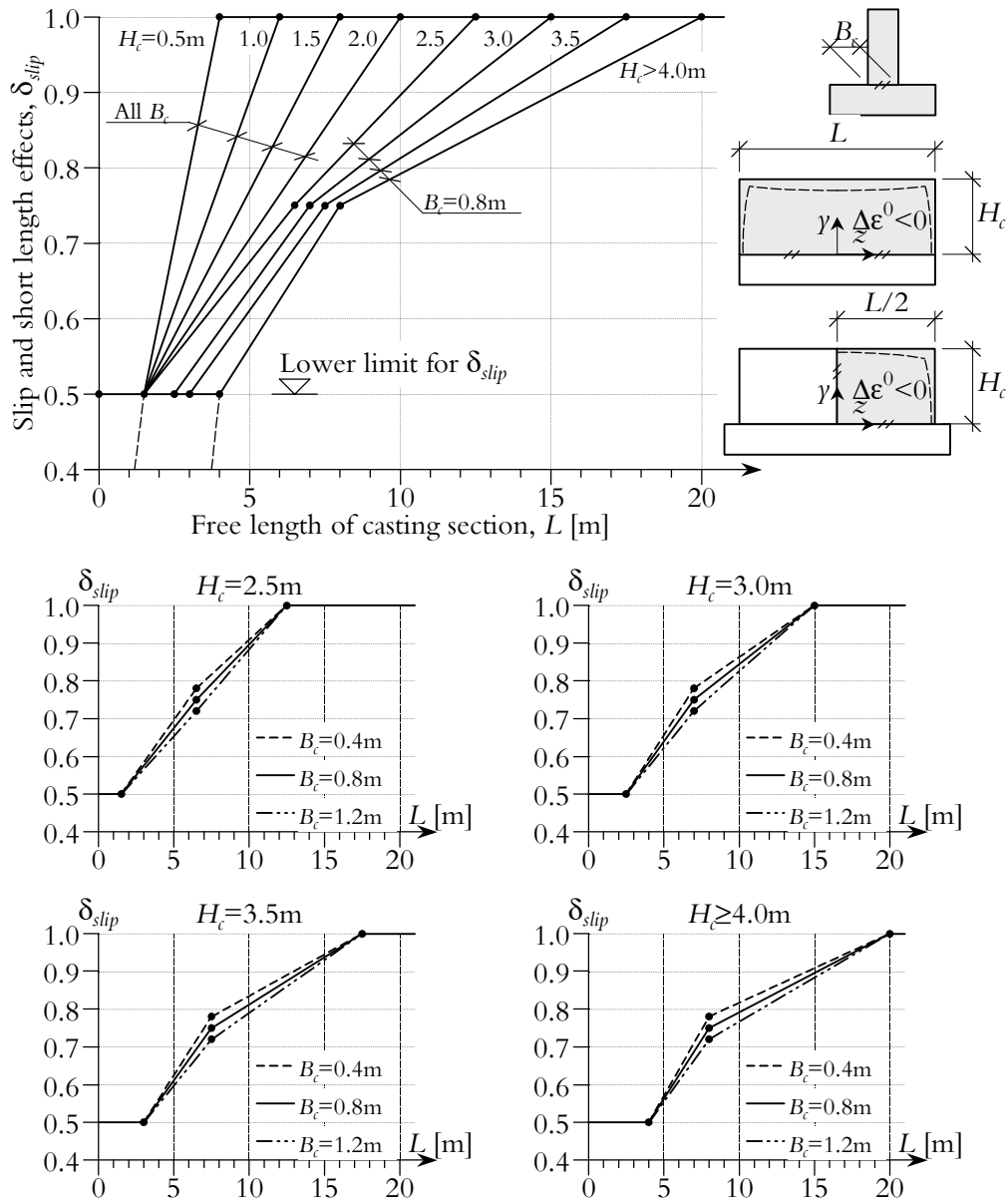A slip failure in a joint between a wall and a slab does not have to be a brittle and fast occurrence. The "failure" might as well take place as a distributed softening of the young concrete adjacent to the joint, which means that no localized crack will be visible in the joint. However, the effect of the "failure" is a reduction of the stresses in the wall, reducing the risk of vertical cracking in the mid-section of the wall.

In Nilsson et al. (1999) and Nilsson (2000) three medium scale tests of wall on slab structures are presented. In these tests it was found that slip failure in the joints between the walls and the slabs took place. The propagation of the slip failures was measured with very brittle crack opening gauges that were glued across the ends of the joints. These recordings showed that the failure was brittle and that the cracks propagated in small distances, which in turn corresponded to the horizontal distances between the vertical reinforcement in the joints.

3.6 General application

By use of the adjustment tools presented above, fully shown in Nilsson (2003), application of the semi-analytical method to any wall on slab structure is possible in the case of free boundary translation and free boundary rotation.

If the structure is subjected to some degree of boundary restraint, additional adjustments are necessary. The basic resilience correction factors should be determined according to sub-section 3.4. This means that structures with length to height ratios greater than a easily calculated limit can be directly analysed. For smaller values of length to height ratios, a method on the safe side is to analyse the structure as if the limit conditions were fulfilled.

4 SUMMARY AND CONCLUSIONS

In this paper the verification and application of the semi-analytical method derived and presented in Nilsson (2003) is shown and described. The verification is done by use of 2920 elastic three-dimensional finite element method calculations as reference restraint distributions. The application needs a number of adjustment tools for fitting the restraint determined by the semi-analytical method to the reference restraint distributions.

The adjustment of the semi-analytical method consists of

- a factor describing effects of high walls, so-called resilience
- effective width of slab
- a factor for effects of relative wall location on slab
- influence of boundary restraint
- correction of resilience due to boundary restraint
- factor taking into account slip failure in joint

The first adjustment accounting for effects of non-linearly varying strains in high walls, the so-called resilience, which is based on a basic resilience factor that should be adjusted for structures subjected to some degree of boundary restraint. The second adjustment consists of the effective width of the slab, which is used together with the basic resilience to obtain the same restraint distributions as the reference distributions for cases subjected to no boundary restraint. The third adjustment changes the effective width of slab depending on the relative location of the wall on the slab. The fourth adjustment regards structures subjected to some degree of boundary restraint, which is used for correction of the resilience as the fifth adjustment. Finally, the method is adjusted for structures with slip failure in the joint between the wall and slab.

For the case of no boundary restraint, any wall on slab structure can fast and easily be calculated. These types of calculations cover most of the interesting cases in practical applications. For cases subjected to some degree of boundary restraint the actual application of the concept of basic resilience correction factors works properly for length to height ratios larger than a certain, easy to calculate limit. For shorter lengths structures a method on the safe side is to analyse the structure as if the limit conditions were fulfilled.

The calculation of restraint variations by the semi-analytical method is both simple and fast and by the adjustment to the three-dimensional finite element method calculations, the method gives reasonable accurate results. The calculations can be simplified in different steps, for instance by only using the resilience and slip failure factors as the adjustment tools.

Further, a comparison between restraint determinations by the semi-analytical method presented in this paper and by evaluations of field measurements on a full-scale structure is presented in Larson et al. (2003).

5   ACKNOWLEDGEMENTS

6   REFERENCES

ACI Committee 207 (1995). Effect of Restraint, Volume Change, and Reinforcement on Cracking of Massive Concrete. ACI Committee 207. ACI 207.2R-95.

Bernander, S (1993). *Balk på elastiskt underlag åverkad av ändmoment M_1* (Beam on Resilient Ground Loaded by Bending End Moments M_1). Göteborg, Sweden: Con-Geo AB. Notes and calculations with diagrams. (In Swedish).

Paper B

Bernander, S (2001). *Analysis of Deformations in an Elastic Halfspace due to Horisontal Loading*. Göteborg, Sweden: Con-Geo AB. Notes and calculations with diagrams. pp. 47.

ConTeSt Pro (2003). *Users manual - Program for Temperature and Stress Calculations in Concrete*. Developed by JEJMS Concrete AB in co-operation with Luleå University of Technology, Cementa AB and Peab AB. Luleå, Sweden: Luleå University of Technology. (In progress May 2003).

Emborg, M (1989). Thermal Stresses in Concrete Structures at Early Ages. Luleå, Sweden: Division of Structural Engineering, Luleå University of Technology. Doctoral Thesis 1989:73D. pp. 285.

JCI (1992). *A Proposal of a Method of Calculating Crack Width due to Thermal Stress* (1992). Tokyo, Japan: Japan Concrete Institute, Committee on Thermal Stress of Massive Concrete Structures. JCI Committee Report. pp. 106.

Larson, M (2000). *Estimation of Crack Risk in Early Age Concrete*. Luleå, Sweden: Division of Structural Engineering, Luleå University of Technology. Licentiate Thesis 2000:10. pp. 170.

Larson, M, Nilsson, M & Jonasson, J-E (2003). *Restraint Coefficients in Thermal Stress Analysis – Application on Full-Scale Field Tests*. pp. 40. (Paper C in this thesis, aimed for external publication).

Löfling, P (1993). *Bestämning av jords hållfasthets- och deformationsegenskaper* (Determination of Strength and Deformation Properties of Soils). Borlänge, Sweden: Swedish Road Administration, Publication 1993:6. pp. 30. (In Swedish).

Nilsson, M (1998). *Inverkan av tvång i gjutfogar och i betongkonstruktioner på elastiskt underlag* (Influence of Restraint in Casting Joints and in Concrete Structures on Elastic Foundation). Luleå, Sweden: Luleå University of Technology, Division of Structural Engineering. Master Thesis 1998:090 CIV. pp. 61. (In Swedish).

Nilsson, M (2000). *Thermal Cracking of Young Concrete – Partial Coefficients, Restraint Effects and Influence of Casting Joints*. Luleå, Sweden: Division of Structural Engineering, Luleå University of Technology. Licentiate Thesis 2000:27. pp. 267. http://epubl.luth.se/1402-1757/2000/27/LTU-LIC-0027-SE.pdf

Nilsson, M, Jonasson, J-E, Emborg, M, Wallin, K & Elfgren, L (2003). *Determination of Restraint in Early Age Concrete Walls on Slabs by a Semi-Analytical Method – Paper 1 Theory and Derivation*. pp. 47. (Paper A in this thesis, aimed for external publication).

Nilsson, M (2003). *Restraint Factors and Partial Coefficients for Crack Risk Analyses of Early Age Concrete Structures - Diagrams and Tables*. Luleå, Sweden: Division of Structural Engineering, Luleå University of Technology. Technical Report 2003:11. pp. 199.

Nilsson, M, Jonasson, J-E, Wallin, K, Emborg, M, Bernander, S & Elfgren, L (1999). Crack Prevention in Walls and Slabs – The Influence of Restraint. In: *Innovation in Concrete Structures, Design and Construction. Proceedings of the International Conference held at the University of Dundee, Scotland, UK on 8-10 September 1999.* Ed. by R. K. Dhir & M. R. Jones. London, UK: Thomas Telford Publishing. pp. 461-471. ISBN: 0 7277 2824 5.

Pettersson, D (1996). *Restraint Stresses Due to Uniform Thermal Action in Walls and Floors of Concrete on a Frictional Surface.* Lund, Sweden: Department of Structural Engineering, Lund Institute of Technology. Report TVBK-7051. pp. 45.

Pettersson, D (1998). *Stresses in Concrete Structures from Ground Restraint.* Lund, Sweden: Department of Structural Engineering, Lund Institute of Technology. Report TVBK-1014. pp. 112.

Rostásy, F, S, Gutsch, A-W & Krauß, M (2001). *Engineering models for the assessment of restraint of slabs by soil and in piles in the early age of concrete.* Luleå, Sweden: Luleå University of Technology, Department of Civil and Mining Engineering. IPACS-report BE96-3843/2001:59-1. ISBN 91-89580-59-1. pp. 135.

Timoshenko, S (1958). Beams on Elastic Foundation. In: *Strength of Materials.* Part II: Advanced Theory and Problems. New York, U.S.A.: Van Nostrand Reinold Company. pp. 565.

7 LIST OF NOTATIONS, DEFINITIONS AND SYMBOLS

Roman upper-case letters

A_a = real cross-section area of adjacent older concrete, [m^2]

$A_{a,eff}$ = effective area of the old concrete, [-]

A_{trans} = transformed area of the cross section, [m^2]

A_c = cross-section area of the young concrete, [m^2]

B_a = real width of slab, [m]

$B_{a,eff}$ = effective width of slab, [m]

B_c = width of wall, [m]

E_{a28} = 28 days modulus of elasticity of the adjacent older concrete, [N/m^2]

H_a = height of slab, [m]

H_c = height of wall, [m]

$I_{trans,y}$ = transformed second moment of inertia of the cross-section for bending around the y-axis, [m^4]

$I_{trans,z}$ = transformed second moment of inertia of the cross-section for bending around the z-axis, [m^4]

K_j = modulus of compression, [N/m^2]

L = length of the structure, [m]

Paper B

L_e = elastic length, [m]
T = temperature, [°C]

Roman lower-case letters

y = vertical co-ordinate from the joint and up-wards, [m]
y' = co-ordinate from the total centroid and up-wards, [m]
y_{cen} = vertical location of the centroid of the transformed cross-section relatively the joint, [m]
z = horizontal co-ordinate from the centre of the slab, [m]
z_{cen} = horizontal location of the centroid of the transformed cross-section relatively the centre of the slab, [m]

Greek upper case letters

X = parameter for determination of effective width of slab, [-]

Greek lower case letters

α = thermal expansion coefficient, [°C^{-1}]
δ_{res} = high wall effect, resilience, [-]
δ^0_{res} = basic resilience factor, [-]
δ^0_{transl} = basic resilience correction factor for translational boundary restraint, [-]
δ^0_{rot} = basic resilience correction factor for rotational boundary restraint, [-]
δ_{slip} = slip in joint effect, [-]
ε = strain, [-]
γ_R = restraint coefficient, [-]
$\gamma_{RR,y}$ = rotational boundary restraint for bending around the y-axis, [-]
$\gamma_{RR,z}$ = rotational boundary restraint for bending around the z-axis, [-]
γ_{RT} = translational boundary restraint, [-]
κ = shape factor for slabs, [-]
ν = Poisson's ratio, [-]
ρ = density, [kg/m^3]
σ^0 = stress at total fixation, [MPa]
σ = stress at studied time, [MPa]
ω = relative location of wall on slab, [-]
ω_{corr} = correction of effective width of slab for relative location of walls on slabs, [-]
ζE_{c28} = modulus of elasticity of the young concrete at the studied time, [N/m^2]

103

Paper C

Restraint Coefficients in Thermal Stress Analyses –
Application on a Full-scale Field Test

By

Mårten Larson

Martin Nilsson

Jan-Erik Jonasson

Mats Emborg

Paper C

Restraint Coefficients in Thermal Stress Analyses – Application on a Full-scale Field Test

By Mårten Larson, Martin Nilsson, Jan-Erik Jonasson and Mats Emborg

M.Sc. Eng. and Tech.Lic. Mårten Larson is a PhD-student in Structural Engineering at Luleå University of Technology, Sweden. His field of research is methods and models for crack estimation in early age concrete.

M.Sc. Eng. and Tech. Lic. Martin Nilsson is a PhD-student in Structural Engineering at Luleå University of Technology, Sweden. His field of research is determination of restraint in young concrete structures.

Tech. Dr. Jan-Erik Jonasson is a Senior Lecturer and Assistant Professor in Structural Engineering at Luleå University of Technology, Sweden. His research speciality is modelling of thermal and moisture conditions and associated structural behaviour of concrete structures.

Tech. Dr. Mats Emborg is partly a Senior Lecturer and Assistant Professor in Structural Engineering at Luleå University of Technology, Sweden, partly Research and Development Manager at Betongindustri AB, Sweden. His research speciality is behaviour of fresh and hardening concrete including self-compacting concrete with and without fibre reinforcement.

ABSTRACT

Modelling of restraint is one of the most important issues that has to be considered in thermal stress analyses enabling reliable thermal crack estimations that will contribute to an improved service life time and function of a concrete structure.

It is shown that the complex structural restraint behaviour can be described by means of restraint coefficients giving an agreeing thermal stress development compared to both more exact Finite Element (FE) calculations and measured stresses in a full-scale structure. The restraint coefficients are in a stress calculation applied as a direct reduc-

tion of the fixation stress during both the expansion and contraction phase of a hardening concrete structural element.

The structural restraint coefficients can be established by means of simple elastic approaches giving an acceptable accuracy compared to both more realistic viscoelastic approaches including models describing the hardening young concrete as well as the measured and observed restraint behaviour of a real full-scale structure.

Keywords: restraint; early age concrete; mass concrete; cracking; resilience; joint slip; wall on slab.

1   INTRODUCTION

The service lifetime and function of a structure is often dependent on what happens during the very early ages of the hardening concrete. Cracking caused by restrained temperature and moisture deformations in the young concrete often leads to an early malfunction of the structure already in the constructional phase. Consequently, it is of great importance that reliable thermal stress estimations and thereby conclusions about cracking risks can be made before this premature damage has appeared. Modelling of the restraint to which a structural element is subjected is, if not the most, at least one of the most important issues that have to be considered in a thermal stress analysis, see Figure 1.1. If a hardening concrete structure may deform freely no stresses will appear and naturally no cracks either. A restrained structure will, on the other hand, rapidly experience both high compressive stresses as the concrete expands during the hydration process and high tensile stresses as it, due to the abating heat development, contracts. The stress development in the structure is during this period significantly influenced by the viscoelastic behaviour of the hardening concrete describing the alteration of the concrete from an almost liquid to a solid state.

Thermal stress estimations are often performed by means of special purpose Finite Element (FE) programs including models describing material properties of the young hardening concrete whereby it is possible to realistically consider the restraint situation in up to three-dimensions (3D). Full 3D-simulations are because of the complexity very time consuming (days) to execute, which in practice has lead to various simplified ways of working. Two- and three-dimensional effects are often treated with different engineering methods whereby the concept of using so-called restraint coefficients described in i.e. ACI (1973), Harrison (1981), Emborg (1989), Kjellman and Olofsson (1999), Larson (2000), Nilsson (2000) or Olofsson et al. (2002) is one way of working. Using restraint coefficients is a very easy and efficient way of incorporating complicated structural restraint effects into a stress calculation.
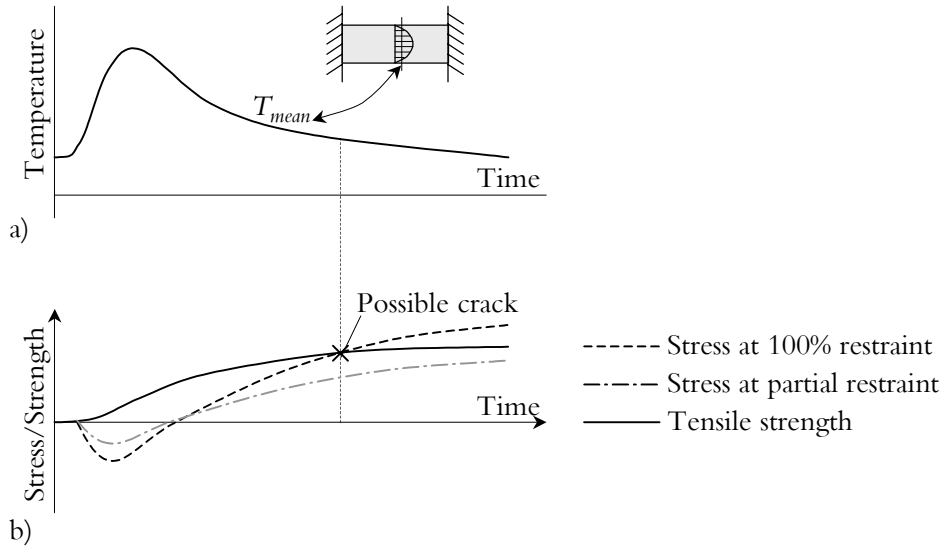
Figure 1.1 *Generalised temperature and stress development in a newly cast concrete element: a) temperature and b) stress development at varying end restraint.*

The concept restraint coefficient is in this study defined as described in for example Larson (2000) by formulating the stress development in a specific point of a structure with

$$\sigma(t) = \int_t R(t,t_0)d\varepsilon(t) + \sigma^{fix}(t) \tag{1.1}$$

where

$$\sigma^{fix}(t) = -\int_t R(t,t_0)d\varepsilon^0(t) \tag{1.2}$$

and

$\varepsilon^0(t)$ is the inelastic strain (the total free strain) at time t, [-]
$\varepsilon(t)$ is the external, measurable strain at time t, [-]
$\sigma^{fix}(t)$ is the fixation stress for $\varepsilon(t) \equiv 0$ at time t, [Pa]
$R(t,t_0)$ is a relaxation function at time t for loading at the age t_0, [Pa]

For a situation of total restraint the stress development will be exactly the same as the fixation stress i.e. $\varepsilon(t) \equiv 0$. This implies that the structural situation for a specific point of a general structure may be described by a restraint coefficient defined by

$$\gamma_R(t) = \frac{\sigma(t)}{\sigma^{fix}(t)} \tag{1.3}$$

where

$\gamma_R \qquad = 0$ at no restraint $\varepsilon(t) = \varepsilon^0(t)$, and

$\gamma_R \qquad = 1$ at no restraint $\varepsilon(t) \equiv 0$.

Usually the restraint coefficients are retrieved from an elastic stress analysis as described in for example ACI (1973), Emborg (1989), Kjellman and Olofsson (1999), Larson (2000), Nilsson (2000) and Olofsson et al. (2002). How this simplified elastic approach influence the evaluated restraint compared to a viscoelastic approach including properties of young concrete and how the restraint coefficients shall be applied in a thermal stress analysis has not yet been sufficiently clarified. Kanstad and Bosnjak (2001) have however shown that there is quite good correlation between thermal stresses calculated with elastically obtained restraint coefficients and stresses calculated with a complete 3D FE-model including the behaviour of young concrete. Very few other studies exist.

The aim of this paper is to:

I.   show that it is possible to evaluate the structural restraint by means of simple elastic approaches within acceptable limits compared to a more realistic viscoelastic approach and the "true" restraint behaviour of a real full scale structure.
II. clarify how the application of restraint coefficients influence a calculated thermal stress development compared to both more exact FE-calculations and measured stresses.

2   FULL SCALE FIELD TESTS

The application of the elastic and viscoelastic restraint approaches is based on a full-scale test whereby a wall is cast on an existing base slab founded on gravel with dimensions according to Figure 2.1. The structure form a part of the Maridal culvert in Oslo, Norway, which has been instrumented for measurements of temperature and strain development as reported in Heimdal et al. (2001) and Bosnjak (2000), see also Figure 2.1 and Figure 2.2. The results from the performed field-test are partly used here to apply and compare different restraint approaches.
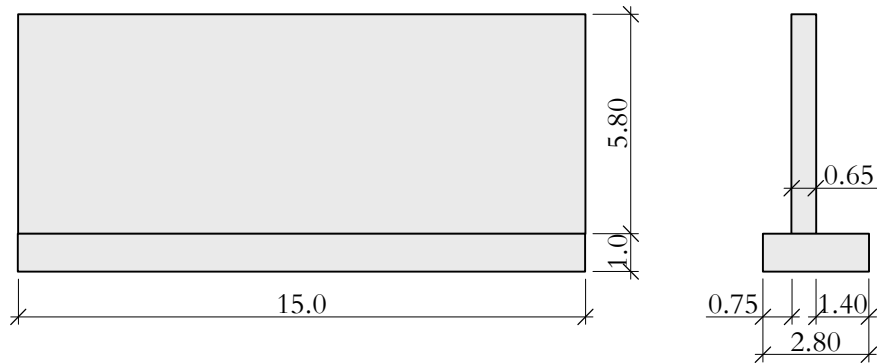
Figure 2.1 *Dimensions in meters of the studied wall and foundation. Description of performed field-tests are given in Heimdal et al. (2001) and Bosnjak (2000).*

The evaluation of restraint coefficients is performed for the mid-section of the studied structure where the cross-section may be considered as almost plane in respect of plane section theory. The measurements in this location have however to a large extent failed and the measured strains in position number 2, 5, 8 and 11 are therefore used in the empirical evaluation instead.
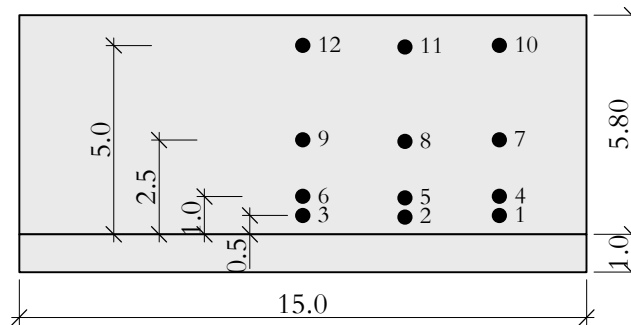
Figure 2.2 *Location of instrumentation and positions for evaluation of restraint coefficients in the wall.*

3 EVALUATION OF RESTRAINT COEFFICIENTS

3.1 Empirical evaluation of restraint

3.1.1 Method

The restraint is evaluated from the measured strain development together with a known maturity dependent creep and relaxation behaviour of the young hardening concrete whereby the restraint coefficient $\gamma_R(t)$ based on Eqs. (1.1) to (1.3) is calculated as

$$\gamma_R(t) = \frac{\sigma(t)}{\sigma^{fix}(t)} = \frac{\int_t R(t,t_0)d\varepsilon^0(t) - \int_t R(t,t_0)d\varepsilon(t)}{\int_t R(t,t_0)d\varepsilon^0(t)} \tag{3.1}$$

With Eq. (3.1) it is now possible to calculate the development of the restraint coefficient from a measured strain $\varepsilon(t)$ if the inelastic strain (the total free strain) $\varepsilon^0(t)$ and the maturity dependent relaxation function $R(t,t_0)$ are known.

3.1.2 Temperature and maturity

The temperature T has been registered in the locations according to Figure 2.2 and the results for position 2, 5, 8 and 11 are presented in Figure 3.1. The initial temperature corresponds to the registered temperature at the apparent setting time of the concrete t_s = 10 hours equivalent time evaluated according to Hedlund (2000) for the concrete used at the Maridal culvert. The apparent setting time is regarded as the age when the concrete alters from an almost liquid to a solid phase, i.e. stresses can start to develop at 10 hours equivalent time and further on, see for instance Hedlund (2000).

The maturity corresponds to the equivalent age t_e as if the hardening process had proceeded at a constant temperature of 20 °C according to

$$t_e = \int_0^t \beta_T dt \tag{3.2}$$

The temperature rate factor β_T describes the difference in hydration rate depending on the temperature. As there seems to be a linear relationship between compressive strength and degree of hydration, Byfors (1980), the hydration rate may be exchanged by the compressive strength rate. This makes it much easier to perform tests for determination of β_T, which can be described by the Arrhenius equation for thermal activation, see e.g. Freisleben Hansen and Pedersen (1977) and Byfors (1980).

$$\beta_T = \exp\left(\theta \cdot \left[\frac{1}{T_{ref}} - \frac{1}{T + 273}\right]\right) \quad \text{for} > \text{-10 °C}$$
$$\beta_T = 0 \qquad\qquad\qquad\qquad \text{for} \leq \text{-10 °C} \tag{3.3}$$

where

T is the measured temperature, [°C]

T_{ref} is the chosen reference temperature (here 20 °C), [°C]

θ is the "activation temperature", which formally can be described as the activation energy divided by the general gas constant according to Freisleben Hansen and Pedersen (1977), [K]
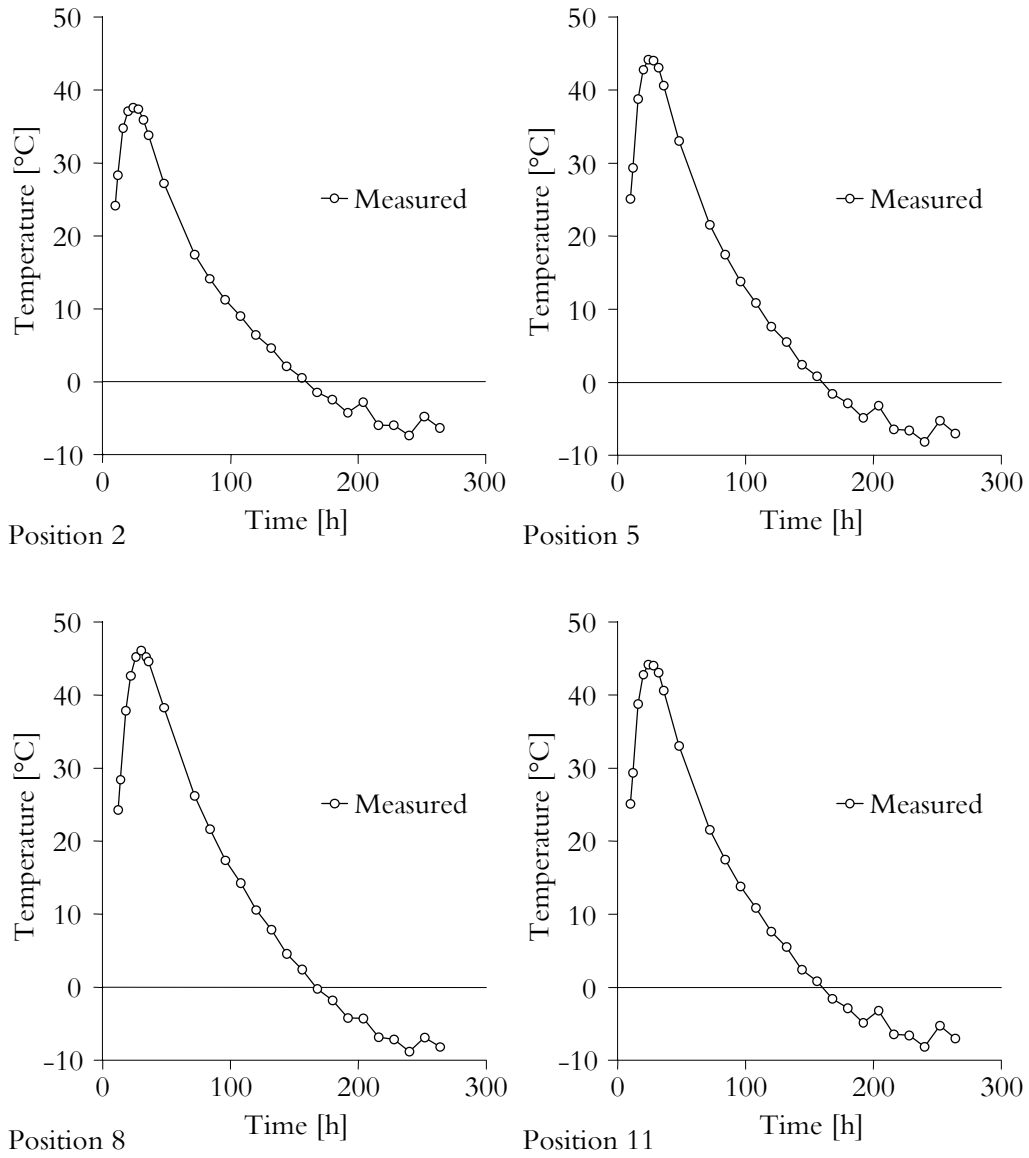
Figure 3.1 *Measured temperature development in positions 2, 5, 8 and 11 according to Figure 2.2.*

The temperature dependency on the activation temperature can according to Jonasson (1984) be described as

$$\theta = \theta_{ref}\left(\frac{30}{T+10}\right)^{\kappa_3} \tag{3.4}$$

in which θ_{ref} and κ_3 are parameters that are to be empirically defined. Parameters valid for the Maridal concrete are given in Appendix A.

3.1.3 Inelastic strain

The inelastic strain or the total free strain development $\varepsilon^0(t)$ originates in young concrete from a combination of thermal dilatation and autogenous shrinkage, which here is modelled according to Hedlund (2000) as

$$\varepsilon^0(t) = \alpha_h \Delta T + \varepsilon_{AD}(t_e) \tag{3.5}$$

where

α_h is the thermal dilatation coefficient, [°C^{-1}]
ΔT is temperature difference, [°C]

The autogenous shrinkage ε_{AD} in Eq. (3.5), adjusted for the actual temperature by means of the factor β_{ST} during the heating and cooling phase of the young concrete, is according to Hedlund (2000) expressed as

$$\varepsilon_{AD}(t_e) = \varepsilon_{ref}(t_e)\beta_{ST}(T) \tag{3.6}$$

where

ε_{ref} is the reference ultimate shrinkage at isothermal conditions ($T = 20$ °C), [–]
$\beta_{ST}(T)$ is temperature effect on autogenous shrinkage, [–]
T is the highest temperature that has been reached so far, which in many cases corresponds to the temperature during the heating phase, [°C]

The reference autogenous shrinkage ε_{ref} can, as described in Hedlund (2000) with denotations according to Figure 3.2, be expressed as a function of equivalent age as

$$\varepsilon_{ref}(t_e) = \begin{cases} 0 & \text{for } t_e < t_{s1} \\ \varepsilon_{s1}\dfrac{t_e - t_{s1}}{t_{s2} - t_{s1}} & \text{for } t_{s1} \le t_e < t_{s2} \\ \varepsilon_{s1} + \varepsilon_{s2}\exp\left(-\left(\dfrac{t_{SH}}{t_e - t_{s2}}\right)^{\kappa_{SH}}\right) & \text{for } t_e \ge t_{s2} \end{cases} \tag{3.7}$$

in which t_{SH} and κ_{SH} are model parameters.
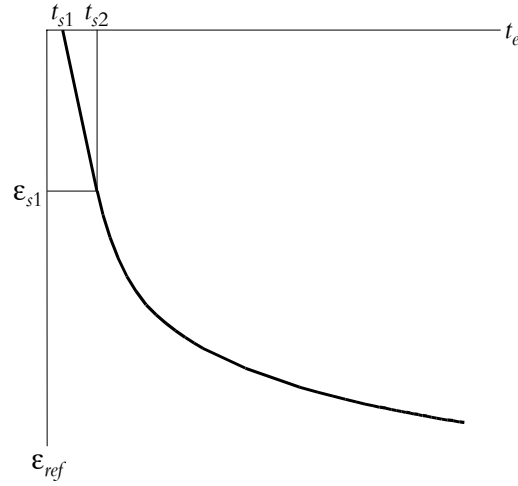
Figure 3.2 *Outline of typical autogenous shrinkage behaviour at early ages.*

The increase of autogenous shrinkage due to temperature in Eq. (3.6) can according to Hedlund (2000) be considered by an empirical model expressed as

$$\beta_{ST}(T) = a_0 + a_1\left(1 - \exp\left(-\left(\frac{T}{T_1}\right)^{b_1}\right)\right) + a_2\left(1 - \exp\left(-\left(\frac{T}{T_2}\right)^{b_2}\right)\right) \qquad (3.8)$$

with following model parameters valid for a NSC (Normal Strength Concrete, water to binder ratio ≥ 0.40):

a_0	0.4	°C	a_2	1.3	–
a_1	0.6	–	T_2	55	°C
T_1	9	°C	b_2	7	–
b_1	2.9	–			

Model parameters for Eqs. (3.5) to (3.8), describing the behaviour of the Maridal concrete, are presented in Appendix A giving a total free strain development $\varepsilon^0(t)$ for position 2, 5, 8 and 11 in the studied wall according to Figure 3.4, see also Hedlund (2000).

Recently, see Utsi (2003), the model description of the autogenous deformation, Eq. (3.6), has been completed with a late swelling. However, this particular concrete seems to be modelled accurately without this swelling, as the agreement between measured and calculated free strain is good in position 11, where the restraining is very low ($\gamma_R \approx 0$), see Figure 3.4.

3.1.4 Measured strain

The strain development $\varepsilon(t)$ has been measured in defined points according to Figure 2.2 and the results are presented in Heimdal et al. (2001) and Bosnjak (2000). Figure 3.4 shows the measured strain in location 2, 5, 8 and 11 of the wall. All measured values have been zeroed at the apparent setting time of the concrete $t_s = 10$ hours equivalent age.

As can be seen in Figure 3.4 there is an instant drop in the measured strains after approximately 108 hours. A crack survey according to Figure 3.3 shows that a crack has appeared close to one of the measured sections whereby point 2 and 5 have registered the phenomenon.

Measured section point 2, 5, 8 and 11 ⇨   5.0m

6.3m   4.2m   4.5m
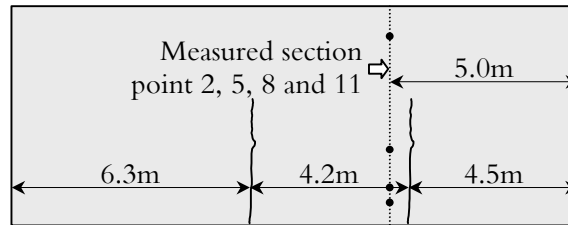
Figure 3.3 *Observed cracking in the studied wall, from Thomassen (1999).*

3.1.5 Differential (restrained) strain

The difference between the total free strain and the measured strain $\Delta\varepsilon(t) = \varepsilon^0(t)-\varepsilon(t)$ represents the restrained part of the deformation that will evolve stresses. As can be seen in Figure 3.4 the concrete reaches failure at a differential strain level of 0.18 ‰ in position 2, which very well correlates to the failure strain of concrete including creep effects for this type of loading, usually 0.14 to 0.2 ‰, see Hedlund (2000). The differential strain level in position 5, where failure also has been registered, is 0.15 ‰.
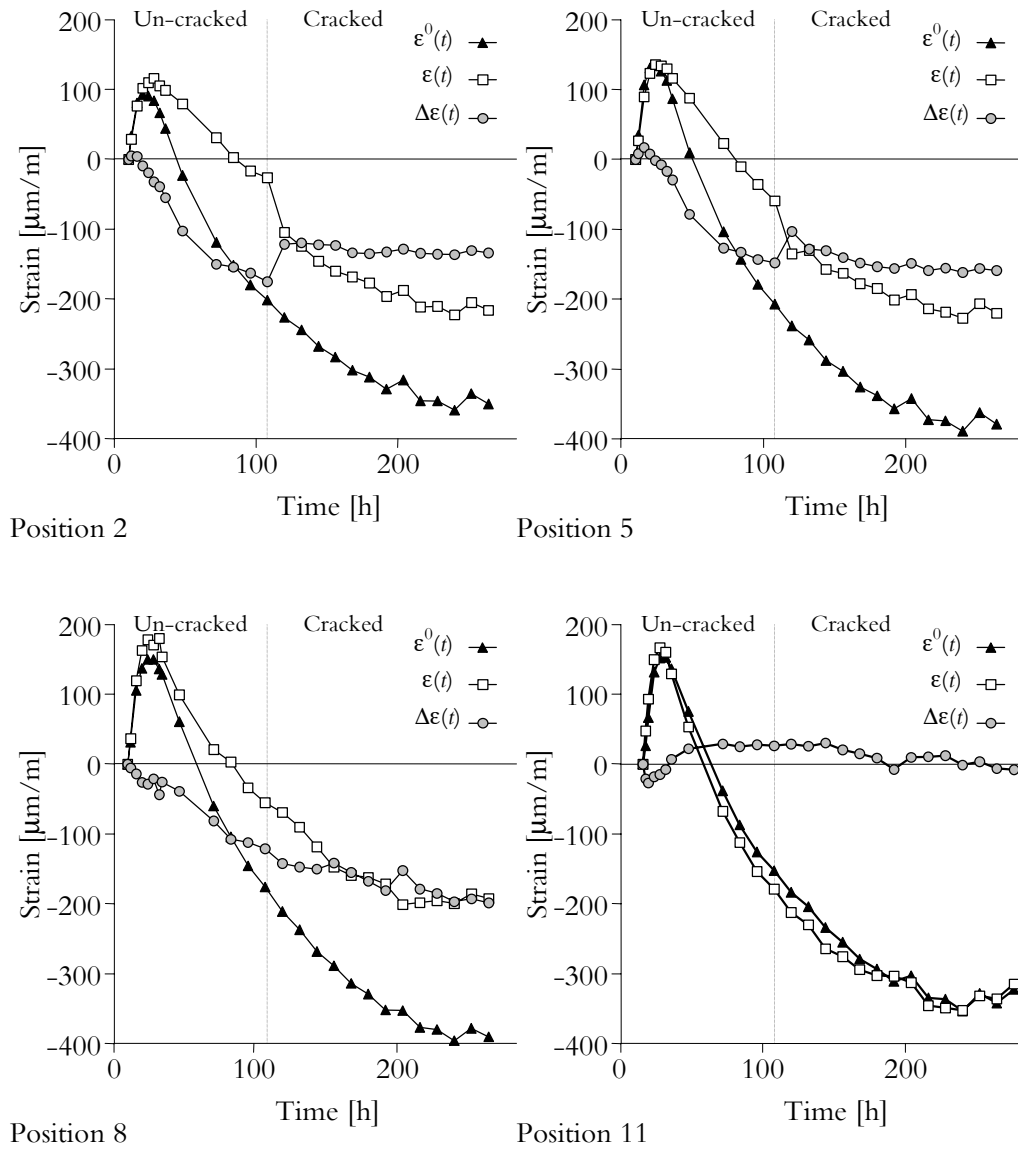
Figure 3.4 *Development of inelastic strain, measured strain and differential (restrained) strain in position 2, 5, 8 and 11 of the wall. After approximately 108 hours there is an instant drop in the measured strains (position 2 and 5), which indicates that a crack arises in the wall at this moment.*

3.1.6 Relaxation function

The relaxation function $R(t,t_0)$ may by means of a simplified method according to Trost (1967) be expressed from a known creep function $\varphi(t,t_0)$ as

117

$$R(\Delta t_{load}, t_0) = E(t_0)\left(1 - \frac{\varphi(\Delta t_{load}, t_0)}{1 + \chi\varphi(\Delta t_{load}, t_0)}\right) \tag{3.9}$$

where

χ is known as the ageing coefficient (Limitations for the ageing coefficient are $0 < \chi \leq 1.0$), [–]

Δt_{load} is time after loading in equivalent time, [d]

t_0 is time of loading in equivalent time, [d]

The creep function $\varphi(\Delta t_{load}, t_0)$ used in this study is derived from the so-called *Linear Logarithmic Model* presented by Larson and Jonasson (2003) as

$$\varphi(\Delta t_{load}, t_0) = \begin{cases} E(t_0)\left(a_1(t_0)\log\left(\dfrac{\Delta t_{load}}{\Delta t_0}\right)\right) & \text{for } \Delta t_0 \leq \Delta t_{load} < \Delta t_1 \\[3mm] E(t_0)\left(a_1(t_0)\log\left(\dfrac{\Delta t_1}{\Delta t_0}\right) + a_2(t_0)\log\left(\dfrac{\Delta t_{load}}{\Delta t_1}\right)\right) & \text{for } \Delta t_{load} \geq \Delta t_1 \end{cases} \tag{3.10}$$

in which Δt_1, $a_1(t_0)$ and $a_2(t_0)$ are model parameter and functions that are to be evaluated from laboratory tests by means of regression.

The functions $a_1(t_0)$ and $a_2(t_0)$ are expressed by

$$a_i(t_0) = a_i^{min} + \left(a_i^{max} - a_i^{min}\right)\exp\left(-\left(\frac{t_0 - t_s}{t_{ai}}\right)^{n_{ai}}\right) \qquad \text{for } i = \{1,2\} \tag{3.11}$$

were index $i = \{1,2\}$, and a_i^{min}, a_i^{max}, t_{ai} and n_{ai} are model parameters that are to be evaluated from laboratory tests by means of regression.

Following parameters have according to Larson and Jonasson (2003) been found to be able to give a satisfactory description for a wide range of concrete mixes and may be used as general constants in the model:

Δt_0	0.001	d
Δt_1	0.1	d
a_1^{min}	0.1	10^{-12}/(Pa log-unit)
a_1^{max}	60	10^{-12}/(Pa log-unit)
a_2^{max}	30	10^{-12}/(Pa log-unit)

The development of the modulus of elasticity is modelled with

$$E(t_0) = E_{ref}\beta_E(t_0) \tag{3.12}$$

in which E_{ref} is the modulus of elasticity at 28 d of age and the relative development $\beta_E(t_0)$ is expressed as

$$\beta_E(t_0) = \begin{cases} 0 & \text{for } t_0 < t_s \\ b_1 \log\left(\dfrac{t_0}{t_s}\right) & \text{for } t_s \leq t_0 < t_B \\ b_1 \log\left(\dfrac{t_B}{t_s}\right) + b_2 \log\left(\dfrac{t_0}{t_B}\right) & \text{for } t_B \leq t_0 < 28 \text{ d} \\ 1 & \text{for } t_0 \geq 28 \text{ d} \end{cases} \tag{3.13}$$

where t_B, b_1 and b_2 are model parameters that are to be evaluated from laboratory tests by means of regression and t_s is the apparent setting time of the concrete.

The model parameters in the creep function described by Eqs. (3.10) to (3.13) are evaluated from creep tests that have been performed at Technical University of Trondheim, Norway (NTNU), according to Bosnjak (2000) giving the model parameters presented in Appendix A and the compliance development shown in Figure 3.5 for the concrete used at the Maridal culvert.
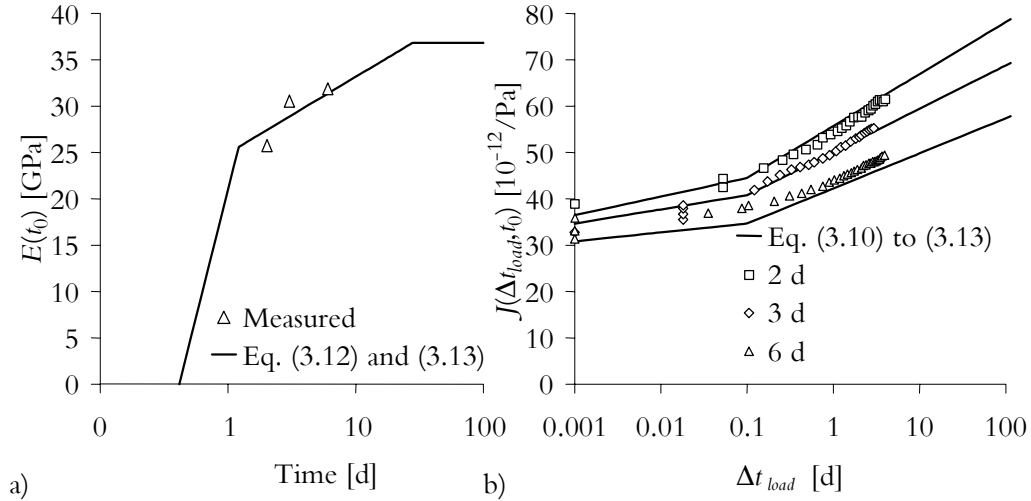
Figure 3.5 *Measured and calculated a) modulus of elasticity* $E(t_0)$ *and b) creep compliance* $J(t,t_0)$. *The creep is modelled by means of Eq. (3.10) to (3.13).*

The creep may also be converted into relaxation by solving the function for the relaxation modulus $R(t,t_0)$ from a compliance function $J(t,t_0)$, which is used in the viscoe-

lastic numerical evaluation of restraint in section 3.2. According to Bažant and Wu (1974) this may be performed by expressing the time t in discrete times t_1, t_2, t_3, ... t_N yielding time steps $\Delta t_j = t_j - t_{j-1}$ and solving following equation

$$\Delta R_j = \frac{(-1)}{J_{j,j-1/2}} \left[\sum_{s=2}^{j-1} \Delta R_s \cdot \left(J_{j,s-1/2} - J_{j-1,s-1/2} \right) + \Delta R_1 \cdot \left(J_{j,0} - J_{j-1,0} \right) \right] \quad (3.14)$$

The formulation has been implemented in a computer program called RELAX (Jonasson (1977) and a revised version by Westman and Jonasson (1999)) whereby creep data obtained from models or tests can be converted into relaxation. This is a more exact method for converting creep into relaxation than the simplified method according to Eq. (3.9). Here the results from the RELAX program are used to find a representative mean value of the ageing coefficient χ, which by means of regression has been evaluated to 0.837. This can be compared to results from Trost (1967) who recommends $0.8 \leq \chi \leq 0.9$ for practical application.

Figure 3.6 shows the development of the relaxation for the Maridal concrete calculated with Eqs. (3.9) to (3.13) ($\chi = 0.837$) and the RELAX program in which the compliance function $J(t,t_0)$ is expressed according to the Linear Logarithmic Model described in Larson and Jonasson (2003).

Figure 3.6 *Comparison between the developments of the relaxation modulus $R(t,t_0)$ obtained from a simplified model according to Eq. (3.9) ($\chi = 0.837$) and by the more exact RELAX program given by Eq. (3.14).*

3.1.7 Restraint coefficients

The restraint coefficient $\gamma_R(t)$ can now be calculated according to Eq. (3.1) for the defined locations in the studied wall. In section 3.5 "Comparison of restraint coefficients"

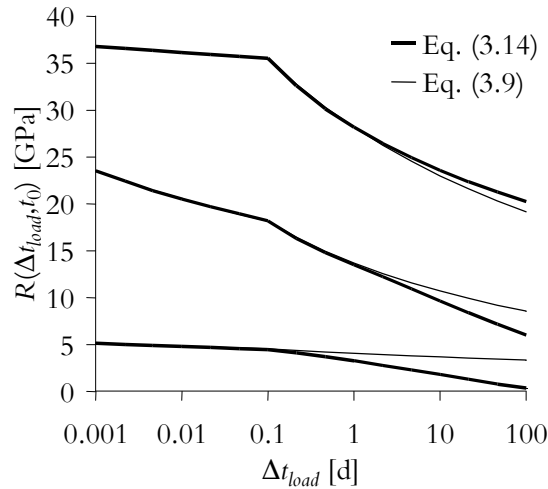the calculated development of the restraint coefficient in position 2, 5, 8 and 11 are shown together with evaluated restraint coefficients according to different methods.

The representative restraint coefficient for the contraction phase is in the empirical evaluation defined as the restraint appearing at the time when the concrete reaches failure i.e. when the cracks arise after 108 hours. Location 2 and 5, which are located close to one of the observed cracks, are however influenced by the non-linear stress strain behaviour that appears as micro cracks starts to develop when the concrete is close to failure. This means that the measured restraint in these locations may be underestimated compared to the locations where no cracking has taken place. To what extent will be further analysed in section 3.5.

3.2 Viscoelastic numerical evaluation of restraint

3.2.1 Method

The stress development $\sigma(t)$ within the defined locations of the restrained wall and the fixation stress $\sigma^{fix}(t)$ are calculated by means of the special purpose FE-program Con-TeSt Pro (2003). A realistic structural restraint development can then be evaluated analogous to Eq. (3.1), which include the thermal deformations and the maturity dependent viscoelastic behaviour of the concrete.

In the following, material models used in ConTeSt Pro (2003) and preconditions for the calculations are presented, see also Table 3.1. The material models have been fitted to material tests performed by Hedlund (2000) and Bosnjak (2000) describing the behaviour of the Maridal concrete. All model parameters are given in Appendix A.

3.2.2 Finite element modelling

For the temperature calculation, the studied structure of Maridal, wall and foundation, is modelled with two-dimensional (2D) 3-node elements. Stresses are analysed in the out of plane direction. Normally, the present length to height ratio of the structure (15/5.8 = 2.6) implies that plane section theory may not be valid, i.e. 2D analysis is expected not to be quite adequate. However, 3D elastic analysis of the actual structure, see Kanstad et al. (2001), shows that the restraint varies almost linearly, which means that plane section theory may yet be valid here as an application model. Further, the structure is founded on gravel with, according to Kanstad et al. (2001), modulus of compression $K_j = 60$ MN/m^2. Together with the actual structure properties this value gives practically no rotational boundary restraint, see Nilsson (2000), which means that free rotation for the structure wall-on-slab may be assumed. Free translation in the out of plane direction is also assumed as well as perfect bond between the wall and foundation.

3.2.3 Heat conduction

The heat transfer in an isotropic media under transient conditions is here modelled with a partial differential equation known as the heat conduction equation expressed by

$$\rho c \frac{\partial T}{\partial t} = \frac{\partial}{\partial x}\left(k_x \frac{\partial T}{\partial x}\right) + \frac{\partial}{\partial y}\left(k_y \frac{\partial T}{\partial y}\right) + Q_h \qquad (3.15)$$

where

x, y	are Cartesian coordinates when studying the cross-section, [m]
T	is temperature, [K]
ρ	is the density, [kg/m^3]
c	is specific heat by weight, [J/kg K]
k_x, k_y	is thermal conductivity in x- and y-direction respectively, [W/m K]
Q_h	is generated heat per unit volume and time, [W/m^3]

Formally, the heat flow at the surfaces of the structure is described as a convective flow by

$$q_n = \frac{\partial T}{\partial n} = h\left(T - T_{env}\right) \qquad (3.16)$$

where

q_n	is the heat flow from the structure normal to the boundary, [W/m^2]
h	is the formal heat transfer coefficient, [W/m^2 K]
T_{env}	is the temperature of the environment, [K]

Following expressions are used to calculate the heat transfer coefficients for the boundaries of the studied cross-section (see also Table 3.1):

$$h_{free} = \begin{cases} 5.6 + 3.95v & v < 5 \text{ m/s} \\ 7.8v^{0.78} & v > 5 \text{ m/s} \end{cases} \qquad (3.17)$$

$$h_{boundary} = \left(\frac{1}{h_{free}} + \sum \frac{l_i}{k_i}\right)^{-1} \qquad (3.18)$$

The wind velocity v is assumed to be 5 m/s as long as the formwork is at place and thereafter 0 m/s due to the fact that scaffolding for the subsequent casting of the culvert top slab surrounds the studied wall rapidly after form removal. This gives following heat transfer coefficients for the different boundaries of the studied wall:

- *Free surface 0 m/s*
    h_{free} = 5.6 W/m^{2}K

- *Formwork on wall 5 m/s*
    l_{form} = 0.018 m, k_{form} = 0.14 W/m K gives h_{form} = 5 W/m^{2}K

Paper C

- *Insulation on top of wall 5 m/s*

  l_{insul} = 0.01 m, k_{insul} = 0.036 W/m K gives h_{insul} = 3.2 W/m^{2}K

3.2.4 Maturity

The maturity development expressed in equivalent age is described by Eq. (3.2) to (3.4) in section 3.1.

3.2.5 Heat development

According to i.e. Ekerfors (1995) and Jonasson (1994) the liberated rate of heat $Q_h(t)$ at a certain time t can be calculated from a known heat development under isothermal conditions $W(t_e)$ as

$$Q_h = \frac{\partial W}{\partial t} = \frac{\partial W}{\partial t_e}\frac{\partial t_e}{\partial t} = \frac{\partial W}{\partial t_e}\beta_T \tag{3.19}$$

with

$$W = B_{ref}q_{cem} \tag{3.20}$$

$$B_{ref} = C + \sum_i\left(k_iB_i\right) \tag{3.21}$$

where

β_T	is defined in Eq. (3.3)
t_e	is defined in Eq. (3.2)
Q_h	is generated heat per unit volume of concrete and time, [W/m^3]
W	is the reaction heat of the concrete per unit weight of the reference binder, [J/kg]
B_{ref}	is the reference binder content of the concrete, [kg/m^3]
k_i	is formal effective factor for binder number i, (-)
q_{cem}	is the reaction heat per weight calculated with respect to the reference binder content, [J/kg]
C	is the Portland cement content of the concrete, [kg/m^3]
B_i	is the additional binder content for binder component number i whereby B_i may for instance be addition of puzzolanic binders like silica fume, blast furnace slag and fly ash, [kg/m^3]

3.2.6 Specific heat and thermal conductivity

The specific heat c indicates how much energy that is required to raise the temperature in a defined amount of material to a certain level. Typical values of the specific heat for ordinary concrete compositions are within the range of 800 to 1200 J/kgK.

The thermal conductivity k indicates the capability of the material to transmit heat. Typical values of the thermal conductivity are within the range of 1.6 to 2.5 W/mK.

3.2.7 Thermal dilatation and shrinkage

Deformations due to thermal dilation and shrinkage in the hardening concrete are modelled according to Eq. (3.5) to (3.8) in section 3.1.

3.2.8 Creep and relaxation

Relaxation is used in the thermal stress analysis, which has been retrieved by means of Eq. (3.14) from a known creep function given by Eqs. (3.10) to (3.13) in section 3.1.

3.2.9 Non-linear stress-strain behaviour

At high tensile stress levels (relative the tensile failure strength) the deformation of the concrete increases progressively with increasing stress i.e. non-linear behaviour is present. This phenomenon is mainly related to the growth of micro-cracks. A stress analysis that not considers the non-linear behaviour in tension will overestimate the tensile stresses.

Here, non-linear stress-strain behaviour at high tensile stresses (pre-peak behaviour) for loading in tension is modelled according to Jonasson (1994) and Hedlund (2000) whereby a virgin stress-strain curve is introduced according to Figure 3.7. Mathematically, this is written as:

$$\frac{\sigma}{f_{ct}} = \frac{\varepsilon_m}{\varepsilon_0} \quad \text{for} \quad \frac{\sigma}{f_{ct}} \leq \alpha_{ct} \tag{3.22}$$

$$\frac{\sigma}{f_{ct}} = 1 - \left(1 - \alpha_{ct}\right) \exp\left(-\left(\frac{\left(\frac{\varepsilon_m}{\varepsilon_0}\right) - \alpha_{ct}}{1 - \alpha_{ct}}\right)\right) \quad \text{for} \quad \frac{\sigma}{f_{ct}} > \alpha_{ct} \tag{3.23}$$

where

f_{ct} is tensile strength, [Pa]

ε_m is material strain (strain related to the stress level), [–]

α_{ct} is relative stress level above which non-liner stress-strain behaviour is present, [–]

ε_0 is f_{ct}/E, i.e. a fictitious strain linearly related to the tensile strength, [–]

Unloading, $\Delta\sigma < 0$, is modelled by use of the elastic modulus at origin, which corresponds to inclination = 1 in Figure 3.7.

Paper C
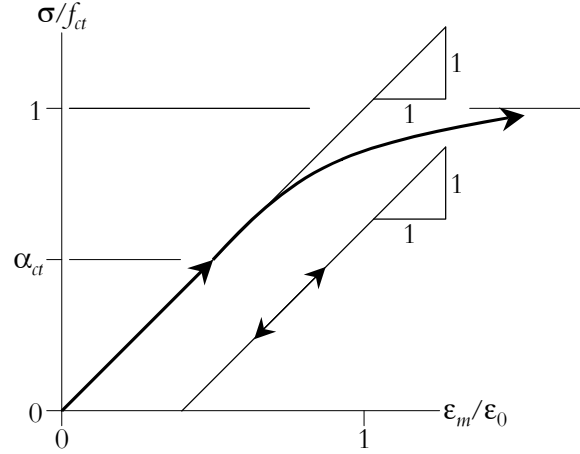
Figure 3.7 *Non-linear stress-strain behaviour at tension according to Jonasson (1994) and Hedlund (2000).*

The unrestrained movements are here expressed as stress induced deformations, Bažant and Chern (1985):

$$\Delta\varepsilon_T^0 = \Delta\varepsilon_T^{free}\left(1 + \rho_T\,\frac{\sigma}{f_{ct}}\,\text{sign}\left(\Delta\varphi\right)\right) \quad\quad (3.24)$$

$$\Delta\varepsilon_\varphi^0 = \Delta\varepsilon_\varphi^{free}\left(1 + \rho_\varphi\,\frac{\sigma}{f_{ct}}\,\text{sign}\left(\Delta\varphi\right)\right) \qu\quad (3.25)$$

where

$\Delta\varepsilon_T^0$ is nonelastic strain, including the stress-induced part, due to a change in temperature, [-]

$\Delta\varepsilon_T^{free}$ is unrestrained and stress-free thermal strain due to thermal changes, [-]

ρ_T is an adjustment factor for stress-induced thermal strain, [-]

$\Delta\varepsilon_\varphi^0$ is nonelastic strain, including the stress-induced part, due to a change in humidity, [-]

$\Delta\varepsilon_\varphi^{free}$ is unrestrained and stress-free moisture strain due to humidity changes, [-]

ρ_φ is an adjustment factor for stress-induced moisture strain, [-]

$\Delta\varphi$ is considered as change in relative pore humidity due to thermal and moisture changes, [-]

The compressive strength development is expressed as described in Jonasson (1994) by using discrete values extracted from a given or measured strength development according to following scheme:

Equivalent age (t_e), [h]	Part of compressive strength at the age of 28 days (f_{cc}^{28}), [‰]
6	η_1
8	η_2
12	η_3
18	η_4
24	η_5
72	η_6
168	η_7

and thereafter applying piece-by-piece linear interpolation in logarithmic time scale. The tensile strength is then estimated in relation to the compressive strength as

$$f_{ct} = f_t^{ref} \left(\frac{f_{cc}}{f_c^{ref}} \right)^{\beta_1}$$

(3.26)

where

f_{ct}	is tensile strength, [Pa]
f_{cc}	is compressive strength, [Pa]
f_t^{ref}	is reference tensile strength, [Pa]
f_c^{ref}	is reference compressive strength, [Pa]
β_1	is a model parameter, [-]

Table 3.1 *Preconditions for viscoelastic evaluation of restraint by means of the special purpose FE-program ConTeSt Pro (2003). Model parameters are given in Appendix A.*

Geometry:	Mid-section in Figure 3.1		
Thermal behaviour:	Heat conduction Maturity Heat development	Eqs. (3.15) to (3.18) Eqs. (3.2) to (3.4) Eqs. (3.19) to (3.21)	
Mechanical behaviour:	Thermal dilatation and shrinkage Creep and relaxation Non linear stress–strain behaviour	Eqs. (3.5) to (3.8) Eqs. (3.10) to (3.14) Eqs. (3.22) to (3.26)	
Heat transfer coefficients:	Free surface	5.6	$[W/m^2 {}^{\circ}C]$
	Insulation on top of wall	3.2 (0–24 h) 5.6 (24– h)	$[W/m^2 {}^{\circ}C]$
	I. Formwork on wall (form removal 24 h)	5.3 (0–24 h) 5.6 (24– h)	$[W/m^2 {}^{\circ}C]$
	II. Formwork on wall (form removal 48 h)	5.3 (0–48 h) 5.6 (48– h)	$[W/m^2 {}^{\circ}C]$
Temperatures:	Initial temperature at casting Ambient temperature	20 Figure 3.8	$[{}^{\circ}C]$ $[{}^{\circ}C]$
Casting:	Filling rate	1	$[m/h]$

3.2.10 Calculated and measured temperature

The ambient temperature was measured, and by connecting these measurements by straight lines the ambient temperature used in the calculations becomes a piece-by-piece linear temperature development, see Figure 3.8.
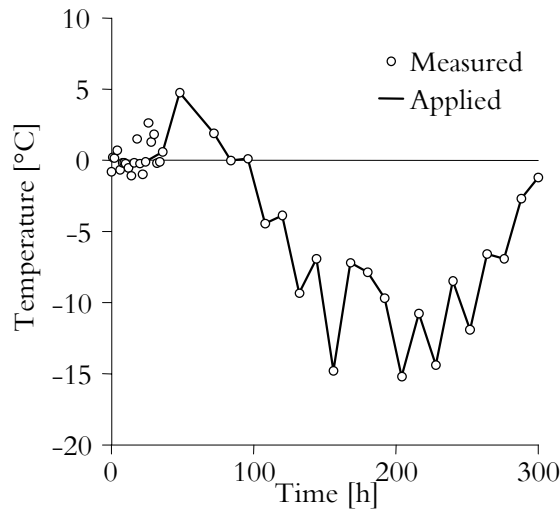
Figure 3.8 *Measured and applied ambient temperature.*

The temperature development in the concrete has been calculated by means of the above given equations and model parameters according to Appendix A for the Maridal concrete giving the results presented in Figure 3.9. As can be seen there is a good correlation between measured and calculated temperature in position 5 and 8 while 2 and 11 show somewhat larger deviation. One possible explanation is that the real "local" concrete might differ somewhat in its properties, but the calculation is only done for one set of parameters.
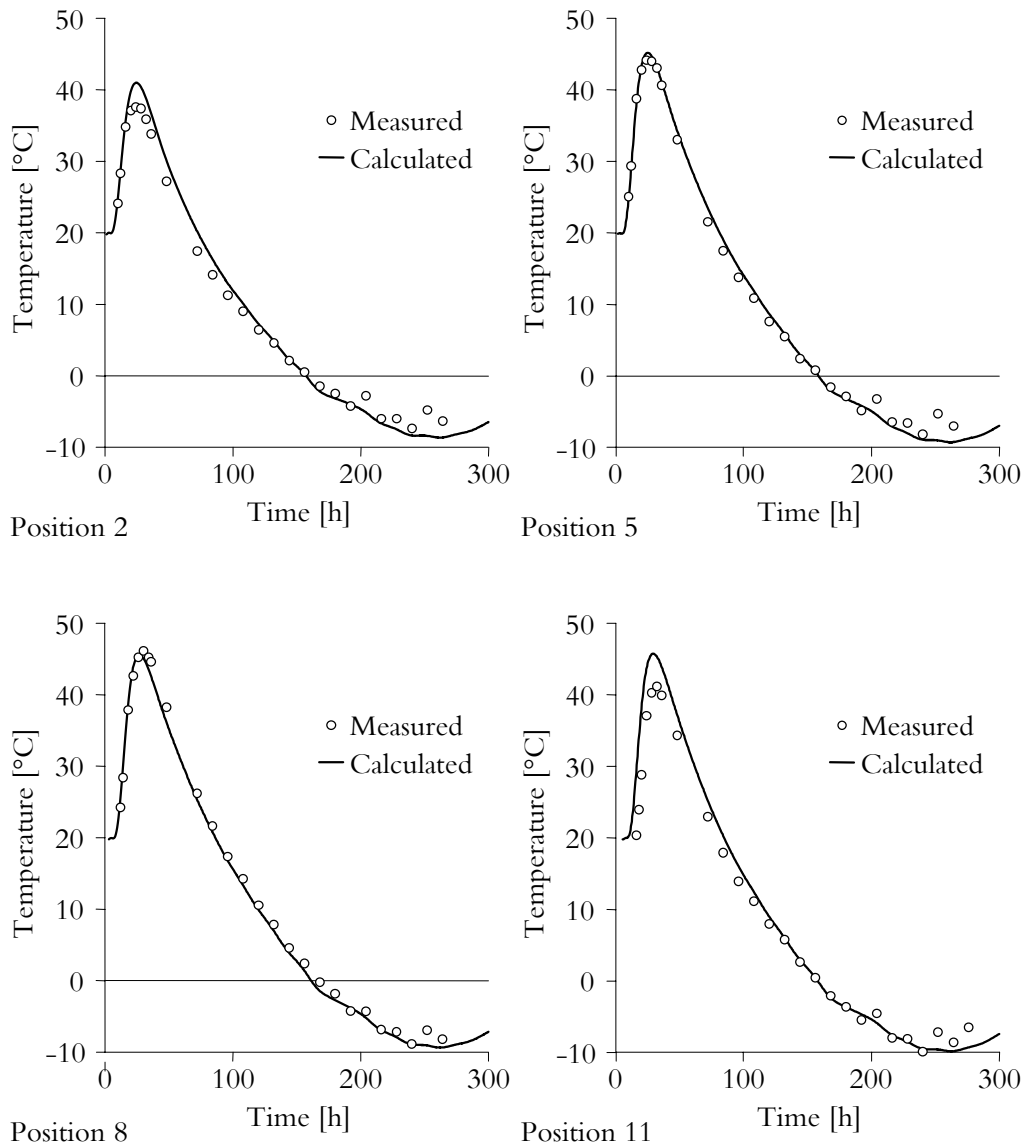
Figure 3.9 *Measured and calculated temperature in location 2, 5, 8 and 11. Calculations have been performed with the special purpose program ConTeSt Pro (2003).*

3.2.11 Restraint coefficients

By means of the calculated stress development $\sigma(t)$ and the fixation stress $\sigma^{fix}(t)$ the restraint development can now be calculated as described by Eq. (3.1). Depending on weather the non-linear stress strain behaviour is considered or not the restraint has been evaluated as:

I. the non-linear stress strain behaviour at high tensile stress levels is considered in the thermal stress analysis giving the closest description of the actual behaviour of the studied culvert wall in which cracks have appeared. This however means that non-linear effects related to the high tensile stress level are included in the evaluated restraint coefficient. The representative restraint coefficient is in this evaluation case defined as the value appearing after 108 hours when cracks according to the measurements arise in the wall.

II. the non-linear stress strain behaviour is not considered in the analysis giving a restraint that is not dependent on the stress level and therefore gives a more general description of the structural restraint behaviour for an undamaged wall and thereby may be comparable to the elastic approaches. Here the representative restraint coefficient is defined at the time when the maximum stress arises in each studied position of the wall.

The evaluated restraint development for the two above outlined cases in the midsection of the wall (position 3, 6, 9 and 12) is shown in Figure 3.12. The evaluated restraint coefficients are given in Table 3.2 and Figure 3.11. As can be seen the nonlinear stress strain behaviour significantly influences the evaluated restraint which will be underestimated compared to a linear analysis, see further section 3.5.

3.3 Elastic numerical evaluation of restraint

3.3.1 Method

In an elastic approach the numerical analysis does not include the thermal and viscoelastic behaviour of the hardening concrete, which considerably simplifies and shortens the computations. Any general purpose FE-program can be used whereby the restrained structural element is subjected to an instant contraction, see for instance Kjellman and Olofsson (1999), Larson (2000) or Olofsson et al. (2002). The calculated stress in a specified location of the element is then compared to the stress that appears if the element is completely restrained whereby a restraint coefficient can be determined as

$$\gamma_R = \frac{\sigma(\zeta E_{c28}, E_a, \varepsilon_c)}{\sigma^{fix}(\zeta E_{c28}, \varepsilon_c)} \tag{3.27}$$

where

σ is the calculated stress from an elastic FE-analysis in the newly cast part of the structure, [Pa]

σ^{fix} is the calculated stress in the newly cast part of the structure at total fixation, [Pa]

ε_c is the contraction to which the newly cast structure is subjected, [-]

E_a is the modulus of elasticity for the adjoining structure, [Pa]

E_{c28} is the modulus of elasticity for the young concrete structure at 28 days equivalent age, [Pa]

Paper C

ζ   is a time factor describing development of the modulus of elasticity, [–]

3.3.2   *Finite element modelling*

The studied structure is modelled with elements and structural boundary conditions in ConTeSt Pro (2003) as described under section 3.2 above.

3.3.3   *Preconditions*

Following parameters are used in the analysis:

- The modulus of elasticity for the adjoining structure E_a is 36.82 GPa
- The modulus of elasticity for the young concrete structure at 28 days equivalent age E_{c28} is 36.82 GPa
- The time factor describing development of the modulus of elasticity ζ is 1.0.

- The contraction to which the newly cast structure is subjected ε_c is described by $\alpha_c \Delta T$ with $\alpha_c = 10 \cdot 10^{-6} \ °C^{-1}$ and $\Delta T = 10 \ °C$, i.e. $\varepsilon_c = 100 \cdot 10^{-6}$.

3.3.4   *Restraint coefficients*

The evaluated restraint coefficients for the mid-section of the wall (position 3, 6, 9 and 12) are given in Table 3.2 and Figure 3.11, see further section 3.5.

3.4   **Elastic analytical evaluation of restraint**

3.4.1   *Method*

An elastic analytical expression to calculate the restraint coefficient γ_R has been derived by Nilsson (2000) under the assumption that plane sections remain plane and that the strains over the height of the structure vary linearly. This may, according to Nilsson (2000), be valid for structures with length to height ratios equal to or larger than approximately five. The expression has been further developed, Nilsson (2003a), for effects of possible slip failure in the joints between the wall and the slab, δ_{slip}, for effect of high wall structures (resilience), δ_{res}, and for un-symmetric structures. The restraint coefficient γ_R is separated into a translational part γ^t_R and two rotational parts γ^{rx}_R and γ^{ry}_R according to

$$\gamma_R = \delta_{slip}\delta_{res} - \gamma^t_R - \gamma^{rx}_R - \gamma^{ry}_R \tag{3.28}$$

where

δ_{slip} slip in joint effect, see Nilsson (2003a & b), [–]
δ_{res} high wall effects, resilience, [–]

The high wall effects, resilience, are in Nilsson (2003a & b) determined by a basic resilience factor and two correction factors for structures subjected to some degree of boundary restraint. Normally, and in this paper, the boundary restraint is negligible,

which implies that the resilience is determined from the basic resilience according to Figure 3.10
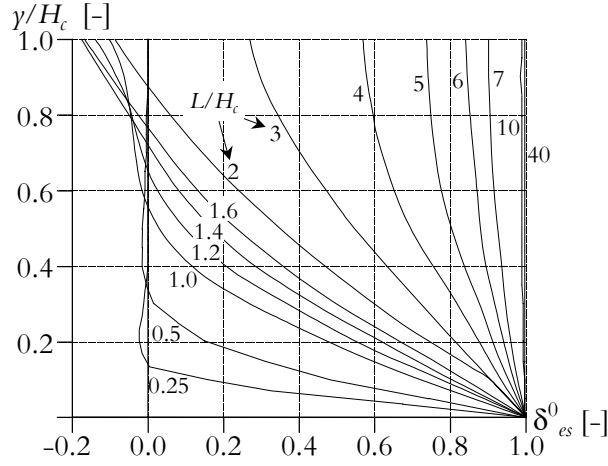
Figure 3.10 *Basic resilience factor* δ^0_{res} *as function of the relative distance above the joint. Nilsson (2003b).*

The curves describing the basic resilience are in Nilsson (2003a & b) described with polynomials according to

$$\delta^0_{res} = a_0 + a_1\left(\frac{\gamma}{H_c}\right) + a_2\left(\frac{\gamma}{H_c}\right)^2 + \ldots + a_i\left(\frac{\gamma}{H_c}\right)^n = \sum_{i=0}^{n} a_i\left(\frac{\gamma}{H_c}\right)^i \qquad (3.29)$$

where $a_0 - a_n$ are the coefficients in the polynomials.

Further, the three additional restraint parts in Eq. (3.28), applied for a newly cast wall on existing slab like the Maridal culvert, are derived using the compensated line theory, supplemented for the high wall effects, and are calculated as

$$\gamma^t_R = (1 - \gamma_{RT})\delta_{slip} \frac{\displaystyle\sum_{i=0}^{n}\frac{a_i}{i+1}}{1 + \dfrac{E_a}{\zeta E_{c28}} \cdot \dfrac{B_{a,eff}H_a}{B_c H_c}} \qquad (3.30)$$

$$\gamma^{rx}_R = (1 - \gamma_{RR,x})\delta_{slip} \frac{(\gamma_{cen} - \gamma)\left(\gamma_{cen}\displaystyle\sum_{i=0}^{n}\frac{a_i}{i+1} - H_c\displaystyle\sum_{i=0}^{n}\frac{a_i}{i+2}\right)}{\dfrac{H_c^2}{12} + \left(\gamma_{cen} - \dfrac{H_c}{2}\right)^2 + \dfrac{E_a}{\zeta E_{c28}}\dfrac{B_{a,eff}H_a}{B_c H_c}\left(\dfrac{H_a^2}{12} + \left(\gamma_{cen} + \dfrac{H_a}{2}\right)^2\right)} \qquad (3.31)$$

132

and

$$\gamma_R^{ry} = (1 - \gamma_{RR,y})\delta_{slip} \frac{(x_{cen} - x)\left(x_{cen} - \omega\dfrac{B_{a,eff} - B_c}{2}\right)}{\dfrac{B_c^2}{12} + \left(x_{cen} - \omega\dfrac{B_{a,eff} - B_c}{2}\right)^2 + \dfrac{E_a}{\zeta E_{c28}}\dfrac{H_a B_{a,eff}}{H_c B_c}\left(\dfrac{B_{a,eff}^2}{12} + x_{cen}^2\right)} \tag{3.32}$$

where

x, y	are Cartesian coordinates in the studied cross-section, [m]
E_a	is the modulus of elasticity for the slab, [Pa]
E_{c28}	is the modulus of elasticity for the young concrete wall at 28 days equivalent time, [Pa]
ζ	is a time factor describing the development of the modulus of elasticity, [-]
$B_{a,eff}$	is the effective width according to Nilsson (2003a & b) of the slab, [m]
H_a	is the height of the slab, [m]
B_c	is the width of the young concrete wall, [m]
H_c	is the height of the young concrete wall, [m]
x	is the horizontal distance from the centre of the slab, [m]
x_{cen}	is the location of the centroid of the transformed cross-section relatively the centre of the slab, [m]
y	is the distance above the casting joint between the slab and the young concrete wall, [m]
z_{cen}	is the location of the centroid of the transformed cross-section relatively the centre of the slab, [m]
γ_{RT}	translational boundary restraint [-]
$\gamma_{RR,x}$	rotational boundary restraint for bending around the x-axis [-]
$\gamma_{RR,y}$	rotational boundary restraint for bending around the y-axis [-]
ω	is the relative location of the wall on the slab. If $\omega = 0$, the wall is located in the middle of the slab, if $\omega = \pm 1$, the wall is located at one of the edges of the slab.

The location of the centroid of the transformed cross-section relative the joint between the wall and the slab and the centre of the slab is calculated from

$$x_{cen} = \frac{\omega\dfrac{B_{a,eff} - B_c}{2}}{1 + \dfrac{E_a}{\zeta E_{c28}}\dfrac{H_a B_{a,eff}}{H_c B_c}} \quad \text{and} \quad y_{cen} = \frac{\dfrac{H_c}{2} - \dfrac{H_a}{2}\dfrac{E_a}{\zeta E_{c28}}\dfrac{H_a B_{a,eff}}{H_c B_c}}{1 + \dfrac{E_a}{\zeta E_{c28}}\dfrac{H_a B_{a,eff}}{H_c B_c}} \tag{3.33}$$

Calculations by Eq. (3.28) with Eqs. (3.29) to (3.33) are hereby denoted Elastic Approach Analytical II, see Table 3.2.

If slip failure in the joint is not considered, if plane sections remain plane (no effects of high walls, or what is denoted resilience) and if no translational nor rotational boundary restraint is present, $\gamma_{RT} = \gamma_{RR,x} = \gamma_{RR,y} = 0$, the analytical expression for the determination of the restraint variation is simplified to, here denoted Elastic Approach Analytical I,

$$\gamma_R = 1 - \frac{1}{1 + \dfrac{E_a}{\zeta E_{c28}} \cdot \dfrac{B_{a,eff} H_a}{B_c H_c}}$$

$$- \frac{(\gamma_{cen} - \gamma)\left(\gamma_{cen} - \dfrac{H_c}{2}\right)}{\dfrac{H_c^2}{12} + \left(\gamma_{cen} - \dfrac{H_c}{2}\right)^2 + \dfrac{E_a}{\zeta E_{c28}} \dfrac{B_{a,eff} H_a}{B_c H_c}\left(\dfrac{H_a^2}{12} + \left(\gamma_{cen} + \dfrac{H_a}{2}\right)^2\right)}$$

$$- \frac{\left(x_{cen} - \omega\dfrac{B_{a,eff} - B_c}{2}\right)^2}{\dfrac{B_c^2}{12} + \left(x_{cen} - \omega\dfrac{B_{a,eff} - B_c}{2}\right)^2 + \dfrac{E_a}{\zeta E_{c28}} \dfrac{H_a B_{a,eff}}{H_c B_c}\left(\dfrac{B_{a,eff}^2}{12} + x_{cen}^2\right)} \qquad (3.34)$$

3.4.2 Restraint coefficients

The restraint is calculated according to Eqs. (3.28) to (3.33) and by Eq. (3.34) whereby following parameters are used in the analysis, see also Figure 2.1 and Figure 2.2:

$\dfrac{E_a}{E_{c28}}$	1.0
ζ	1.0
$\dfrac{B_{a,eff}}{B_c}$	0.7427
$\dfrac{H_a}{H_c}$	0.1724
γ	0.5, 1.0, 2.5 and 5.0 m
H_c	5.8 m

The evaluated restraint coefficients for the mid-section of the wall (position 3, 6, 9 and 12) are given in Table 3.2 and Figure 3.11, see further sub-section 3.5.

3.5   Comparison of restraint coefficients

In this section all restraint coefficients determined by different methods described in sections 3.1 to 3.4 are collected and compared. The major result is that the empirical and viscoelastic numerical non-linear approaches give the best picture of the actual structural restraint behaviour of the studied wall while the viscoelastic numerical linear,

elastic numerical and elastic analytical approaches give a more general description of how an undamaged wall behave, see further below.

As can be seen in Figure 3.12 there is a large variation of the evaluated restraint close to the zero stress state, which is related to the division of small stress values in Eq. (3.1). An additional reason for the deviation of the measured restraint at early ages is that the strain gauges measure deformation in the reinforcement which does not have full contact with the, at this time, still plastic concrete. As the wall then starts to contract the restraint develops from an initial high level down to a more or less constant value. In position 2 and 5 it can clearly be seen how the non–linear behaviour affects the restraint situations as the wall approaches failure. The non linear behaviour will in this specific case influence the restraint in position 2 in the order of approximately 14 % compared to a linear analysis at the time when the structure reaches failure (after 108 hours).

The evaluated restraint coefficients are given in Table 3.2 and in Figure 3.11 they are presented as a function of the relation height over the foundation y to the height of the wall H_c. The overall correlation between the different approaches is very good but with some deviations that have to be further explained.

Although plane section theory is applied the restraint evaluated according to the viscoelastic approach does not give coefficients following a straight line from the bottom to the top of the wall. The largest deviation is at the lower part of the wall (position 2) where the major portion of the deviation arises due to the non–linear behaviour when the structure reaches failure. This location is however, as can be seen in Figure 3.9, also influenced by a lower temperature giving less thermal dilatation and a slower development of the E–modulus and creep that in turn will give a lower value of the restraint coefficient. In this study the deviation in restraint between the viscoelastic and elastic approaches is comparatively small but in structures with large temperature differences the influence on the evaluated restraint coefficient may be significant.

Table 3.2 *Representative restraint coefficients evaluated according to viscoelastic and elastic approaches with numerical and analytical methods compared to measured restraint after 108 hours when the wall reaches failure.*

Method Loca- tion	Empirical approach Measured (After 108 h)	Viscoelastic approach		Elastic approach		
		Numerical I. Non-linear (After 108 h)	Numerical II. Linear (At σ_{max})	Numerical	Analytical	
					I	II
2	0.604	–	–	–	–	–
3	–	0.584	0.555	0.603	0.576	0.577
5	0.482	–	–	–	–	–
6	–	0.539	0.515	0.510	0.479	0.480
8	0.385	–	–	–	–	–
9	0.312	0.302	0.255	0.231	0.198	0.172
11	–0.130	–	–	–	–	–
12	–	–0.241	–0.222	–0.234	–0.266	–0.226
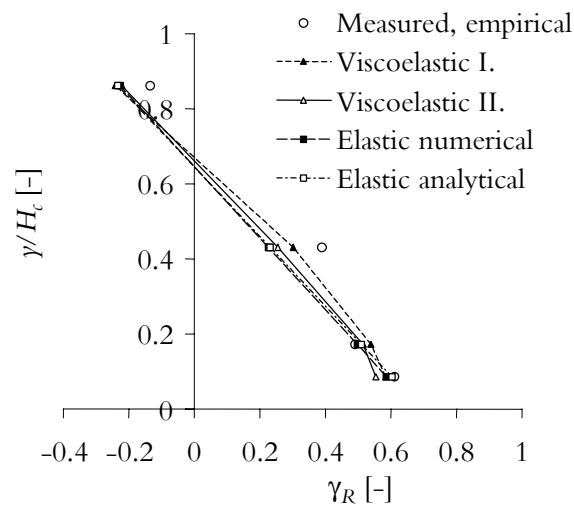
Figure 3.11 *Comparison of restraint coefficients in the mid-section of the wall evaluated with viscoelastic and elastic approaches presented as a function of the relation height over the foundation y to the height of the wall H_c. The measured restraint in point 2, 5, 8 and 11 is also given in the figure.*
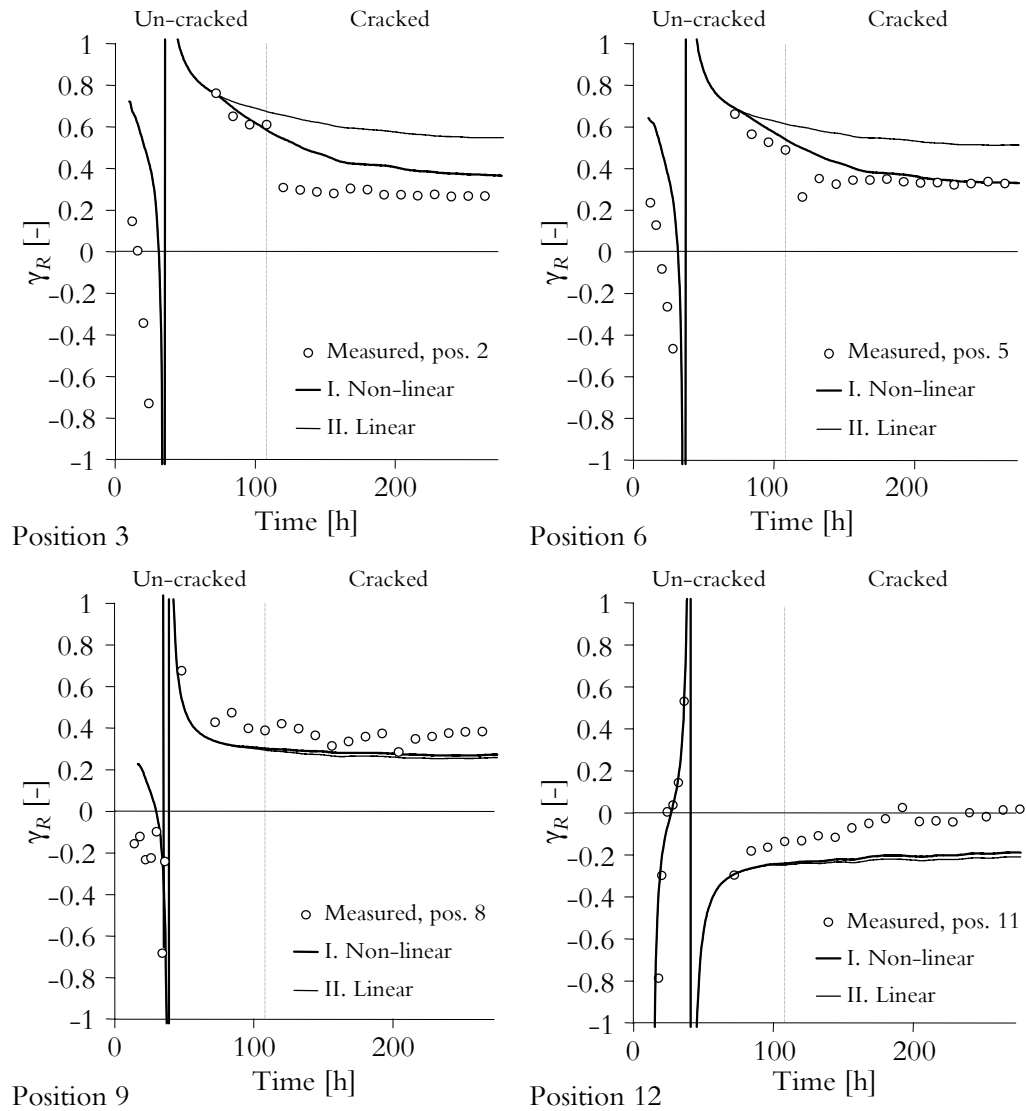
Figure 3.12 Measured and calculated (viscoelastic numerical approach) development of the restraint coefficient $\gamma_R(t)$ according to Eq. (3.1). I. denotes that the non-linear stress strain behaviour at high tensile stresses has been considered and II. that it has not. Note that the positions of the measured (empirical approach) values are Nos. 2, 5, 8 and 11 while the viscoelastic approach is valid for positions Nos. 3, 6, 9 and 12.

4   THERMAL STRESSES

4.1 Application of restraint coefficient in stress analysis

The application of restraint coefficients in thermal stress analysis is as here shown in Eqs. (1.1) to (1.3), described by

$$\sigma(t) = \gamma_R \sigma^{fix}(t) \tag{4.1}$$

where the fixation stress $\sigma^{fix}(t)$, including the material behaviour of the hardening concrete described in section 3.2, can be calculated without knowing the structural behaviour of the actual structure that is to be analysed. The structural behaviour is considered by the restraint coefficient γ_R solely.

To clarify how the application of restraint coefficients influence a calculated thermal stress development following stress calculations are performed for the mid-section (position 3, 6, 9 and 11) of the studied wall where plane section theory may be assumed to be valid (see also Figure 4.1):

- *Measured*   The stress development is calculated from the measured strain development in position 2, 5, 8 and 11 as described in section 3.1.
- *FEM non-linear*   The stress development is calculated by means of the special purpose Finite Element (FE) program ConTeSt Pro as described in section 3.2 whereby the non-linear stress strain behaviour at high tensile stresses is considered. This calculation gives the closest description of the studied structure.
- *FEM linear*   As described under "FEM non-linear" but without considering the non-linear behaviour. This calculation is comparable to the concept of using restraint coefficients explained below.
- *Coefficient*   The stress development is calculated according to Eq. (4.1) from the fixation stress $\sigma^{fix}(t)$ with the restraint coefficients obtained by the elastic analytical approach given in Table 3.2.

4.1   Comparison of stresses

4.1.1   Measured and FEM non-linear

As can be seen in Figure 4.1 the correlation between the measured and calculated stress development is rather good. This means that the preconditions given in section 3.2 regarding structural behaviour and material modelling are good enough for description of this particular situation.
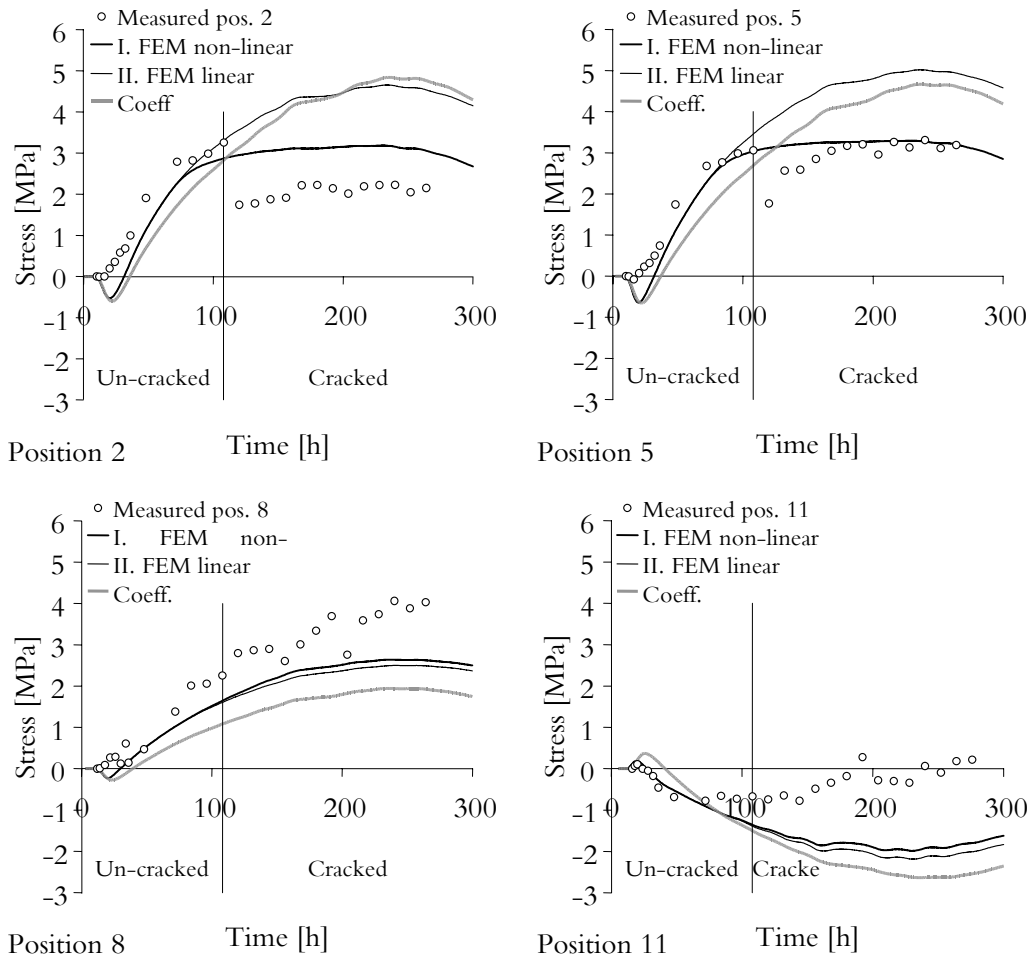
Figure 4.1 *Calculated stress development by means of numerical FE-analysis and restraint coefficient evaluated by means of an elastic analytical approach compared to measured stresses in positions nearby. I. denotes that the non-linear stress strain behaviour at high tensile stresses has been considered and II. that it has not.*

As also described in Hedlund (2000) it has been shown that it is possible to use results from individual tests of different material properties and put them together in a thermal stress calculation giving a satisfactory description of the stress development.

Regarding the structural boundary conditions it has here again been stated that a structure founded on soft ground, i.e. gravel, silt or clay, may be assumed to have free translation and free rotation.

The modelling of the non-linear stress-strain behaviour at high tensile stress levels seems to give an accurate description of the stress development when micro cracks start

to develop and the structure finally reaches failure. This behaviour can also clearly be recognized in the measured results from the field test at the positions where failure has been observed (position 2 and 5).

4.1.2   FEM linear and Coefficient

Using the concept of describing the structural behaviour by means of a restraint coefficient give, as shown in Figure 4.1, an acceptable picture of the stress development calculated with numerical FEM. Here the most important issue is to confirm that the coefficient approach give reliable results and does not underestimate the maximum stress during the contraction phase as this is used as a design criterion in practical application. As can be seen this condition is satisfactorily fulfilled.

5   CONCLUSIONS

It is shown that it is possible to evaluate the structural restraint by means of simple elastic approaches. Compared to a more realistic viscoelastic approach and the measured restraint behaviour of a real full scale structure the elastic approaches give consistent results. In structures with large temperature variations, however, there might be significant deviations due to different development of the maturity dependent material properties. This has not been analysed here but should be set under further focus.

It can clearly be stated that the concept of using restraint coefficients in thermal stress analysis will work for practical application. The coefficient approach give reliable results and does not underestimate the maximum stress during the contraction phase. The non-linear stress strain behaviour at high tensile stresses has in this respect a less important role to play. This due to the fact that cracks shall be avoided and a correct description of the stress development should be obtained at stress levels when the relation between stress and strain still is more or less linear.

ACKNOWLEDGMENT

REFERENCES

Bažant, Z P and Wu, S T (1974). Rate-type Creep Law of Concrete Based on Maxwell Chain. J. RILEM. In: *Material and Structure, Vol. 7/1974, pp 45-60.*

Bažant, Z P and Chern, J-C (1985). Concrete Creep at Variable Humidity – Constitutive Law and Mechanisms. In: *Material and Structures, Vol. 18, pp 1 - 20.*

Paper C

Bosnjak, B (2000). *Self-Induced Cracking Problems in Hardening Concrete Structures*. Division of Structural Engineering, The Norwegian University of Science and Technology, Doctoral Thesis 2000:121, 152 pp.

Byfors, J (1980). *Plain Concrete at Early Ages*. Swedish Cement and Concrete Research Institute, Fo/Research 3:80, Stockholm.

ACI, R W (1973) (Chairman). *Effect of Restraint, Volume Change and Reinforcement on Cracking of Massive Concrete*. American Concrete Institute Committee, report no ACI 207.2R-73, 10 pp.

ConTeSt Pro (2003). *Users manual - Program for Temperature and Stress Calculations in Concrete*. Developed by JEJMS Concrete AB in co-operation with Luleå University of Technology, Cementa AB and Peab AB. Luleå, Sweden: Luleå University of Technology. (In progress May 2003).

Ekerfors, K (1995). *Mognadsutveckling i ung betong - Temperaturkänslighet, hållfasthet och värmeutveckling (Maturity development in young concrete - Temperature sensitivity, strength and heat development, in Swedish)*. Division of Structural Engineering, Luleå University of Technology, Licentiate Thesis 1995:34L, 136 pp.

Emborg, M (1989). *Thermal Stresses in Concrete Structures at Early Ages*. Division of Structural Engineering, Luleå University of Technology, Doctoral Thesis 1989:73D, 280 pp.

Emborg, M and Bernander, S (1994). *Modeller för beräkning av temperaturspänningar och sprickrisk. Kapitel 16.10 i Betonghandboken - Material (Models for Calculation of Thermal Stresses and Cracking Risks. Chapter 16.10 in the Swedish Handbook for Concrete Constructions - Material. In Swedish)*. Svensk Byggtjänst och Cementa AB, Stockholm 1994.

Freisleben Hansen, P and Pedersen, E J (1977). Måleinstrument til kontrol af betons hærdening (Maturity Computer for controlled curing and hardening of concrete, in Danish). In: *Journal of Nordic Concrete Federation, No 1:1977, Stockholm, pp 21-25*.

Harrison, T. A. (1981). *Early-age thermal crack control in concrete*. London, England: CIRIA, Construction Industry Research and Information Association. Report 91. ISSN: 0305-408X. ISBN: 0 86017 166 3. pp. 48.

Hedlund, H (2000). *Hardening Concrete − Measurements and Evaluation of Non-elastic Deformation and Associated restraint stresses*. Division of Structural Engineering, Luleå University of Technology, Doctoral Thesis 2000:25, 394 pp.

Heimdal, E, Kanstad, T and Kompen, R (2001). *Maridal Culvert Norway − Field Tests II*. Published by Luleå University of Technology, Division of Structural Engineering, IPACS Report, ISBN 91-89580-74-5.

Jonasson, J-E (1984). *Slipform Construction - Calculations for Assessing Protection Against Early Freezing*. Swedish Cement and Concrete Research Institute, Fo/Research 4:84, Stockholm, 70 pp.

Jonasson, J-E (1994). *Modelling of Temperature, Moisture and Stresses in Young Concrete*. Division of Structural Engineering, Luleå University of Technology, Doctoral Thesis 1994:156D, 225 pp.

Kanstad, T and Bosnjak, D (2001). *3D Neural Network Calculations of Culvert Walls by Diana – Verification, Theoretical and Practical Background*. Published by Luleå University of Technology, Division of Structural Engineering, IPACS Report, ISBN 91-89580-61-3.

Kjellman, O and Olofsson, J (1999). *3D Structural Analysis of Crack Risk in Hardening Concrete Structures - Verification of a Three-step Engineering Method*. Published by Luleå University of Technology, Division of Structural Engineering, IPACS Report, ISBN 91-89580-53-2.

Larson, M (2000). *Estimation of Crack Risk in Early Age Concrete – Simplified Methods for Practical Use*. Division of Structural Engineering, Luleå University of Technology, Licentiate Thesis 2000:10, 170 pp.

Larson, M and Jonasson, J-E (2003). *Linear Logarithmic Model for Concrete Creep – I. Formulation and Evaluation*. In progress.

Nilsson, M (2000). *Thermal Cracking of Young Concrete – Partial Coefficients, Restraint Effects and Influence of Casting Joints*. Luleå, Sweden: Luleå University of Technology, Division of Structural Engineering. Licentiate Thesis 2000:27. pp. 267. http://epubl.luth.se/1402-1757/2000/27/LTU-LIC-0027-SE.pdf

Nilsson, M (2003). *Determination of Restraint in Early Age Concrete Walls on Slabs by a Semi-Analytical Method – Paper 2 Verification and Application*. (Paper B in this thesis, aimed for external publication).

Olofsson, J, Hedlund, H and Uhlán, M (2002). *Slab Cast on Rock Ground – Model for Restraint Estimation*. Published by Luleå University of Technology, Division of Structural Engineering, IPACS Report, ISBN 91-89580-XY-Z, In progress.

Thomassen, A K (1999). *Temperature and Strain Calculations Related to the Field Tests at the Maridals Culvert*. NOR-IPACS report STF22 A99761, ISBN 82-14-01062-4.

Trost, H (1967). Auswirkungen des Superpositionsprinzips auf Kriech- und Relaxationsprobleme bei Beton Spannbeton. In: *Beton und Stahlbau, Vol. 62, 1967, pp 230-238*.

Utsi, S (2003). *Self-Compacting Concrete – Properties of fresh and hardening concrete for civil engineering applications*. Luleå, Sweden: Division of Structural Engineering, Luleå University of Technology. Licentiate Thesis 2003:19. (In progress).

Paper C

Westman G and Jonasson J-E (1999). *Conversion of creep data to relaxation data by the program RELAX*. Division of Structural Engineering, Luleå University of Technology, Skrift 199:06, 23 pp.

APPENDIX A   MATERIAL PROPERTIES OF THE MARIDAL CONCRETE

A.1   Thermal and mechanical properties

In Table A.1 to A.4 parameter values for the models used in the empirical evaluation in section 3.1 and the viscoelastic numerical evaluation in section 3.2 (ConTeSt Pro package) are given. The results come from tests and material modelling given in Hedlund (2000) and Bosnjak (2000) and have in some cases been revised based on the results from the full-scale field tests.

Table A.1 *Some mix parameters of the tested Maridal concrete. w_0 is the mixing water content, C is the cement content, B is the total binder content and SF is condensed silica fume content (B = C + SF).*

w_0/C	–	0.44
w_0/B w_0/B	–	0.42
C (CEM I 52.5)	kg/m^3	347.8 to 354.8
SF/C	–	0.05
Air	%	3.5 to 4.8

Table A.2 *Thermal properties for the Maridal concrete.*

ρ	kg/m^3	2350
c	J/kg K	1100 (1000) [*]
λ	W/m K	2.2 (2.1) [*]
W_c	J/kg	335000 (355000) [*]
C	kg/m^3	350
λ_1	–	1.15
t_1	h	9.5
κ_1	–	2.75
Δt_{e0}	h	3
β_D	–	1
θ_{ref}	K	4400
κ_3	–	0
t_s	h	10
[*] *Adjusted after comparison with results from field test. Original values are given within brackets.*		

Table A.3 *Mechanical properties for the Maridal concrete.*

Poison ratio	ν	–	0.18
Creep and relaxation	Δt_0	d	0.001
	Δt_1	d	0.1
	a_1^{min}	10^{-12}/(Pa log–unit)	0.1
	a_1^{max}	10^{-12}/(Pa log–unit)	60
	a_2^{max}	10^{-12}/(Pa log–unit)	30
	a_2^{min}	10^{-12}/(Pa log–unit)	6.939
	t_{a1}	d	0.01
	n_{a1}	–	0.198
	t_{a2}	d	0.677
	n_{a2}	–	0.604
	E_{ref}	GPa	36.82
	t_B	d	1.212
	b_1	1/(log–unit)	1.498
	b_2	1/(log–unit)	0.224
	χ	–	0.837
Non linear stress strain behaviour	f_{cc}^{28}	MPa	76
	η_1 (6 h)	‰	17
	η_2 (8 h)	‰	25
	η_3 (12 h)	‰	53
	η_4 (18 h)	‰	155
	η_5 (24 h)	‰	224
	η_6 (72 h)	‰	560
	η_7 (168 h)	‰	803
	f_t^{ref}	MPa	3.7 (3.35) [*]
	f_c^{ref}	MPa	73
	β_1	–	0.667
	α_{CT}	–	0.8 (0.6) [*]
	ρ_T	–	–
	ρ_φ	–	–
	k_φ	–	2 (4) [*]

[*] *Adjusted after comparison with results from field test. Original values are given within brackets.*

Table A.3 *Continuation.*

Inelastic strain	α_h	$10^{-6}/K$	9.3
	θ_T	K	5000
	ε_{s1}	–	–
	t_{s1}	d	0.167
	ε_{s2}	10^{-6}	–150
	t_{s2}	d	0.417
	t_{SH}	d	5
	κ_{SH}	–	0.3

Table A.4 *Relaxation values for the Maridal concrete adapted for the Maxwell-chain model used in ConTeSt Pro (2003). All parameters defined in description of the RELAX program, see Westman and Jonasson (1999).*

```
16   8   0.005   0.417

0.416   0.517   0.759   1.114   1.635   2.4   3.522   5.17   7.589   11.138   16.349
23.997   35.223   51.7   75.885   111.384

0.01   0.01   0.01   0.01   0.01   0.01   0.01   0.01
0.3932   0.1187   1.3153   1.5064   1.5295   1.0659   1.0584   –1.7825
1.787   0.9   3.384   2.8237   3.1092   2.0874   2.1143   –1.6421
3.4328   1.9287   5.1396   3.4756   4.0241   2.6328   2.7041   0.5983
3.4116   1.9024   5.4611   3.4564   3.92   2.5665   2.6351   3.6849
2.9417   1.692   5.4758   3.2672   3.6053   2.3648   2.4258   6.5906
2.5103   1.4581   5.5665   3.1456   3.3669   2.2121   2.2674   9.1608
2.1028   1.2017   5.8149   3.1145   3.2381   2.1269   2.1809   11.2309
1.7169   0.9279   6.2626   3.1772   3.2221   2.1095   2.1675   12.7484
1.3566   0.6475   6.892   3.3145   3.2934   2.1424   2.2097   13.7974
1.0289   0.3737   7.6459   3.4914   3.4085   2.2042   2.2816   14.5427
0.7406   0.1168   8.4661   3.6688   3.5357   2.2773   2.363   15.136
0.4759   –0.1172   8.9394   3.7346   3.6233   2.3152   2.4121   15.4471
0.2668   –0.3068   9.1224   3.7657   3.6566   2.3253   2.4281   15.5406
0.1178   –0.4457   9.2556   3.789   3.682   2.3322   2.4395   15.6056
0.015   –0.5434   9.3488   3.8055   3.7007   2.3367   2.4473   15.6496
```

Paper D

**Partial Coefficient for Thermal Cracking Problems
Determined by a Probabilistic Method**

By

Martin Nilsson

Lennart Elfgren

Paper D

Partial Coefficient for Thermal Cracking Problems Determined by a Probabilistic Method

Martin Nilsson
Doctoral Student, Tech. Lic.
Department of Civil and Mining Engineering
Division of Structural Engineering
Luleå University of Technology
SE-971 87 Luleå, Sweden
E-mail: Martin.Nilsson@ce.luth.se

Lennart Elfgren
Professor, Tech. Dr.
Department of Civil and Mining Engineering
Division of Structural Engineering
Luleå University of Technology
SE-971 87 Luleå, Sweden
E-mail: Lennart.Elfgren@ce.luth.se

ABSTRACT

The aim of this work is to calculate partial coefficients for thermal cracking problems of young concrete and to compare the results with the values stated in the Swedish building code for bridges, [1]. The code values are only based on experiences and logical reasoning, whereas the calculated values form a more theoretical base for their determination. The coefficients are calculated with a probabilistic method. Various possible variations of the used variables have been studied showing the wide range of possible results depending on the input. However, with use of material properties and reason-

able assumptions related to thermal cracking problems, fairly good agreement has been found between the stated values in the Swedish code [1] and the values obtained through the probabilistic method.

The calculated values are based on many assumptions and assumed values and should therefore not be seen as what is correct but rather more as an indication on the reasonableness of the values stated in the Swedish code. Further investigations, calculations and judgements must be performed before wider conclusions can be drawn.

Keywords: Partial coefficients, Safety factors, Young concrete, Probabilistic method, Cracking

1 INTRODUCTION

A structure or a structural member should be designed in such a way that safety and serviceability are always maintained. This means that no relevant limit state conditions should be exceeded with an in beforehand-determined probability. For young concrete structures it is important to prevent surface and through cracks due to e.g. temperature and/or temperature gradients during the hydration phase. Such cracks do not affect the total bearing capacity of a structure, the safety, but can influence the aesthetics and cause leakage and durability problems, the serviceability, that must be taken care of by e.g. injection.

The risk of thermal cracking in young concrete structures is commonly estimated as the ratio between the calculated maximum tensile stress and the actual tensile strength. Alternatively, the ratio between the calculated maximum tensile strain and the actual ultimate tensile strain is used, which will be the case here. If a determined ratio is smaller than a so-called crack safety value, a structure is assumed to fulfil the requirements for avoiding thermal cracking. Depending on the effects of cracking and the accuracy in determining material properties, the Swedish building codes for bridges, [1], states different crack safety values as measures of the risk of cracking.

The risk of cracking due to temperature and temperature gradients can be estimated, according to [1], by three different methods. In Method 1 certain demands are specified on i.e. the casting and the air temperatures, the maximum cement content and the minimum value of the water cement ratio. Demands are also stated on the thickness and height of the structural members, the casting length, and when form stripping is allowed. In Method 2 and Method 3, which are more elaborate, certain values of the crack safety are prescribed depending on the accuracy in the determination of material data. Method 2 implies that requirements in a certain handbook, [2], should be applied. The requirements have been established by numerous thermal stress analyses. Further, material data that should be used are given in the code. In Method 3, the risk of cracking is estimated very accurately with tried and documented computer software and material properties.

The risk of cracking should not be larger than the partial coefficients given in Table 1, the crack safety values according to [1]. The environmental classes in the legend of the first column are according to the Swedish building code for concrete, [3]. Environmental class A2 stands for "Moderately reinforcement aggressive", class A3 stands for "Very reinforcement aggressive" and class A4 stands for "Extremely reinforcement aggressive", further see Section 4.2.

Table 1 *Partial coefficients - or crack safety values - for Method 2 and Method 3 given in [1]. For Method 2 values from the two right columns are used where C is the cement content [kg/m³].*

Environm. class	Method 3 Complete material data	Method 2 Material data given in the code	
		$360 \leq C \leq 430 kg/m^3$	$430 \leq C \leq 460 kg/m^3$
A2	1.11	1.25	1.42
A3	1.18	1.33	1.54
A4	1.25	1.42	1.67

The crack safety values can be referred to what usually are called partial coefficients based on probabilistic methods, see e.g. [4], [5], [6], [7] and [8]. A method for determination of partial coefficients will be presented here. Further, a determination of partial coefficients for thermal cracking problems, that is the crack safety values in [1], will follow as an attempt to indicate the reasonableness in the stated values. The method and the results are more thoroughly presented and described in [8]. The determination is based on material properties, assumptions on load situations and other conditions typical for thermal cracking problems.

2 PARTIAL COEFFICIENTS

2.1 Limit state function and safety index

The safety against failure can be estimated by a limit state condition in terms of a resistance parameter *r* and a stress parameter *s*. The limit state condition, $\Theta(\cdot)$, can be expressed as the resistance parameter *r* reduced by the stress parameter *s* as

$$\Theta(\cdot) = r - s \geq 0 \tag{1}$$

Usually, the resistance parameter *r* is the material strength and the load parameter *s* is the stresses caused by acting loads. Depending on their relative size, the limit state condition is not exceeded if the resistance is larger than or equal to the stress, $r \geq s$, and it is

exceeded if the resistance is smaller than the stress, $r < s$.

The two parameters are regarded as two normally distributed stochastic variables with given probability density functions, $f_r(r)$ and $f_s(s)$, see Figure 1a). From the presumption that the resistance parameter r and the stress parameter s are stochastic variables, the limit state condition is also a stochastic variable. Assuming the resistance parameter r and the stress parameter s being normally distributed also the limit state condition Θ is normally distributed with the probability density function $f_\Theta(\Theta)$, Figure 1b).
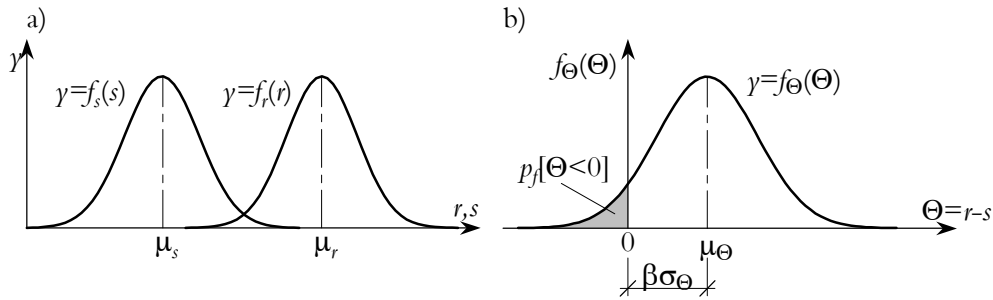

Figure 1 *a) Probability density functions for the stress parameter, $f_s(s)$, and the resistance parameter, $f_r(r)$, b) Probability density function for the limit state condition Θ, $f_\Theta(\Theta)$.*

The probability of exceeding a limit state condition, $p_f[\Theta = r\text{–}s < 0]$, is equal to the area of the shaded surface in Figure 1b). In the figure, the distance, with the standard deviation σ_Θ as unit, from the mean value μ_Θ to the failure limit, $\Theta = 0$, is written as $\beta\sigma_\Theta$. The coefficient β is the so-called safety index, introduced by Cornell in [9], and is, according to the figure, determined as

$$\beta = \frac{\mu_\Theta}{\sigma_\Theta} \qquad (2)$$

How much larger the resistance r should be than the stress s is often specified in building codes in different safety classes and through specified values of the safety index β. The safety index β is defined by a formal probability of failure, that is, of exceeding the limit sate condition. The safety index β is often coupled to safety classes in building codes, see e.g. [6], [7], [10]. If the risk of human injuries is low, often referred to safety class 1, the probability of failure is $p_f = 10^{-4}$ and the safety index $\beta = 3.72$. The same principle applies to safety classes 2 and 3, see Table 2.

Paper D

Table 2 *Correspondence between safety class, safety index and probability of failure, [1], [10].*

Safety class	1	2	3
Safety index β	3.72	4.26	4.75
Probability of failure, p_f	10^{-4}	10^{-5}	10^{-6}

2.2 Partial coefficients

The partial coefficient method is based on characteristic values and partial coefficients for verification that prescribed safety requirements are fulfilled. Generally, for the limit state condition in Eq. (1), partial coefficients are used as follows

$$\Theta = r_d - s_d = \frac{r_c}{\gamma_r} - \gamma_s s_c \geq 0 \qquad (3)$$

where d indicates design values, c indicates characteristic values and γ_r and γ_s are the partial coefficients for the resistance parameter r and the stress parameter s, respectively.

For the risk of thermal cracking of young concrete, the partial coefficients in Table 1 are the product of the partial coefficients for the resistance parameter r and the stress parameter s, $\gamma_r\gamma_s$, compare with Eq. (3),

$$\frac{r_c}{s_c} \geq \gamma_r\gamma_s \qquad (4)$$

In this case, all partial coefficients have been collected in one coefficient limiting the ratio between the resistance parameter and the load parameter.

3 THE PROBABILISTIC METHOD

3.1 Equations for determination of partial coefficients

A method, further referred to as the probabilistic method, will be used to determine alternative values of the partial coefficients, safety values, for thermal cracking problems, given in Table 1. The method has the advantage of being consequent but it also includes many approximations. The results can therefore not be used directly without additional judgements. The following determination of the partial coefficients will be formulated in terms of strains. The procedure in general is based on a method presented by Lars Östlund in [11], reprinted in [12], and adopted on thermal cracking problems in [8]. As design condition with partial coefficients for thermal cracking problems, Eq. (4) will be used as the limit state condition.

The resistance parameter r is defined as the product of a factor C_r describing uncertainties in the calculation method, of a factor a for the geometric quantity, a factor ρ transferring concrete strain in a test specimen at failure to concrete strain in real structures, and a factor ε that is the ultimate strain, see APPENDIX A.

$$r = C_r a \rho \varepsilon \tag{5}$$

The load parameter is defined as the product of a factor C_s describing uncertainties in the calculation method, a factor γ_R describing the restraint, see [8], and the sum of the thermal strain and the shrinkage induced strain, see APPENDIX A.

$$s = C_s \gamma_R (b \varepsilon_T + c \varepsilon_{sh}) \tag{6}$$

where b and c are deterministic coefficients that are used when either the temperature induced strain is of greater importance than the shrinkage strain, or the opposite.

By introducing

$$\frac{C_r}{C_s} = C \quad \text{with coefficient of variation } V_C = \sqrt{V_{Cr}^2 + V_{Cs}^2} \tag{7}$$

Eq. (5) and (6) in Eq. (1) give the limit state equation

$$\Theta(\cdot) = C a \rho \varepsilon - \gamma_R (b \varepsilon_T + c \varepsilon_{sh}) \tag{8}$$

When calculating partial coefficients by the probabilistic method, the following design values are used for the stochastic variables r, ε_T and ε_{sh}.

$$r_d = \mu_r \exp(-\alpha_r \beta V_r) \tag{9}$$

$$\varepsilon_{T,d} = \mu_T \left(1 - \alpha_T \beta V_T\right) \tag{10}$$

$$\varepsilon_{sh,d} = \mu_{sh} \left(1 - \alpha_{sh} \beta V_{sh}\right) \tag{11}$$

where α_r, α_T and α_{sh} are so-called sensitivity coefficients determined as

$$\alpha_i = \frac{\kappa_i}{\sqrt{\Sigma \kappa_i^2}} = \frac{\kappa_i}{\sqrt{\kappa_r^2 + \kappa_T^2 + \kappa_{sh}^2}}; \quad \text{with } i = r, \ T \text{ and } sh \tag{12}$$

which must fulfil the condition

Paper D

$$\alpha_r^2 + \alpha_T^2 + \alpha_{sh}^2 = 1 \tag{13}$$

The sensitivity coefficients take values between -1 and 1 and are positive for favourable factors, the resistance parameters, and negative for unfavourable, the load/stress parameters. The larger the coefficient is, the larger the importance of the uncertainty is in the corresponding variable.

In the calculation of the partial coefficients for thermal cracking problems of concrete, it is very difficult to give any absolute values of the mean values of the strains of shrinkage and temperature changes. However, the relation between them is simpler to estimate. Therefore, a coefficient ν_{sh} is introduced stating the ratio between the mean values of the strains of shrinkage and of the temperature change

$$\nu_{sh} = \frac{c\mu_{sh}}{b\mu_T} \tag{14}$$

Eqs. (9) to (11) and Eq. (14) in Eq. (8) give the design condition with design values of the variables

$$\frac{\mu_r}{b\gamma_R\mu_T}\exp(-\alpha_r\beta V_r) - \left(1 - \alpha_T\beta V_T\right) - \nu_{sh}\left(1 - \alpha_{sh}\beta V_{sh}\right) = 0 \tag{15}$$

By introducing the help variables

$$Z = \frac{\mu_r}{b\gamma_R\mu_T}$$

and

$$\psi_1 = \left(1 - \alpha_T\beta V_T\right) + \nu_{sh}\left(1 - \alpha_{sh}\beta V_{sh}\right)$$

Eq. (15) can be re-written as

$$Z = \psi_1\exp(\alpha_r\beta V_r) \tag{16}$$

By introducing partial coefficients for the design values in Eqs. (9) through (11) one obtain

$$r_d = \frac{r_c}{\gamma_r} = \frac{\mu_r}{\gamma_r}\exp(-k_r V_r) \tag{17}$$

155

$$s_d = \gamma_s \gamma_R \left(b\varepsilon_{T,c} + c\varepsilon_{sh,c} \right) = \gamma_s \gamma_R \left(b\mu_T (1 + k_T V_T) + c\mu_{sh}(1 + k_{sh}V_{sh}) \right) \qquad (18)$$

where r_c, $\varepsilon_{T,c}$ and $\varepsilon_{sh,c}$ are the characteristic values of the resistance parameter, the temperature and the shrinkage induced strains, respectively. The limit state condition is then written as

$$\frac{\mu_r}{\gamma_r} \exp(-k_r V_r) - \gamma_s \gamma_R \left(b\mu_T (1 + k_T V_T) + c\mu_{sh}(1 + k_{sh}V_{sh}) \right) \geq 0 \qquad (19)$$

The coefficient k depends of actual fractile value for normal distribution variables, see Table 10 in APPENDIX A. In the same way as above, with $Z = \mu_r / b\gamma_R\mu_T$, $\nu_{sh} = c\mu_{sh}/b\mu_T$ and $\psi_2 = (1 + k_T V_T) + \nu_{sh}(1 + k_{sh}V_{sh})$, Eq. (19) can be re-written as

$$\gamma_s \gamma_r \leq \frac{Z}{\psi_2} \exp(-k_r V_r) = \frac{Z}{\psi_2} \frac{r_c}{\mu_r} \qquad (20)$$

By calculating Z, see APPENDIX A, and r_c/μ_r by Eq. (A.4) with $x_{i,c}/\mu_i = \exp(-\alpha_i \beta V_i) = \exp(-k_i V_i)$, the partial coefficient $\gamma_r \gamma_s$ can be determined.

More thorough descriptions of the determination of the partial coefficients can be seen in APPENDIX A and references [8], [11] and [12].

3.2 Numerical values

Varying the variables shown in Table 3 and keeping all others constant in the equations above, calculations of partial coefficients for thermal cracking problems of young concrete have been performed.

ν_{sh} is defined in Eq. (14) and states the ratio between the mean values of the strains of shrinkage and of the strains of temperature change. b and c are varied to simulate situations where one of the two strain components has smaller or larger influence. Especially in high strength concrete the shrinkage is considerable implying larger values of c. V_ε is the coefficient of variation of the actual concrete (actual ultimate strain ε_{cu}). V_C is the coefficient of variation of the methods used for estimating the risk of thermal cracking. Compare V_C with Methods 1 to 3 in Section 1 where e.g. $V_C = 0.15$ for Method 1, $V_C = 0.10$ for Method 2 and $V_C = 0.05$ for Method 3. These values are just an attempt to estimate the accuracy in the methods and should not be seen as what is correct. The safety index β is varied to coincide with safety classes 1 and 3 with probabilities of failure of 10^{-4} and 10^{-6} respectively, see Table 2.

Table 3 *Variables varied in the determination of partial coefficients for thermal cracking problems.*

Variable	Values
ν_{sh}	$0.01\dfrac{c}{b}$, $0.20\dfrac{c}{b}$, $0.50\dfrac{c}{b}$, $1.00\dfrac{c}{b}$, $2.00\dfrac{c}{b}$
b	1/3, 1, 3
c	1/3, 1, 3
V_ε	0.05, 0.10, 0.15, 0.20, 0.25
V_C	0.05, 0.10, 0.15, 0.20, 0.25
β	3.72, 4.75

The coefficient of variation of the temperature induced strains is given the value V_T = 0.08 according to [16]. The coefficient of variation of the shrinkage is given the value V_{sh} = 0.20. This value is a bit smaller than what can be determined from [17]. The values of k_T and k_{sh} are both 1.65 coinciding with 95 % fractile values of the temperature and shrinkage induced strains, respectively, see Table 4.

The coefficients of variations of the geometry parameter V_a and of the factor transferring strength in test specimens to real structures V_ρ are both given the value 0, that is $V_a = 0$ and $V_\rho = 0$. The coefficient of variation of the geometry is assumed to be very low since in civil engineering structures, any divergences from the right measures do not significantly affect the risk of thermal cracking. For the concrete ultimate strain, 45% fractile value is assumed giving $k_\varepsilon = 0.13$. The coefficient k is for normal distribution variables and can be found in general statistic textbooks, see Table 10 in APPENDIX A. The value of the ultimate strain for the concrete is chosen slightly below the mean value bearing in mind that thermal cracking only causes flaws and costs for repair and reduction of the life of the structure but not total failure. For the accuracy in the design method C, for the geometry parameter a and for the factor transferring the ultimate strain in test specimens to real structures ρ, the coefficient k is chosen $k_C = k_a = k_\rho = 1.65$ assuming 5% fractile values, see Table 4 below and Table 10 in APPENDIX A.

Table 4 *Constant values for the resistance parameters C, a, ρ and ε and the load parameters ε_T and ε_{sh} used in the determination of the partial coefficients.*

k_C	V_a	k_a	V_ρ	k_ρ	k_ε	V_T	k_T	V_{sh}	k_{sh}
1.65	0	1.65	0	1.65	0.13	0.08	1.65	0.20	1.65

3.3 Calculation of partial coefficients

3.3.1 Example of calculation of partial coefficients

The following presumptions and values are used to illustrate the calculation of partial coefficients. Let the influence of the imposed volume changes be equal, $b = c = 1$. The mean value of the volume change due to shrinkage is one hundredth of the mean value of the imposed volume change due to the temperature change, $\nu_{sh} = 0.01 \cdot 1/1 = 0.01$. Further, the variation coefficients of the strength of the concrete and the calculation method are assumed to be five percent, $V_\varepsilon = V_C = 0.05$. The safety index $\beta = 3.72$ refers to safety class 1. The following values for the resistance parameter, the sensitivity values α and the help values ψ, N and Z are obtained, Table 5 and Table 6.

Table 5 *Calculated values for the resistance parameter.*

V_r	C_c/μ_C	a_c/μ_a	ρ_c/μ_ρ	$\varepsilon_c/\mu_\varepsilon$	r_c/μ_r
0.071	0.921	1.000	1.000	0.994	0.915

Table 6 *Calculated sensitivity values α and help-values ψ_1, N and Z.*

α'_{sh}	α_T	ψ_1	N	α_φ	α_T	α_r	Z
–0.017	–0.682	1.213	0.117	–0.017	–0.682	0.731	1.470

The partial coefficient for this case is then calculated as, Eq. (20)

$$\gamma_r\gamma_s = \frac{Z}{\psi_2}\frac{r_c}{\mu_r} = \frac{1.470}{(1+1.65\cdot0.08)+0.01(1+1.65\cdot0.20)}0.915 = 1.174$$

implying that the resistance parameter must be about 1.17 times larger than the load parameter for not exceeding the limit state condition.

3.3.2 Final calculation of partial coefficients

All the partial coefficients calculated with values according to the description and Table 3 above are presented in Figure 2 to Figure 6 below. In all the diagrams, the curves from the lowest to the upper most one represent V_C = 0.05, 0.10, 0.15, 0.20 and 0.25, respectively. See [8] for more descriptions of the calculations and the results.

In Figure 2 to Figure 6 it can be seen that with increased safety index β, the partial coefficient $γ_r γ_s$ increases and is varying over a larger range depending on the values of V_C. When the coefficient b increases also the partial coefficient increases, and when b decreases the partial coefficient decreases, compare Figure 3 and Figure 4 with Figure 2. For the coefficient c, the opposite is valid. When c increases, the partial coefficient decreases and when c decreases, the partial coefficient increases, compare Figure 5 and Figure 6 with Figure 2.
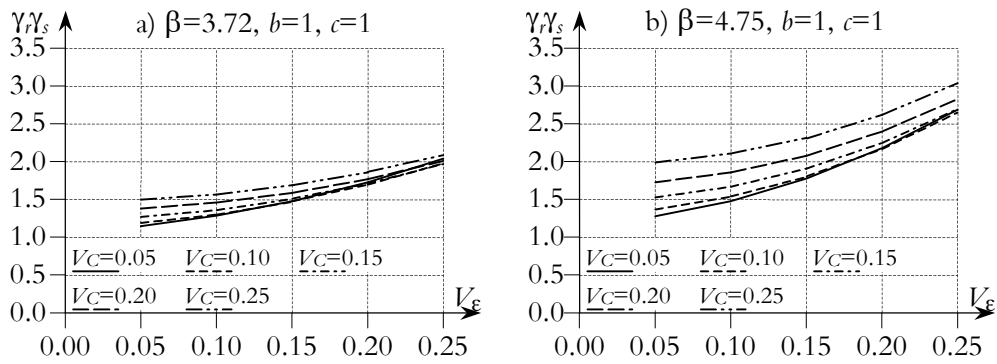

Figure 2 Partial coefficient $γ_r γ_s$ for a) β=3.72, b=1 and c=1, b) β=4.75, b=1 and c=1.

Figure 3 Partial coefficient $γ_r γ_s$ for a) β=3.72, b=1/3 and c=1, b) β=4.75, b=1/3 and c=1.
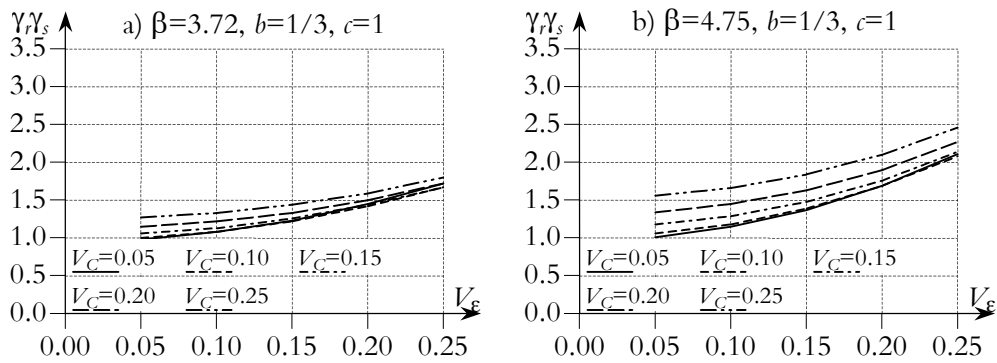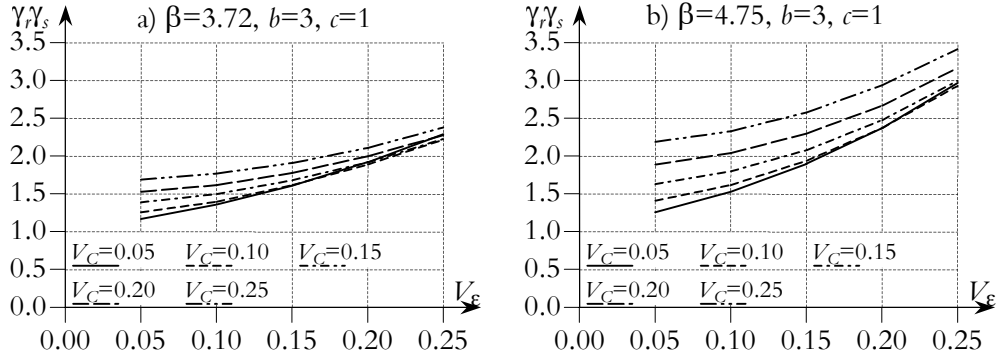
Figure 4 *Partial coefficient* $\gamma_r\gamma_s$ *for a)* β=3.72, b=3 and c=1, b) β=4.75, b=3 and c=1.
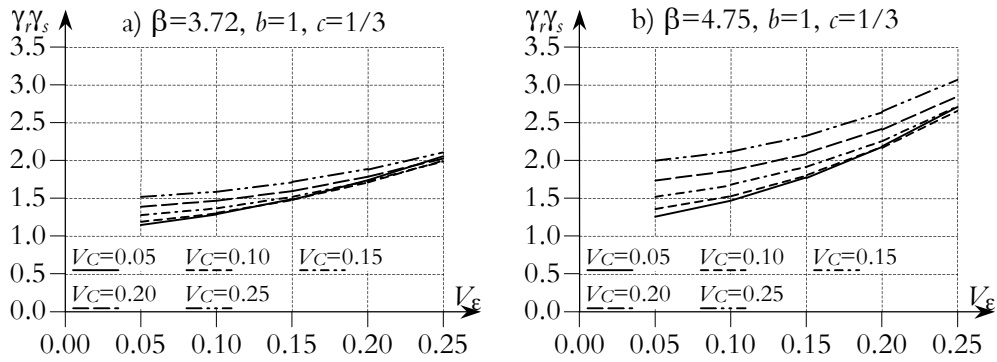

Figure 5 *Partial coefficient* $\gamma_r\gamma_s$ *for a)* β=3.72, b=1 and c=1/3, b) β=4.75, b=1 and c=1/3.
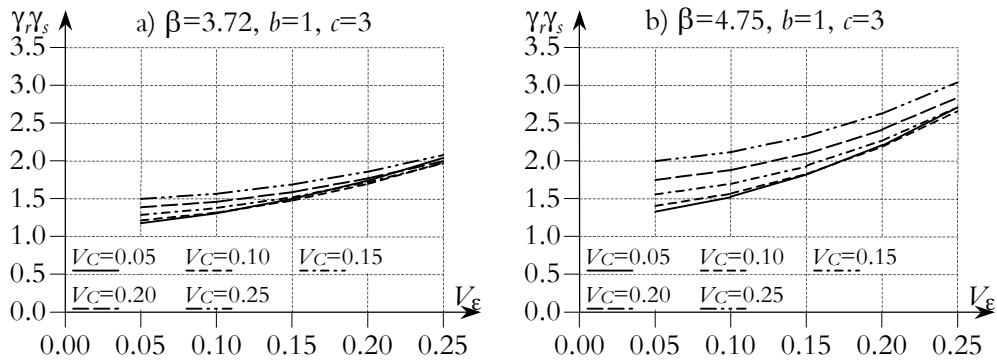

Figure 6 *Partial coefficient* $\gamma_r\gamma_s$ *for a)* β=3.72, b=1 and c=3, b) β=4.75, b=1 and c=3.

160

Paper D

4 RESULTS

4.1   Final values of partial coefficients

Final values of the partial coefficient $\gamma_r\gamma_s$ are determined from the previous calculations with $b = c = 1$, $\beta = 3.72$ and with coefficients of variation, $V_C = 0.05$ and $V_\varepsilon = 0.05$, 0.10 and 0.15. The values are chosen to coincide with the first row in Table 1. For Method 3 (the column of complete material data) the models of analysis (computer software) are very well documented and tried and should give results not varying much from reality. Therefore, the coefficient of variation for the method of calculation is chosen to be small, $V_C = 0.05$. For Method 2, (columns for material data given in [1]) lots of calculations and judgements are behind, [2], implying good accuracy of the analyses, again $V_C = 0.05$. The differences in accuracy of material data are taken into account by varying the coefficient of variation of the material V_ε as stated, $V_\varepsilon = 0.05$, 0.10 and 0.15. Again, $k_T = k_{sh} = 1.65$ for 95 % fractile values. Further, as an extension of the final determination of the partial coefficients, 55 % fractile values are assumed for the temperature and the shrinkage induced strains to coincide with the assumed fractile value of the ultimate strain (45 % fractile), see Section 3.2. For environmental class A2 and $V_\varepsilon = 0.05$, 0.10 and 0.15, the partial coefficient $\gamma_r\gamma_s$ is taken as the values of the lowest curve in Figure 2a) presented in Table 7.

Table 7 *Partial coefficient $\gamma_r\gamma_s$ from calculation with the probabilistic method for environmental class A2 and V_ε = 0.05, 0.10 and 0.15.*

Environm. class	k_T, k_{sh}	Complete material data V_ε=0.05	Material data given in the code	
			$360{\leq}C{\leq}430$kg/m^3 V_ε=0.10	$430{\leq}C{\leq}460$kg/m^3 V_ε=0.15
A2	0.13 (55% fractile)	1.36	1.52	1.75
	1.65 (95% fractile)	1.15	1.29	1.48

4.2   Effects of exceeding the limit state condition

The calculation of partial coefficients above is chosen to be valid for environmental class A2. The effects of exceeding the limit state condition (cracking) in a structural member are smaller in environmental class A2 than in classes A3 and A4. Therefore an extra partial coefficient γ_n is introduced. The values of the extra partial coefficient γ_n are chosen as the mean ratio between the values in the rows in Table 1, see Table 8.

Table 8 *Partial coefficient γ$_n$ depending on environmental classes.*

	Environmental class		
	A2	A3	A4
γ$_n$	1.00	1.07	1.14

Final values of the partial coefficient γ$_r$γ$_s$ are obtained from Table 7 with partial coefficient γ$_n$ in Table 8, see Table 9.

Table 9 *Final values of partial coefficient γ$_r$γ$_s$ as determined by probabilistic method.*

Environm. class	k$_T$, k$_{sh}$	Complete material data	Material data given in the code	
			360≤C≤430kg/m^3	430≤C≤460kg/m^3
A2	0.13 (55% fractile)	1.36	1.52	1.75
	1.65 (95% fractile)	1.15	1.29	1.48
A3	0.13 (55% fractile)	1.45	1.62	1.87
	1.65 (95% fractile)	1.23	1.38	1.58
A4	0.13 (55% fractile)	1.56	1.74	2.00
	1.65 (95% fractile)	1.32	1.48	1.70

A comparison with the values that are stated in [1] and the values of the partial coefficients obtained by the probabilistic method are depicted in Figure 7. As can be seen, the values for $k_T = k_{sh} = 1.65$ (95 % fractile values) are little higher than the values given in [1]. The values show good agreement even though the uncertainties in the chosen values of the variables used in the probabilistic method are large and that the partial coefficients stated in [1] only are based on experiences. For $k_T = k_{sh} = 0.13$ (55 % fractile values), the partial coefficients are much higher than the values in [1]. The reason for this is that with only 55 % fractile values of the temperature and the shrinkage induced strains, the risk of exceeding these values is increased. This implies an increased risk of exceeding the limit state condition, whereupon higher partial coefficients are needed.
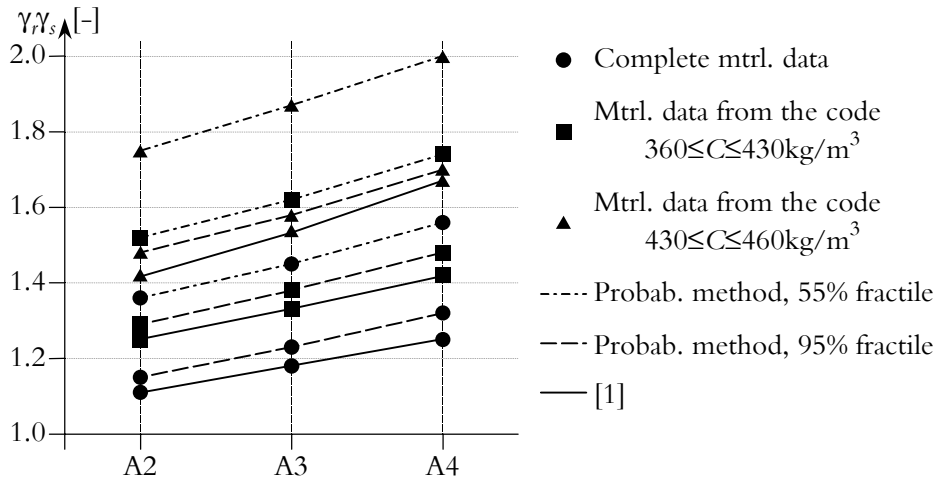
Paper D

Figure 7 *Comparison between partial coefficients stated in [1] and partial coefficients obtained by the probabilistic method.*

5 DISCUSSION

It is possible to calculate partial coefficients for thermal cracking problems of young concrete. The values presented above coincide well with the crack safety values stated in the Swedish building code for bridges, [1]. However, the calculated values of the partial coefficient are based on many assumptions and simplifications and they shall not be seen as what is absolutely true right, further judgements are always necessary.

The used coefficients of variation of the thermal changes and of the shrinkage need further investigation. The values are roughly taken from [16] and are only assumed values that have not been well verified.

The crack safety values in [1] are all based on experience, so also these values are a bit vague. The calculated partial coefficients presented here can be seen as an attempt to verify the values in [1]. However, all estimations of the risks of thermal cracking of young concrete have to be based on more judgements and analyses of the problems as a whole rather than on the crack safety values given in [1].

The differences in the partial coefficient between the environmental classes need further investigations. The values that are stated in [1] are only based on logical argu- ments by the persons who have written the code, meaning that higher environmental class needs higher partial coefficients.

163

ACKNOWLEDGEMENT

REFERENCES

[1]   BRO 94 (1999). *BRO94 Allmän teknisk beskrivning för broar, 9. Förteckning.* (General Technical Description for Bridges, 9. Catalogue). Borlänge, Sweden: Swedish National Road Administration. Publ 1999:20. pp. 139. ISSN 1401-9612. (In Swedish).
      Bro 2002 (2002). *Bro 2002. Allmän teknisk beskrivning för broar, 4 Betongkonstruktioner.* (General Technical Description for Bridges, 4. Concrete structures). Borlänge, Sweden: Swedish National Road Administration. (In Swedish).

[2]   Emborg, M, Bernander, S, Ekefors, K, Groth, P & Hedlund, H (1997). *Temperatursprickor i betongkonstruktioner - Beräkningsmetoder för hydratationsspänningar och diagram för några vanliga typfall* (Temperature Cracks in Concrete Structures – Calculation Methods for Hydration Stresses and Diagrams for some Common Typical Examples). Luleå, Sweden: Luleå University of Technology. Technical Report 1997:02. 100 pp. ISSN 1402-1536. (In Swedish).

[3]   BBK94 (1994). *Boverkets handbok om betongkonstruktioner.* (The Swedish Building Administrations Handbook on Concrete Structures). Part 2 – Material, Performance and Control. Stockholm, Sweden: The Swedish Building Administration, Division of Buildings. pp. 116. ISBN 91-7332-687-9. (In Swedish).

[4]   Schneider, J (1997). Introduction to Safety and Reliability of Structures. In: *Structural Engineering Documents, 5.* Zürich: IABSE, International Association for Bridges and Structural Engineering. 138 pp.

[5]   AK79/81 (1982). *Allmänna regler för bärande konstruktioner. Principer, rekommendationer och kommentarer samt exempel på tillämpning.* (General Regulations for Structures. Principles, Recomendations, Comments and Examples of Application). Stockholm, Sweden: Statens Planverk, Rapport nr 50, Liber 1982, pp. 159. ISBN 91-38-07090-1. (In Swedish).

[6]   NKB78 (1978). *Retningslinier for last- og sikkerhetsbestemmelser for baerende konstruktioner* (Guiding Rules for Loads and Safety Regulations for Structures). NKB-rapport nr. 35. 146 pp. ISBN 87-503-2951-0. (In Swedish).

[7]   NKB87 (1987). *Retningslinier for last- og sikkerhetsbestemmelser for baerende konstruktioner* (Guiding Rules for Loads and Safety Regulations for Structures). NKB-rapport nr. 55. 107+55 pp. ISBN 87-503-6991-1, ISSN 0359-9981. (In Swedish).

[8]   Nilsson, M (2001). *Thermal Cracking of Young Concrete - Partial Coefficients, Restraint Effects and Influence of Casting Joints.* Luleå, Sweden: Division of Structural

Engineering, Luleå University of Technology. Licentiate Thesis 2000:27. pp. 267.

[9] Cornell, C A (1969). A probability-based structural code. In: *ACI Journal, Vol. 66*, pp. 974-985.

[10] BBK94 (1995). *Boverkets handbok om betongkonstruktioner.* (The Swedish Building Administrations Handbook on Concrete Structures). Part 1 - Design. Stockholm, Sweden: The Swedish Building Administration, Division of Buildings. pp. 185. ISBN 91-7147-235-5. (In Swedish).

[11] Östlund, L (1997). *Studium av erforderligt värde på partialkoefficienten för tåglast vid dimensionering av järnvägsbroar* (Study of Necessary Value of the Partial Coefficient for Load of Trains at Design of Railway Bridges). Borlänge, Sweden: Swedish Railroad Administration. Investigation on behalf of the Swedish Railroad Administration. pp. 19. (In Swedish).

[12] Nilsson, M, Ohlsson, U & Elfgren, L (2000). *Partialkoefficienter för betongbroar längs Malmbanan* (Partial Coefficients for Concrete Bridges along Malmbanan). Luleå, Sweden: Luleå University of Technology. Technical report 1999:03. 66 pp. ISSN 1402-1536. (In Swedish).

[13] Larson, M (2000). *Estimation of Crack Risk in Early Age Concrete.* Luleå, Sweden: Division of Structural Engineering, Luleå University of Technology. Licentiate Thesis 2000:10. pp. 170.

[14] Jonasson, J-E, Wallin, K, Emborg, M, Gram, A, Saleh, I, Nilsson, M, Larson, M and Hedlund, H (2001). *Tempertursprickor i betongkonstruktioner − Handbok med diagram för sprickriskbedömning inklusive åtgärder för några typfall; Del D och E* (Temperature cracks in concrete structures - Handbook with diagrams for crack risk estimation including measures for some typical cases). Luleå, Sweden: Division of Structural Engineering, Luleå University of Technology. Technical Report 2001:14. (In Swedish, in progress).

[15] ConTeSt Pro (1999). *Användarhandbok - ConTeSt Pro* (Users manual – Program for Temperature and Stress Calculations in Concrete). Developed by JEJMS Concrete AB in co-operation with Luleå University of Technology, Cementa AB and Peab Öst AB. Danderyd, Sweden: Cementa AB. pp. 207. (In Swedish).

[16] Jonasson, J-E, Emborg, M & Bernander, S (1994). Temperatur, mognadsutveckling och egenspänningar i ung betong (Temperature, Maturity Growth and Eigenstresses in Young Concrete). In: *Betonghandbok - Material.* (Concrete Handbook – Material). Edition 2. Stockholm, Sweden: AB Svensk Byggtjänst and Cementa AB. pp. 547-607. ISBN 91-7332-709-3. (In Swedish).

[17] Jonasson, J-E (1994). Krympning hos hårdnad betong (Shrinkage in Hardened Concrete). In: *Betonghandbok - Material.* (Concrete Handbook - Material). Edition 2. Stockholm, Sweden: AB Svensk Byggtjänst and Cementa AB. pp. 524-545. ISBN 91-7332-709-3. (In Swedish).

APPENDIX A

Below a derivation follows of equations used in the determination of partial coefficients for thermal cracking problems.

A.1 Resistance parameter

The resistance parameter r is expressed as, [11]

$$r = C_r a \rho \varepsilon \qquad (A.1)$$

where C_r is a factor describing uncertainties in the calculation method on the resistance parameter such as determination of material properties. C_r is a stochastic variable with mean μ_{Cr} and coefficient of variation V_{Cr}. a is a geometric quantity (e.g. cross-section area). a is a stochastic variable with mean μ_a and coefficient of variation V_a. ρ is a factor transferring concrete strain from test specimen at failure to concrete strain in real structures. ρ is a stochastic variable with mean μ_ρ and coefficient of variation V_ρ. ε is the actual concrete ultimate strain. ε is a stochastic variable with mean μ_ε and coefficient of variation V_ε. The stochastic variables r, C_r, a, ρ and ε are assumed to be logarithmic normally distributed.

The mean value of the resistance parameter is

$$\mu_r = \mu_{Cr} \mu_a \mu_\rho \mu_\varepsilon \qquad (A.2)$$

and the coefficient of variation, if terms of higher order are neglected,

$$V_r \approx \sqrt{V_{Cr}^2 + V_a^2 + V_\rho^2 + V_\varepsilon^2} \qquad (A.3)$$

Eq. (A.1) divided by Eq. (A.2) gives, if using characteristic values,

$$\frac{r_c}{\mu_r} = \frac{C_{rc}}{\mu_{Cr}} \frac{a_c}{\mu_a} \frac{\rho_c}{\mu_\rho} \frac{\varepsilon_c}{\mu_\varepsilon} \qquad (A.4)$$

which will be used further on in the final calculation of the partial coefficients, see Eq. (A.21) below.

A.2 Load parameter

The load parameter s for thermal cracking problems can be formulated, in terms of strains, as

$$s = C_s \gamma_R (b(\varepsilon_{T1} + \varepsilon_{T2}) + c\varepsilon_{sh})$$

166

where C_s is uncertainties in the calculation method on the load parameter and is assumed to have the same value for all the loads. C_s describes uncertainties in the determination of the strains by e.g. manual methods, see [13] and [14], or by finite element calculations, see [15]. C_s is a stochastic variable with mean μ_{Cs} and coefficient of variation V_{Cs}. γ_R is the coefficient of restraint and is a deterministic coefficient, $0 \leq \gamma_R \leq 1$. For further explanations and the determination of the coefficient of restraint, see [8]. ε_{T1} is the non-elastic strain of volume changes from differences between the casting temperature and the adjacent temperature. ε_{T2} is the non-elastic strain of volume changes from differences between the maximum temperature and the casting temperature. Below, the temperature-induced strains are combined into one parameter, ε_T, which is a stochastic variable with mean μ_T and coefficient of variation V_T. ε_{sh} is the strain of volume changes from shrinkage and is a stochastic variable with mean μ_{sh} and coefficient of variation V_{sh}. b and c are both deterministic coefficients, $0 \leq b$ and $0 \leq c$. The stochastic variables ε_T and ε_{sh} are assumed to be normally distributed. The deterministic coefficients b and c are used when either the temperature-induced strain is of greater importance than the shrinkage strain, or the opposite. Now, the load parameter is

$$s = C_s \gamma_R (b\varepsilon_T + c\varepsilon_{sh}) \tag{A.5}$$

The variables are put together so that the mean value of the stress parameter is

$$\mu_s = \gamma_R \left(b\mu_T + c\mu_{sh} \right) \tag{A.6}$$

By introducing the following relation

$$\frac{C_r}{C_s} = C; \quad V_C = \sqrt{V_{Cr}^2 + V_{Cs}^2} \tag{A.7}$$

the limit state condition, Eq. (1), is simplified to

$$\Theta(\cdot) = Ca\rho\varepsilon - \gamma_R (b\varepsilon_T + c\varepsilon_{sh}) \tag{A.8}$$

A coefficient ν_{sh} is introduced stating the ratio between the mean values of the strains of shrinkage and of the temperature change

$$\nu_{sh} = \frac{c\mu_{sh}}{b\mu_T} \tag{A.9}$$

A.3   Design condition

When calculating partial coefficients by the probabilistic method, the following design

values and help values κ are used for the stochastic variables r, ε_T and ε_{sh}.

$$r_d = \mu_r \exp(-\alpha_r \beta V_r) \quad \kappa_r = r_d V_r \tag{A.10}$$

$$\varepsilon_{T,d} = \mu_T \left(1 - \alpha_T \beta V_T\right) \quad \kappa_T = -b\gamma_R \mu_T V_T \tag{A.11}$$

$$\varepsilon_{sh,d} = \mu_{sh} \left(1 - \alpha_{sh} \beta V_{sh}\right) \quad \kappa_{sh} = -c\gamma_R \mu_{sh} V_{sh} \tag{A.12}$$

When using design values in Eq. (3), the equal sign is valid, which together with Eq. (A.5) gives

$$r_d - b\gamma_R \varepsilon_{T,d} - c\gamma_R \varepsilon_{sh,d} = 0 \tag{A.13}$$

In the expressions above, α are so-called sensitivity coefficients determined as

$$\alpha_i = \frac{\kappa_i}{\sqrt{\Sigma \kappa_i^2}} = \frac{\kappa_i}{\sqrt{\kappa_r^2 + \kappa_T^2 + \kappa_{sh}^2}}; \quad \text{with } i = r, \ T \text{ and } sh \tag{A.14}$$

which must fulfil the condition

$$\alpha_r^2 + \alpha_T^2 + \alpha_{sh}^2 = 1 \tag{A.15}$$

$c\mu_{sh} = \nu_{sh} b \mu_T$ according to Eq. (A.9) and design values according to Eqs. (A.10) to (A.12) inserted in Eq. (A.13) give

$$\frac{\mu_r}{b\gamma_R \mu_T} \exp(-\alpha_r \beta V_r) - \left(1 - \alpha_T \beta V_T\right) - \nu_{sh} \left(1 - \alpha_{sh} \beta V_{sh}\right) = 0 \tag{A.16}$$

By introducing the help variables

$$Z = \frac{\mu_r}{b\gamma_R \mu_T}$$

and

$$\psi_1 = \left(1 - \alpha_T \beta V_T\right) + \nu_{sh} \left(1 - \alpha_{sh} \beta V_{sh}\right) \tag{A.17}$$

Eq. (A.16) is simplified to

$$Z \exp(-\alpha_r \beta V_r) - \psi_1 = 0$$

Paper D

where from

$$Z = \psi_1 \exp(\alpha_r \beta V_r) \tag{A.18}$$

Z can be determined if the values of α_i (with $i = r$, T and sh), β, ν_{sh}, b, c and V_i are known. The steps for calculating Z can be as follows:

(1) A value of α'_{sh} is assumed

(2) $\alpha'_T = \dfrac{\kappa_T}{\sqrt{\Sigma\kappa_i^2}} = \dfrac{-b\gamma_R\mu_T V_T}{-c\gamma_R\mu_{sh}V_{sh}}\alpha'_{sh} = \dfrac{V_T\alpha'_{sh}}{\nu_{sh}V_{sh}}$ is calculated

(3) ψ is calculated with Eq. (A.17), α'_{sh} and α'_T

(4) $r_d = \mu_r \exp(-\alpha_r\beta V_r) = \mu_r\dfrac{\psi_1}{Z} = b\gamma_R\mu_T\psi_1$ and $\kappa_r = r_d V_r$ are calculated

(5) $N = \dfrac{\sqrt{\Sigma\kappa_i^2}}{b\gamma_R\mu_T} = \sqrt{(V_T)^2 + (\nu_{sh}V_{sh})^2 + (\psi_1 V_r)^2}$

(6) $\alpha_{sh} = \dfrac{\kappa_{sh}}{\sqrt{\Sigma\kappa_i^2}} = \dfrac{-\gamma_R b\mu_T\nu_{sh}V_{sh}}{\sqrt{\Sigma\kappa_i^2}} = \dfrac{-\nu_{sh}V_{sh}}{N}$ is calculated and compared to α'_{sh}

(7) When $\alpha'_{sh} \approx \alpha_{sh}$, $\alpha_T = \dfrac{-V_T}{N}$ and $\alpha_r = \dfrac{\psi_1 V_r}{N}$ are calculated

(8) Check of $\Sigma\alpha_i^2 = 1$

(9) Z is calculated by Eq. (A.18).

The value of Z is used below in the calculation of the partial coefficients.

A.4   Partial coefficients

The design values in Eqs. (A.10) through (A.12) can alternatively be expressed with partial coefficients as

$$r_d = \frac{r_c}{\gamma_r} = \frac{\mu_r}{\gamma_r}\exp(-k_r V_r) \tag{A.19}$$

$$s_d = \gamma_s\gamma_R\left(b\varepsilon_{T,c} + c\varepsilon_{sh,c}\right) = \gamma_s\gamma_R\left(b\mu_T(1 + k_T V_T) + c\mu_{sh}(1 + k_{sh}V_{sh})\right) \tag{A.20}$$

which in the limit state condition, Eq. (3), give

$$\frac{\mu_r}{\gamma_r}\exp(-k_r V_r) - \gamma_s\gamma_R\left(b\mu_T(1 + k_T V_T) + c\mu_{sh}(1 + k_{sh}V_{sh})\right) \geq 0$$

With $Z = \mu_r/b\gamma_R\mu_T$, $\nu_{sh} = c\mu_{sh}/b\mu_T$ and $\psi_2 = (1 + k_T V_T) + \nu_{sh}(1 + k_{sh}V_{sh})$ it can be re-

written as

$$\gamma_s \gamma_r \leq \frac{Z}{\psi_2} \exp(-k_r V_r) = \frac{Z}{\psi_2} \frac{r_c}{\mu_r} \tag{A.21}$$

giving the partial coefficients $\gamma_r \gamma_s$. Z is calculated according to Section A.3 and r_c/μ_r is calculated from Eq. (A.4) with $x_{i,c}/\mu_i = \exp(-\alpha_i \beta V_i) = \exp(-k_i V_i)$. k_i depends on actual fractile value, which for normally distributed functions can be found in any table for the normal distribution, see Table 10 below.

Table 10 *Coefficient k as function of fractile for normal distribution.*

Fractile	0.05	0.10	0.15	0.20	0.25	0.30	0.35	0.40	0.45
k	1.65	1.28	1.04	0.84	0.67	0.52	0.39	0.25	0.13

Doctoral and Licentiate Theses from the
Division of Structural Engineering
Luleå University of Technology

Doctoral Theses

1980   Ulf Arne Girhammar: *Dynamic Fail-safe Behaviour of Steel Structures*. Doctoral Thesis 1980:06D. pp. 309.

1983   Kent Gylltoft: *Fracture Mechanics Models for Fatigue in Concrete Structures*. Doctoral Thesis 1983:25D. pp. 210.

1988   Lennart Fransson: *Thermal Ice Pressure on Structures in Ice Covers*. Doctoral Thesis 1988:67D. pp. 161.

1989   Mats Emborg: *Thermal Stresses in Concrete Structures at Early Ages*. Doctoral Thesis 1989:73D, 2nd Edition, 1990. pp. 285.

1993   Lars Stehn: T*ensile Fracture of Ice. Test Methods and Fracture Mechanics Analysis*. Doctoral Thesis 1993:129D. pp. 136.

1994   Björn Täljsten: *Plate Bonding. Strengthening of Existing Concrete Structures with Epoxy Bonded Plates of Steel or Fibre Reinforced Plastics*. Doctoral Thesis 1994:152D, 2nd Edition 1994. pp. 308.

1994   Jan-Erik Jonasson: *Modelling of Temperature, Moisture and Stresses in Young Concrete*. Doctoral Thesis 1994:153D. pp. 225.

1995   Ulf Ohlsson: *Fracture Mechanics Analysis of Concrete Structures*. Doctoral Thesis 1995:179D. pp. 94.

1998   Keivan Noghabai: *Effect of Tension Softening on the Performance of Concrete Structures. Experimental, Analytical and Computational Studies*. Doctoral Thesis 1998:21. pp. 147.

1999   Gustaf Westman: *Concrete Creep and Thermal Stresses. New creep models and their effects on stress developments*. Doctoral Thesis 1999:10. pp. 301.

1999   Henrik Gabrielsson: *Ductility in High Performance Concrete Structures. An experimental investigation and a theoretical study of prestressed hollow core slabs and prestressed cylindrical pole elements*. Doctoral Thesis 1999:15. pp. 283.

2000   Patrik Groth: *Fibre Reinforced Concrete. Fracture mechanics methods applied on self-compacting concrete and energetically modified binders*. Doctoral Thesis 2000:04. pp. 214.

2000   Hans Hedlund: *Hardening concrete. Measurements and evaluation of non-elastic deformation and associated restraint stresses*. Doctoral Thesis 2000:25, 394 pp. ISBN 91–89580–00–1.

2003   Anders Carolin: *Carbon Fibre Reinforced Polymers for Strengthening of Structural Members*. Doctoral Thesis 2003:18, June 2003. 190 pp. ISBN 91–89580–04–4.

2003 Martin Nilsson: *Restraint Factors and Partial Coefficients for Crack Risk Analyses of Early Age Concrete Structures*. Doctoral Thesis 2003:19. pp. 170. ISBN: 91-89580-05-2.

2003 Mårten Larson: *Thermal Crack Estimation in Early Age Concrete – Models and Methods for Practical Application*. Doctoral Thesis 2003:20. pp. 190. ISBN: 91-86580-06-0.

Licentiate Theses

1984 Lennart Fransson: *Bärförmåga hos ett flytande istäcke. Beräkningsmodeller och experimentella studier av naturlig is och av is förstärkt med armering.* (Load-carrying Capacity of a Floating Ice Cover. Analytical Models and Experimental Studies of Natural Ice and of Ice Strengthened with Reinforcement) Licentiate Thesis 1984:012L, 2nd Edition, 1988. pp. 137.

1985 Mats Emborg: *Temperature Stresses in Massive Concrete Structures. Viscoelastic Models and Laboratory Tests*. Licentiate Thesis 1985:011L, 2nd Edition, 1988. pp. 163.

1987 Christer Hjalmarsson: *Effektbehov i bostadshus. Experimentell bestämning av effektbehov i små- och flerbostadshus* (Heating Demand in Single and Multi Family Houses. A comparison of Models for Calculation and Methods for Measurement). Licentiate Thesis 1987:009L. pp. 72.

1990 Björn Täljsten: *Förstärkning av betongkonstruktioner genom pålimning av stålplåtar.* (Concrete Structures Strengthened by Externally Bonded Steel Plates). Licentiate Thesis 1990:06L. pp. 205.

1990 Ulf Ohlsson: *Fracture Mechanics Studies of Concrete Structures*. Licentiate Thesis 1990:07L. pp. 66.

1990 Lars Stehn: *Fracture Toughness of Sea Ice. Development of a Test System Based on Chevron Notched Specimens*. Licentiate Thesis 1990:11L. pp. 88.

1992 Per Anders Daerga: *Some Experimental Fracture Mechanics Studies in Mode I of Concrete and Wood*. Licentiate Thesis 1992:12L, 2nd Edition. pp. 76.

1993 Henrik Gabrielsson: *Shear Capacity of Beams of Reinforced High Performance Concrete*. Licentiate Thesis 1993:21L, 2nd Edition. pp. 111.

1995 Keivan Noghabai: *Splitting of Concrete in the Anchoring Zone of Deformed Bars. A fracture mechanics approach to bond*. Licentiate Thesis 1995:26L, 2nd Edition. pp. 131+46.

1995 Gustaf Westman: *Thermal Cracking in High Performance Concrete. Viscoelastic Models and Laboratory Tests*. Licentiate Thesis 1995:27L. pp. 123.

1995 Katarina Ekerfors: *Mognadsutveckling i ung betong. Temperaturkänslighet, hållfasthet och värmeutveckling.* (Maturity Development in Young Concrete. Temperature

Sensitivity, Strength and Heat Development). Licentiate Thesis 1995:34L. pp. 136.

1996   Patrik Groth: *Cracking in Concrete. Crack Prevention with Air-Cooling and Crack Distribution with Steel Fibre Reinforcement*. Licentiate Thesis 1996:37L. pp. 126.

1996   Hans Hedlund: *Stresses in High Performance Concrete due to Temperature and Moisture Variations at Early Ages*. Licentiate Thesis 1996:38L. pp. 240.

2000   Mårten Larsson: *Estimation of Crack Risk in Early Age Concrete. Simplified methods for practical use*. Licentiate Thesis 2000:10. pp. 171.

2000   Stig Bernander: *Progressive Landslides in Long Natural Slopes. Formation, potential extension, and configuration of finished slides in strain-softening soils*. Licentiate Thesis 2000:16. pp. 135.

2000   Martin Nilsson: *Thermal Cracking of young concrete. Partial coefficients, restraint effects and influences of casting joints*. Licentiate Thesis 2000:27. pp. 267.

2000   Erik Nordström: *Steel Fibre Corrosion in Cracks. Durability of sprayed concrete*. Licentiate Thesis 2000:49, December 2000. pp. 103.

2001   Anders Carolin: *Strengthening of concrete structures with CFRP – Shear strengthening and full-scale applications*. Licentiate Thesis 2001:01. pp. 120. ISBN 91-89580-01-X

2001   Håkan Thun: *Evaluation of concrete structures. Strength development and fatigue capacity*. Licentiate Thesis 2001:25. pp. 164. ISBN 91-89580-08-2.

2002   Patrice Godonue: *Preliminary Design and Analysis of Pedestrian FRP Bridge Deck*. Licentiate Thesis 2002:18, 203 pp

2002   Jonas Carlswärd : *Steel fibre reinforced concrete toppings exposed to shrinkage and temperature deformations*. Licentiate Thesis 2002:33. pp. 112.

2003   Anders Rönneblad: *Product Models for Concrete Structures - Standards, Applications and Implementations*. Licentiate Thesis 2003:22.

2003   Håkan Nordin: *Strengthening of Concrete Structures with Pre-Stressed CFRP*. Licentiate Thesis 2003:25.

2003   Sofia Utsi: *Self-Compacting Concrete - Properties of fresh and hardening concrete for civil engineering applications*. Licentiate Thesis 2003:19.